

**AES/PE/10-42**

**Sedimentology and 3D architecture of a bioclastic calcarenite complex on Favignana, southern Italy: Implications for reservoir modelling**

**15/12/2010**

**R.A. Kijl**







**Title** : Sedimentology and 3D architecture of a bioclastic calcarenite complex on Favignana, southern Italy: Implications for reservoir modelling

**Author** : R.A. Kil

**Keywords** : Sicily, sedimentology, bioclastic calcarenite, cool-water carbonates, foramol, high energy shelf, multi-point statistics, reservoir modelling

**Date** : 15/12/2010

**Supervisor** : Dr. A. Moscariello

**TA Report number** : AES/PE/10-42

**Graduation committee** : Dr. A. Moscariello <sup>1</sup>  
Prof.dr. S.M. Luthi <sup>1</sup>  
Prof.dr. P.L. de Boer <sup>2</sup>  
Dr. X.M. Marquez <sup>3</sup>  
Ir. A. Janszen <sup>1</sup>

**Postal Address** : Section for Petroleum Engineering  
Faculty of Civil Engineering and Geosciences  
Delft University of Technology  
P.O. Box 5048  
2600 GA Delft, The Netherlands

**Telephone** : +31 (0)15 2781328 (secretary)

**Telefax** : +31 (0)15 2781189

<sup>1</sup> Delft University of Technology, Delft, The Netherlands

<sup>2</sup> University of Utrecht, Utrecht, The Netherlands

<sup>3</sup> Shell Exploration & Production, Rijswijk, The Netherlands

Front page illustration: the Cala Rossa bay with Punta San Vituzzo dipping towards the North.

Copyright © 2010 Section for Petroleum Engineering. All rights reserved.

No parts of this publication may be reproduced, stored in a retrieval system, or transmitted, in any form or by any means, electronic, mechanical, photocopying, recording, or otherwise, without the prior written permission of the section for Petroleum Engineering.



# Acknowledgements

The research project that I have been working on for the past year could not have been realised without the support from quite a number of people. Starting with the people that were not directly involved in the project, but who have been helpful in the last couple of months. I would like to thank Anouk, my family and my fellow students for their support and 'gezelligheid'.

From people that were involved in this study, I would like to thank my thesis supervisor Andrea Moscariello. His enthusiasm for the project is inspiring, and his suggestions have been very useful. Beside, his network on Favignana and Italian language skills opened many doors that would have remained closed to 'outsiders'.

The fieldwork is made possible by the Molengraaff fund. Their contributions to geological research projects are very valuable and therefore I'd like to acknowledge the board of the Molengraaff fund for the granted subsidy. Furthermore, the use of Petrel would not have been possible without the generosity of Schlumberger for providing the licences.

For all their ideas in the field considering sediment transport and the conceptual geological environment, I'd like to acknowledge Poppe de Boer, Joris Eggenhuisen and Arnoud Slootman from the University of Utrecht. Most of them have also been on Favignana during my two visits, and their contributions have been very helpful. Another person who generously shared her experience in examining the thin sections is Xiomara Marquez from Shell.

The handling of the samples was challenging due to the brittle rock properties, therefore my thanks to Dick Delforterie for his expertise in making the thin sections and the plugs. The unusually permeable samples required an alternative experimental set-up. Wim Verwaal and Karel Heller, thank you for the effort in making this work properly.

For his extremely useful contribution to this project in the form of detailed (digital) maps of Favignana, I would like to thank Paolo D'Angelo from the *Area Marinara Protetta delle Isole Egadi*. These maps made the creation of an up-to-date and accurate model of the island a more convenient.

Last but not least, after a long day in the field the doors of *Amici del Mare* were always wide open. Rino, Uccio and the rest of the staff, thank you for the hospitality, the delicious food and the only available (internet)connection to the outside world during Favignana's quiet winter period.



# Abstract

The island of Favignana provides an exceptional three-dimensional insight in the architecture of a Lower Pleistocene bioclastic calcarenite complex. Due to the degree of quarrying, a large amount of outcrops is available in the eastern part of the island. Two campaigns resulted in the logging of stratigraphic sections, recording of sedimentary structures and palaeo-transport orientations, analysis of the fossil content and the collection of samples in order to test the reservoir potential of the calcarenite — associated with foramol skeletal grain types.

A correlation between palaeo-transport directions and the stratigraphic logs distributed over the whole fieldwork area led to a conceptual geological model. Sediments were generated in the shallow temperate water of the Mediterranean, and are subsequently transported and/or reworked by storm events. Deposition on top of the middle to Upper Pliocene Trubi clay most likely took place in a topographic low between the already existing mountainous structures of Favignana and the nearby Levanzo island. A system of large scours characterised the depositional processes — which are described by three phases — significantly. Propagation of the calcarenite complex was dominated by a southeastern direction, making the Favignana calcarenite complex a rare example in the Mediterranean, as comparable deposits in the area propagate on a shelf towards the open sea instead of towards a major land mass.

The use of a multi-point statistics algorithm, which is a suitable option when a large dataset and a good conceptual model are available, led to the generation of a facies model. Based on the analysis performed on the calcarenite samples, the reservoir potential is high, with porosity values of up to 0.65 bulk rock fraction and a permeability of tens of darcy. Because the fieldwork area has never been buried to depth, little diagenesis — such as cementation, compaction and fracturing — has taken place.

The Favignana calcarenite is believed to be a relevant and important analogue for a several carbonate hydrocarbon fields in various regions of the world such as South America and Middle East. The detailed understanding of sedimentary facies distribution, internal architecture and reservoir property variability can therefore assist to guide and/or optimize the development of those reservoirs. In particular, the Favignana calcarenite is thought to be a relevant analogue for the Perla gas field in Venezuela, a giant reservoir consisting of foramol carbonates, and the reservoirs formed by the Asmari limestone in the Zagros basin.



# Riassunto

## **Sedimentologia e architettura tridimensionale del complesso calcarenitico bioclastico di Favignana (Italia meridionale): Implicazioni per la modellizzazione di giacimenti**

L'isola di Favignana offre una visione tridimensionale dell'architettura interna e stratigrafia di un complesso sedimentario di calcarenite bioclastiche del Pleistocene inferiore caratterizzate da una tipica associazione a foramol. Grazie alla presenza di un gran numero di cave per lestrazione di pietre da costruzione, una grande quantità di affioramenti di eccezionale qualità è disponibile nell'area di studio, situata nella parte orientale dell'isola. Durante due campagne di terreno si sono eseguite: misurazione di sezioni stratigrafiche, descrizione di strutture sedimentarie, raccolta di dati di paleo-trasporto, analisi del contenuto di fossili e la raccolta di campioni al fine di testare le potenziali caratteristiche di un simile giacimento formato da calcareniti.

Una correlazione tra le direzioni di paleo-trasporto e il record stratigrafico complessivo dell'intera area di studio ha permesso la definizione di un modello geologico concettuale tridimensionale. Le biocalcareniti, depositatesi al di sopra delle argille della Formazione di Trubi (Pliocene superiore), si sono accumulate molto probabilmente in corrispondenza di un basso topografico tra le strutture già esistenti della montagna di Favignana (Monte Santa Caterina) e la vicina isola di Levanzo. Il processo di accumulo delle bio-calcareniti, è definito complessivamente da tre momenti con caratteristiche sedimentarie differenti e conseguente formazione di dune di diverse dimensioni. La fine della fase deposizionale dell'intero complesso, è caratterizzata da importanti processi erosivi e gravitativi risultanti in larghe incisioni, profonde fino a 20 m, successivamente riempite da processi di accumulo rapido. In base alle osservazioni micro- e macro-tessiturali (basate sulle strutture sedimentarie e le direzioni di paleo-trasporto), le biocalcareniti di Favignana si sono generate in acque temperate fredde in una località probabilmente situata a nord o nord-ovest della posizione attuale. In seguito i sedimenti sarebbero quindi stati trasportati e/o rielaborati da correnti associate a eventi di tempesta come indicato dalla propagazione del complesso di bio-calcareniti, dominata da una direzione di trasporto verso sud-est. In base alla paleogeografia attuale, tale caratteristica architetturale rende l'accumulo bio-calcarenitico di Favignana un singolare esempio nel Mediterraneo. Infatti, simili complessi tendono a svilupparsi verso il mare aperto e acque più profonde piuttosto che verso la terra ferma e zone costiere e acque meno profonde come sembra avvenire nel caso studiato.

La modellizzazione tridimensionale della distribuzione di facies del complesso bio-calcarenitico è stata eseguita utilizzando l'algoritmo multi-point statistics, che è un'opzione adatta quando sono disponibili un set di dati di grandi dimensioni e un buon modello geologico concettuale. In base alle analisi di laboratorio compiute sui campioni di bio-calcarenite, il potenziale per un giacimento simile è molto alto, con valori di porosità fino al 65% e una permeabilità di decine di Darcy. Poiché l'area di studio non è mai stata sepolta a profondità elevate, processi diagenetici non hanno influenzato in maniera critica la tessitura originale di tali rocce. Ciononostante, cementazione, compattazione e fratturazione possono notevolmente influire nel modificare le caratteristiche tessiturali e di potenziale flusso dell'ammasso roccioso. In ogni modo, in base ai promettenti risultati dei test di laboratorio, è ipotizzabile che una frazione considerevole della porosità e permeabilità possa essere conservata anche dopo processi post-deposizionali.

Le bio-calcareniti di Favignana riscuotono un grande interesse per la loro similitudine con molti giacimenti di idrocarburi in rocce carbonatiche localizzati in altre regioni del mondo quali il Sud America e Medio Oriente. La comprensione di dettaglio delle facies sedimentarie, l'architettura e distribuzione di proprietà quali la porosità e permeabilità può quindi aiutare a guidare e/o ottimizzare lo sviluppo di tali giacimenti. In particolare, le bio-calcareniti di Favignana sono un riferimento importante per il campo di gas Perla in Venezuela, un giacimento gigante composto da carbonati tipo foramol e i giacimenti formati dal calcare Asmari nel bacino dello Zagros.



# List of Figures

2.1	Location of Favignana and an illustration showing the age of the researched area. . . . .	4
2.2	Morphology of the fieldwork area. . . . .	4
2.3	Overview of the Mediterranean area showing the structures related to the Alpine orogeny. Image from the public domain, free of copyright. . . . .	7
2.4	A simplified geological map of Favignana, with a cross section corresponding to the XX' line in the map. Map and profile are modified after Abate et al. (1997) and Tavarnelli et al. (2003). . . . .	7
3.1	The principle of the apparent dip. By definition, $\beta \leq \alpha$ for an apparent dip $\beta$ and a real dip $\alpha$ . . . . .	9
3.2	The principle of drilling cores from samples, and the result when the cores were washed from drilling debris. . . . .	10
3.3	Schematic overview of the experimental set-up used for the permeability measurements. .	13
3.4	Examples of a calcarenite plug prepared for permeability tests, including the rubber bicycle inner tyre that serves as a seal. . . . .	13
4.1	Bed geometries as function of the grain size on the horizontal axis, and the mean flow velocity on the vertical axis. . . . .	17
4.2	Classification of carbonate grain types by Lees & Buller (1972). . . . .	18
4.3	Thin section examples showing fossil content and diagenetic processes. The size of the red scale bar is respectively 500 $\mu\text{m}$ and 200 $\mu\text{m}$ for the 10x and 4x magnifications. Abrasion due to the creation of thin sections may have changed the original grain orientations. Images and interpretation courtesy of Dr. X. Marquez. . . . .	21
4.4	Examples of fossils as observed in the field. Unless indicated otherwise, hand lenses for scale.	22
4.5	More examples of fossils as observed in the field. . . . .	23
4.6	Two main types of cross-lamination as observed on Favignana. Note the difference in geometry visible on the cross section perpendicular to the main flow direction. See also figure 4.1 for flow regimes. Figure courtesy of Southard (1996). . . . .	28
4.7	Field examples of sedimentary structures outcropping in eastern Favignana. The photographs illustrate massive calcarenites and parallel- and undulated lamination. . . . .	30
4.8	Field examples of scour fills, tabular cross-stratification and large foresets. . . . .	31
4.9	Field examples of trough cross-stratification, bioturbation and the (Trubi) clay. . . . .	32
4.10	Sedimentary logs from fieldwork at eleven pseudo-well locations, which are illustrated in the map. Well spacing varies significantly and is therefore not to scale. . . . .	33
4.11	Pie chart data obtained from field observations and facies assemblage. . . . .	35
4.12	Overview of palaeo-transport directions as observed in the field. . . . .	35
4.13	Cross plot showing porosity versus permeability obtained from core analysis of the samples. Sections 3.3.1 and 3.3.2 describe the laboratory experiments. . . . .	37
4.14	Experimental results of the permeability tests on samples. . . . .	37
5.1	Schematic map of the Aegadian islands showing the major transport directions and possible locations of carbonate generation platforms. . . . .	39
5.2	The well logs from the fieldwork data (figure 4.10) with an interpreted conceptual facies model. . . . .	43

5.3	Conceptual model of the Favignana calcarenite with respect to the present-day situation.	43
6.1	Training image grid for the MPS algorithm. North is upper left, facies colour according to general facies legend. . . . .	46
6.2	Facies model resulting from the MPS method showing a plan view, two cross sections and a fence with stratigraphic log locations. The values of Y-axes in cross-sections are in metres above mean sea level. . . . .	49
6.3	Conceptual structural reservoir prospective of the Favignana calcarenite. A cross section from northwest to southeast is given, with Favignana on the right. Vertical scale is exaggerated. . . . .	53
7.1	Water escape structures at two different scales. . . . .	55
7.2	Isopach map of the area west of Favignana. . . . .	57
7.3	Terraces in the Marsala calcarenite deposits between Trapani and Mazara del Vallo on the mainland of Sicily as described by D'Angelo & Vernuccio (1996). . . . .	58
7.4	Example of some calcarenite terraces near the city of Marsala, looking south. The city of Marsala is just out of the view on the right. . . . .	58
A.1	Geological map of the onshore area of western Sicily. The complexity of the geological structures in Sicily contrasts considerably with the relatively undeformed Pleistocene clastic carbonates (marked on the map). Map modified after Catalano et al. (2002). . . . .	69
A.2	Nautical map of the Aegadian archipelago showing the islands of Favignana, Levanzo and Marettimo. Image courtesy of the <i>Area Marinara Protetta delle Isole Egadi</i> . . . . .	70
A.3	Map of Favignana showing the locations as they are used in this report. . . . .	71
A.4	The fieldwork area on the eastern part of Favignana. The quarries are indicated in red. . . . .	72
A.5	Chronostratigraphical correlation of the Lower Pleistocene to present day situation. . . . .	73
B.1	Locations of the photo panels shown in this appendix. . . . .	74
B.2	Outcrop of the eastern part of Cala Rossa. The change from a more planar bedding to dunes with linear crest and finally undulated crest is clearly visible. Also notice the end of a set of dunes with tabular cross-lamination, overlain by trough cross-laminated units. Person for scale. . . . .	75
B.3	Photo panel of the Scala Cavallo cliff face. Note the large scours incising the older sedimentary rock. . . . .	76
B.4	High energy development of a scour and fill system. Similar geometries are observed elsewhere, however of smaller scale. . . . .	77
B.5	Large foresets in the Cala Azurra bay, prograding to the southeast. . . . .	78
B.6	Abandoned quarry south of the Scalo Cavallo cliff to illustrate the general thickness of the calcarenite. Note the 'skyscraper' left behind in the centre of the quarry, which is about 20m high. . . . .	78
C.1	Overview of the thin sections with polarisation filter activated. . . . .	82
D.1	Facies logs in all fieldwork locations, which are used as input in the facies model. The trajectory is shown in the top left, and the dotted line represents the surface of the island. Elevation in metres above mean sea level. . . . .	84
D.2	Intermediate slices of the training image used in the MPS modelling algorithm. The north is pointing upwards, scale not relevant. . . . .	85
D.3	Probability maps of the facies functioning as additional input data in the modelling process.	86
D.4	Probability maps of the facies functioning as additional input data in the modelling process (continued). . . . .	87
D.5	Close-ups of the final Multi-point statistics model of eastern Favignana. . . . .	88
D.6	The eastern Favignana porosity model. . . . .	89
D.7	Facies model of eastern Favignana resulting from a SIS algorithm. . . . .	90
D.8	Facies model of eastern Favignana resulting from a TGS algorithm. . . . .	91
E.1	Procedure to create a seal around the samples used for permeability tests. . . . .	93

# List of Tables

3.1	Overview of the samples, the type and the number of plugs and thin sections obtained in the laboratory. Note: sample 7 could not be used because of poor cementation conditions.	10
6.1	Average petrophysical properties of the facies in the model, including the sample sources. Numbers according to table 3.1. . . . .	50
6.2	Results of the volume calculation of the potential Favignana oil reservoir. BV is the bulk volume, PV the pore volume and HCPV is hydrocarbon pore volume — or the pore volume occupied by hydrocarbons. All volumes are in $[10^6 \text{ m}^3]$ . . . . .	53
A.1	List of maps of Favignana used in this study. . . . .	68
B.1	Overview of the geological photo panels. . . . .	74
C.1	Facies overview . . . . .	80
C.2	Results of laboratory experiments on plugs from the Favignana calcarenite. Porosity and permeability are listed in the rightmost columns. Plugs with indicated with H are taken horizontally, V indicates vertical plugs. . . . .	81
D.1	List of figures used to illustrate different aspects of the Favignana facies model. . . . .	83

# List of Symbols

Symbol	Description	SI Unit
A	Cross sectional area	m <sup>2</sup>
$\rho$	Density	kg/m <sup>3</sup>
D	Diameter	m
$\mu$	Dynamic viscosity	Pa s
Q	Flow rate	m <sup>3</sup> /s
F	Froude number	-
GOC	Gas oil contact	m
g	Gravitational constant	m/s <sup>2</sup>
D <sub>gr</sub>	Grain size (diameter)	$\mu$ m
h	Height	m
L	Length	m
B <sub>o</sub>	Oil formation volume factor	rb/sb
OWC	Oil water contact	m
$\mathcal{O}$	Order of magnitude	n/a
k	Permeability	10 <sup>-12</sup> m <sup>2</sup> or D
$\Phi$	Porosity	-
p	Pressure	Pa or kg/(m s <sup>2</sup> )
T	Thickness	m
t	Time	s
V	Volume	m <sup>3</sup>
H	Water tank level	m

# List of Abbreviations

Abbreviation	Description
AMSL	Above mean sea level
BP	Before Present
b	Bulk
BV	Bulk volume $[(10^6) \text{ m}^3]$
GSLIB	Geostatistical software library
GPS	Global positioning system
HCPV	Hydrocarbon pore volume $[(10^6) \text{ m}^3]$
ma	Matrix
MSL	Mean sea level
Ma	Mega-annum: million years ago
MPS	Multi-point statistics
PV	Pore volume $[(10^6) \text{ m}^3]$
SIS	Sequential Indicator Simulation
STOIIP	Stock tank oil initially in place $[(10^6) \text{ m}^3]$
TGS	Truncated Gaussian Simulation

# Contents

Acknowledgements	i
Abstract	iii
Riassunto ( <i>Italiano</i> )	v
List of Figures	viii
List of Tables	ix
List of Symbols	x
List of Abbreviations	xi
Table of Contents	xii
<b>1 Introduction</b>	<b>1</b>
<b>2 Geographical and geological setting</b>	<b>3</b>
2.1 Location . . . . .	3
2.2 Morphology . . . . .	3
2.3 Geological setting . . . . .	5
<b>3 Methods</b>	<b>8</b>
3.1 Stratigraphic description . . . . .	8
3.2 Sampling . . . . .	9
3.3 Reservoir properties . . . . .	11
3.3.1 Porosity . . . . .	11
3.3.2 Permeability . . . . .	12
3.4 3D Geological modelling . . . . .	15
<b>4 Favignana calcarenite</b>	<b>16</b>
4.1 Background . . . . .	16
4.2 Sedimentary microfacies . . . . .	17
4.2.1 Foramol . . . . .	17
4.2.2 Fossil content . . . . .	18
4.2.3 Diagenesis . . . . .	20
4.3 Sedimentary macrofacies . . . . .	24
4.3.1 Massive calcarenite . . . . .	24
4.3.2 Parallel laminated units . . . . .	25
4.3.3 Undulated lamination and scour fills . . . . .	25
4.3.4 Tabular cross-stratification . . . . .	26
4.3.5 Large scale foresets . . . . .	26
4.3.6 Trough cross-stratified units . . . . .	27
4.3.7 Massive bioturbated units . . . . .	27

4.3.8	Clay . . . . .	28
4.4	Stratigraphic logs and facies distribution . . . . .	34
4.5	Palaeo-transport directions . . . . .	34
4.6	Reservoir properties . . . . .	36
4.6.1	Porosity . . . . .	36
4.6.2	Permeability . . . . .	36
<b>5</b>	<b>Conceptual geological model</b>	<b>38</b>
5.1	Sediment supply . . . . .	38
5.2	Transport mechanism . . . . .	39
5.3	Depositional environment . . . . .	40
<b>6</b>	<b>Reservoir modelling</b>	<b>44</b>
6.1	Facies model . . . . .	44
6.1.1	Geostatistical algorithm . . . . .	45
6.1.2	Training image . . . . .	45
6.1.3	Additional data . . . . .	47
6.1.4	Facies modelling results . . . . .	47
6.2	Property modelling . . . . .	50
6.3	Reservoir implications . . . . .	50
<b>7</b>	<b>Discussion</b>	<b>54</b>
7.1	Sedimentation deformation structures . . . . .	54
7.2	Reservoir properties . . . . .	54
7.3	Location on shelf . . . . .	55
7.4	Tectonic and eustatic processes . . . . .	57
7.5	Reservoir analogues . . . . .	59
7.6	Modelling algorithms . . . . .	60
7.6.1	Object modelling . . . . .	60
7.6.2	Sequential indicator simulation . . . . .	60
7.6.3	Truncated Gaussian simulation . . . . .	61
7.6.4	Indicator kriging . . . . .	61
<b>8</b>	<b>Conclusions</b>	<b>62</b>
<b>9</b>	<b>Recommendations</b>	<b>64</b>
	<b>References</b>	<b>66</b>
<b>A</b>	<b>Maps and charts</b>	<b>68</b>
<b>B</b>	<b>Geological photo panels</b>	<b>74</b>
<b>C</b>	<b>Facies description and properties</b>	<b>79</b>
<b>D</b>	<b>Modelling results</b>	<b>83</b>
<b>E</b>	<b>Tutorials</b>	<b>92</b>
E.1	Falling head experiment . . . . .	92
E.2	Import maps from CAD files . . . . .	94
E.3	Field data in pie charts . . . . .	94
E.4	Probability maps . . . . .	95

# 1 Introduction

The eastern part of the island of Favignana (eastern Sicily, Italy) presents extensive exposures of a bioclastic sand wedge complex of exceptional quality. Access to the outcrops is easy because almost all of them are situated in quarries which have been exploited since hundreds of years. This study presents an unprecedented three-dimensional insight through a potential hydrocarbon reservoir analogue.

Preliminary research and a quick investigation in the field (A. Moscariello, personal communication) showed that the eastern Favignana rock type was a promising study area, and it could therefore be useful as an analogue for existing hydrocarbon producing fields. The study of reservoir analogues can be very helpful in improving the ultimate recovery and production rates of a comparable oil or gas field. It has been proved to be a useful method to improve the understanding of the reservoir geometry and flow behaviour of hydrocarbon producing reservoirs (Bhushan & Hopkinson, 2002). Through the information extracted from an analogue, 1) well placement; 2) production intervals; 3) water flood strategy; or 4) other enhanced oil recovery methods can be optimised to a better extent.

Analogues have proven to be a useful comparison with reservoirs because of their exposure at the surface. One of the challenges in the production of hydrocarbons is to access key information which would unravel the detailed architecture and internal geometry of the reservoir. Typical reservoirs are situated up to several kilometres below the surface, and data are often very detailed but limited to the near-wellbore area — such as petrophysical data — or in a low resolution and available over a large area — like seismic surveys. The advantage of studying analogues is that the analysis of reservoir rock can be done on all scales, from microscopic analysis of small fragments of rocks to depositional environment and its associated geometries and lateral distribution.

The aim of this study is to 1) describe the sediment facies; 2) reconstruct the internal architecture; 3) determine reservoir properties; and 4) build a facies model of the eastern part of Favignana. This covers a large amount of data, from millimetre to reservoir scale. A fieldwork campaign during the winter period was organised. Prior to the start of the project, the deliverables of the research were defined as:

- Stratigraphical and facies logs
- Microscopic description
- Reservoir properties (porosity - permeability)



- Facies maps and photo panels
- Conceptual geological model of eastern Favignana
- Three dimensional geological models of facies and reservoir units

A reservoir model in the subsurface is usually based on well data combined with a conceptual model of the regional geology. While a subsurface model is unlikely to be totally correct it is commonly accepted that, despite the errors, it can be used as a simplification of the reality. Similarly, a three-dimensional facies model of an outcropping rock package, due to the limited standard software capability will also not be entirely correct. However, in the case of Favignana the errors generated by the modelling algorithm will be visible due to the high density of quarries and outcrops.

This study represents the first attempt to describe the internal structure of the eastern Favignana calcarenite, instead of treating it as one unit, as done so far (Abate et al., 1997; D'Angelo et al., 2005; Tavarnelli et al., 2003). The large number of outcrops of large dimensions and the large variety of different facies makes definition of reservoir units which can represent the complex reservoir architecture a challenging task.

## 2 Geographical and geological setting

### 2.1 Location

The island of Favignana is part of the Aegadian archipelago. Together with Levanzo and Marettimo it forms a group of rather small islands located approximately five kilometres from the west coast of Sicily, southern Italy (see figure A.2 in appendix A). Figure A.3 — in the same appendix — is a detailed map of Favignana, showing elevation, buildings and roads, as well as geographical names of locations described in this report.

This study focusses on the bioclastic carbonate deposits on the eastern part of Favignana. Most of the houses on the island are build with stones extracted from this rock, locally known as *tufo*. This name, however, does not refer to rocks with volcanic origin, known as tuff. Some claim the *tufo*, which is a common name assigned to similar soft sedimentary rocks throughout Italy, is named after the sound a hammer makes while hitting the rock.

### 2.2 Morphology

Favignana differs from the other two Aegadian islands when looking at its morphological characteristics. While Levanzo and Marettimo practically only consist of a mountain rising from the sea, Favignana's Monte Santa Caterina is flanked by areas with lower relief (figure 2.2a). The eastern side of the mountain shows a more than 50 metres high cliff in the north, with a surface gradually dipping to the south. Compared to the 300 metres high Monte Santa Caterina this can be considered relatively flat. The south dipping surface can theoretically be caused by either depositional or erosional processes. However, observations made during this study indicate that sedimentary structures are truncated in the top part — see figure 2.2b — hence suggesting an erosive nature of the topography.

The situation of the main quarried areas is shown in figure A.4. Quarrying has been going on for hundreds of years, and was first concentrated on the outcrops along the coast. This is where the oldest quarries can be found. Transportation of the mined rock was easy due to the access from the sea. Later, people started to quarry the rock more inland. Some interesting observations can be made on the geometry of

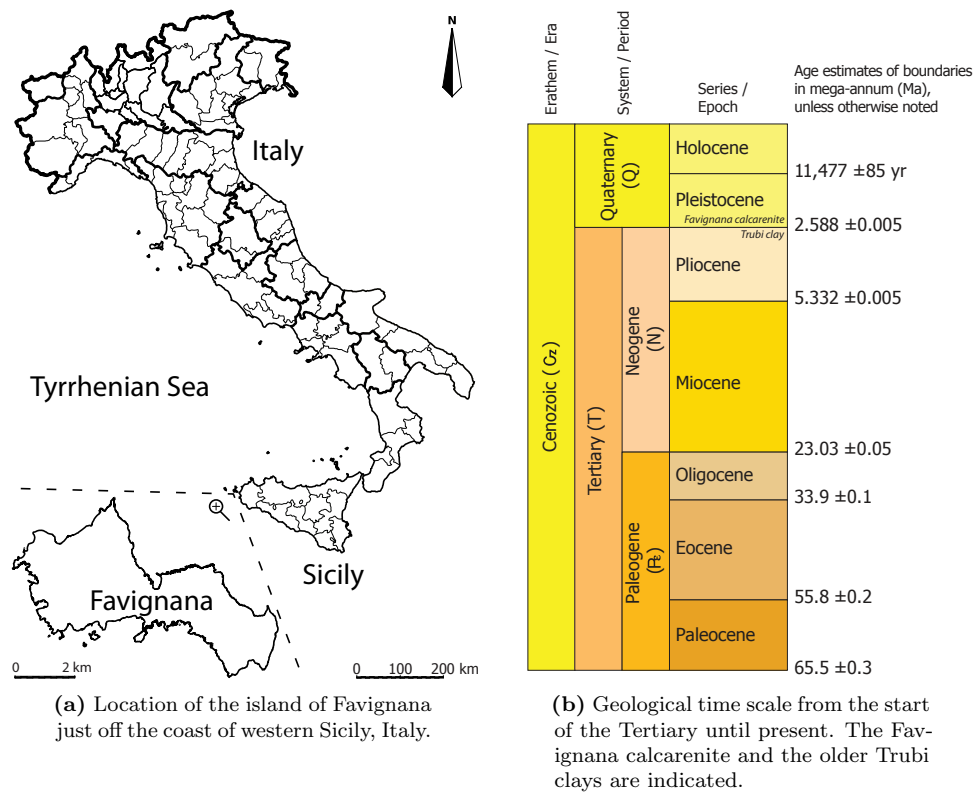


**Figure 2.1** – Location of Favignana and an illustration showing the age of the researched area.



(a) Eastern Favignana as seen from Monte Santa Caterina. Seen from more than 300 metres elevation the area has a rather low-profile character. On the foreground the Town of Favignana, right above it the Scalo Cavallo cliff. View is towards the east, with the mainland of Sicily on the background.



(b) View on the western part of Cala Rossa and Punta san Vittuzzo. The truncated sedimentary structures are an indicator for erosive processes.

**Figure 2.2** – Morphology of the fieldwork area.

the excavations. The elevation of the lowest quarried part never drops below sea level. An explanation might be found in groundwater problems, because of the highly permeable rock. Secondly, the worst quality rock is often left behind, i.e. not quarried. In a lot of fractured areas this can be observed, because fractures decrease the ability to serve as building material.

Outcrop quality in these quarries varies considerably. Depending in the age and the degree of weathering the ability to observe sedimentary structures varies. A too young quarry still shows the cuts made by mining equipment, and sedimentary structures were not able to become visible on the outcrop rock face. The result is a — for the human eye — homogeneous wall with a regular grid of cuts. On the other side, some very old quarries with exposure to seawater are weathered, colouring the rock to a blackish surface. In the perfect conditions the quarries are old enough for the wind to erode part of the wall, exposing sedimentary structures, and not too close to a source of water to develop a high degree of weathering.

## 2.3 Geological setting

The geological setting of Favignana is geometrically related to the same geological history which affected the larger island of Sicily, southern Italy. In the Mesozoic, the African and the Eurasian plates were bounded by a passive continental margin. The African plate moves north and collides with the European continent, creating several mountain ranges in the Mediterranean area, including the Apennines, the Alps and the Pyrenees. An overview of all the Tertiary structures as a result of the Alpine orogeny is given in figure 2.3.

During this Alpine orogeny stage different thrust sheets developed, superposing each other. The island of Sicily is therefore characterised by a fairly complex structural setting of folds and east-west trending thrust belts (see figure A.1 for a geological map of the onshore part of western Sicily). The structurally interesting part of Favignana can be subdivided into two main tectonic units; the Monte Santa Caterina unit and the Punta Faraglione unit (Incandela, 1996; Tavarnelli et al., 2003). A simplified geological map — see figure 2.4a — shows the position of both units.

**The Monte Santa Caterina unit** consists of upper Triassic to Lower Jurassic platform carbonates. They show a grading upward trend to the middle Jurassic - Eocene limestones and marls. The latter are pelagic — or deep marine — deposits. An unconformity follows with on top Miocene limestones deposited in relatively shallow depths. The youngest sediments in this unit are Tortonian and Messinian marls and clays.

**The Punta Faraglione unit** superposes the Monte Santa Caterina unit and is basically built up with the same stratigraphic column.

The Monte Santa Caterina unit overthrusts the Punta Faraglione unit on the most western part of the island, as shown in figure 2.4a. The mountain of Monte Santa Caterina itself consists mainly of a

thrust fault that overrides the Punta Faraglione unit with a horizontal displacement of more than three thousand metres (Incandela, 1996; Tavarnelli et al., 2003).

Post orogenic extension caused the introduction of normal faults. Favignana is a good example of such a stage of extension after a major stage of thrusting. The geological cross section in figure 2.4b illustrates both the compressional and extensional structures in Monte Santa Caterina. Uplift in the area occurred during a third phase, caused by the still ongoing compression between the African and Eurasian plates.

Monte Santa Caterina is flanked on its eastern side by much younger deposits of Lower Pleistocene bioclastic deposits (Abate et al., 1997; D'Angelo et al., 2005). This puts the border between the Trubi Formation and the calcarenite at the Plio - Pleistocene boundary.

The other islands of the Aegadian archipelago, Marettimo in the east and Levanzo in the north, show the same stratigraphical succession as Monte Santa Caterina on Favignana. However on the other two islands no Lower Pleistocene terraces are present. Whether the latter were never deposited, or because they are eroded or not uplifted is uncertain. Between Favignana and Marettimo a deep channel of more than 200 metres exists. Figure A.2 illustrates this in a nautical map of the Aegadian islands. The fact that the shelf is interrupted by such a channel can have important consequences for the transport mechanism of sediments. The conceptual geological model in chapter 5 will address with those issues.

Because the young age and the nowadays relatively calm structural setting, tectonic deformation and other post-sedimentary processes are limited. Parts of the east Favignana calcarenites show fractures, indicating some minor tectonic influence. Offsets are generally less than a couple of centimetres. The elevation of the eastern part of Favignana, which can be up to fifty metres, suggests that some uplift must have taken place. A sea level of that height is not realistic for the Lower Pleistocene Mediterranean.

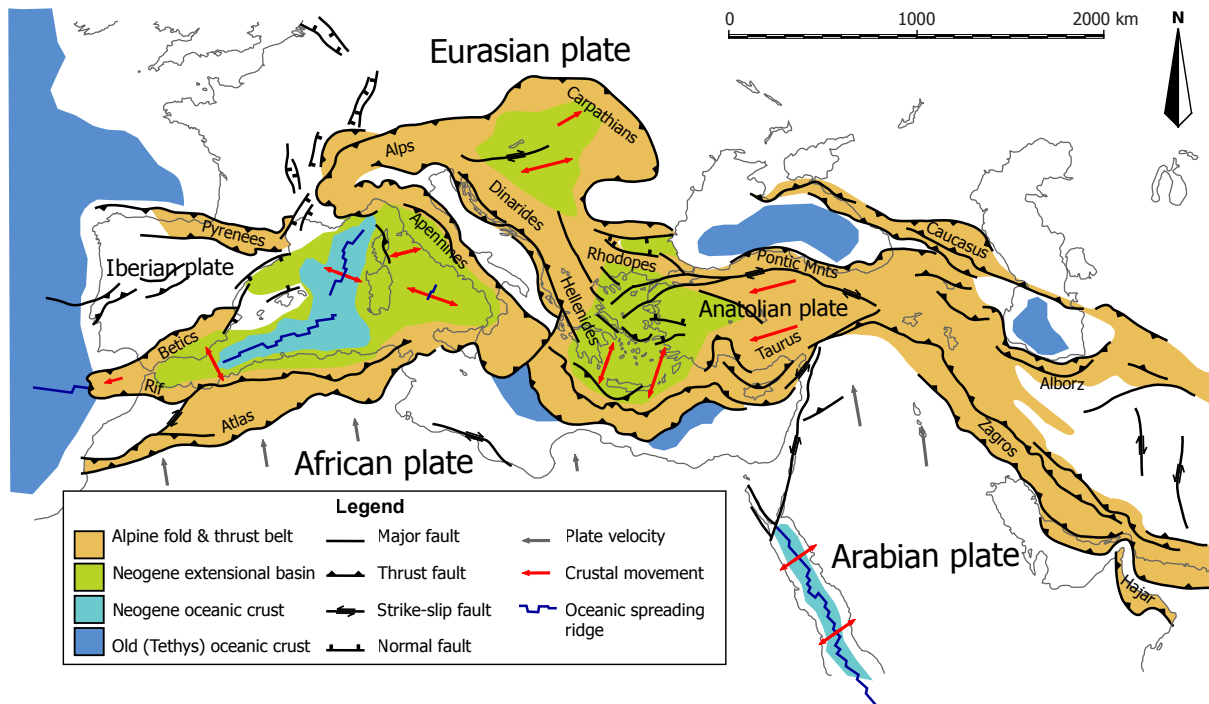


**Figure 2.3** – Overview of the Mediterranean area showing the structures related to the Alpine orogeny. Image from the public domain, free of copyright.

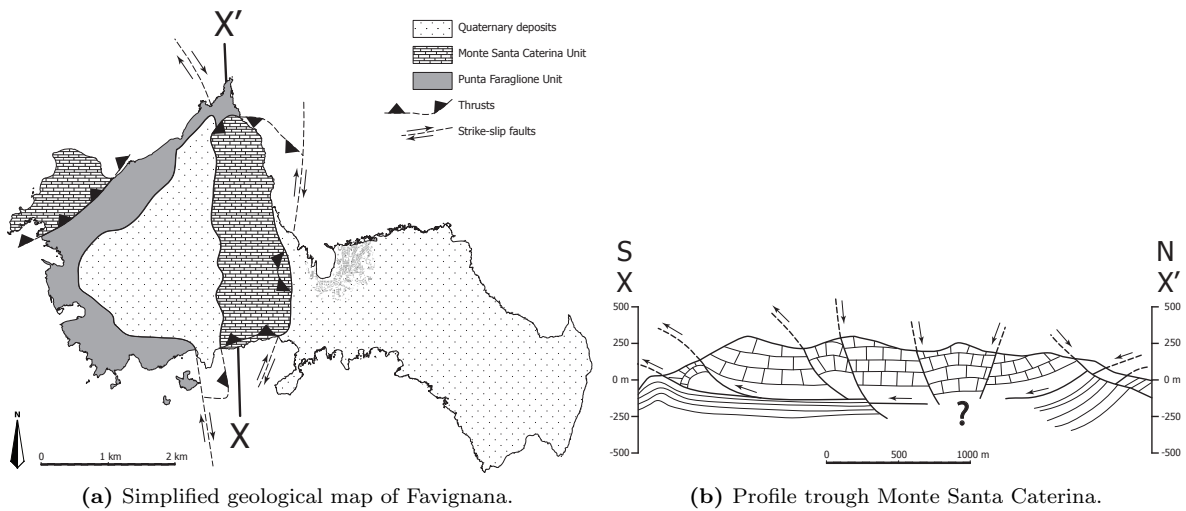


**Figure 2.4** – A simplified geological map of Favignana, with a cross section corresponding to the XX' line in the map. Map and profile are modified after Abate et al. (1997) and Tavarnelli et al. (2003).

## 3 Methods

The fieldwork included several types of data collection. Because this project focuses on describing the Favignana bioclastic sands from a reservoir point of view, a combination of stratigraphical sections and samples have been used. The methods of data collection and data treatment will be described in this section.

### 3.1 Stratigraphic description

East Favignana houses an extensive system of quarries, providing good outcrop quality. Some stratigraphical sections provide excellent outcrop accessibility and a good potential to create stratigraphic logs. Others are more remote or out of reach, and those have been evaluated by using photo panels.

The location of every pseudo-well is measured using a GPS device, which is usually horizontally accurate to five metres. Because the GPS elevation is less accurate because of locally high quarry walls — in the order of multiple metres off — elevation is extracted from a digital model of the Favignana surface. This model was available in AutoCAD format, and was then converted to data readable by the Petrel modelling software. The workflow used in this process is described in appendix E.2. Each section is documented with photos, if possible including a large scale five metre long ruler. This device is also used to keep track of thickness and depth.

The calcarenite deposits consist of a large variety of calcareous remains of living material. Very few siliceous or clay-type minerals are present in the matrix. Texture depends on the type of skeletons and the amount of reworking. The base of the Favignana system shows a major clay unit, differing considerably in composition and texture. The amount of transport and the related energy determines the degree of fragmentation. This has consequences for the grain size. Grain-size analysis is performed by examining thin sections, however microscope magnifications are generally too high to capture a representative area of such coarse-grained material. Instead of using a microscope, a standard mirror reflex camera with high resolution was used in order to capture the entire thin section instead of only a small portion.

Sedimentary structures are a good indication of the processes that were active during deposition. The structures observed in the quarries and outcrops on Favignana will be used to describe the conceptual

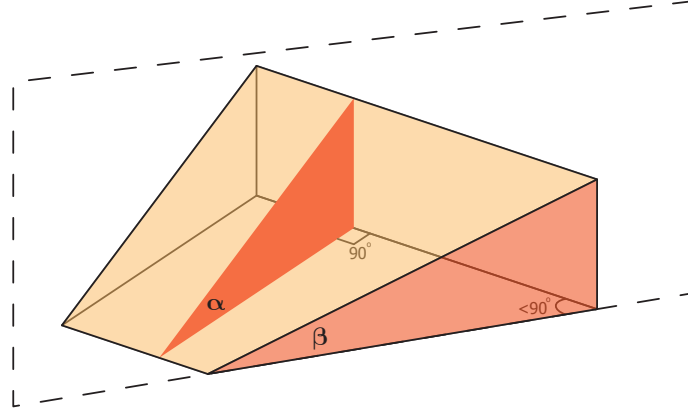


**Figure 3.1** – The principle of the apparent dip. By definition,  $\beta \leq \alpha$  for an apparent dip  $\beta$  and a real dip  $\alpha$ .

geological model. A good three-dimensional insight is crucial in order to make a reliable subdivision. Generally an outcrop face exposing only one orientation does not provide sufficient information to extract the transport direction. The fact that the quarries on Favignana provide outcrop walls in almost all orientations, often perpendicular to each other, makes interpolation and reconstruction of transport directions easier. Thus, for each sedimentary structure in an outcrop, an attempt to obtain the palaeotransport direction was made. In some cases — for reasons described earlier — the outcrop quality was too bad to make reliable observations. For those parts of the section the sedimentary structures and transport directions are unknown.

The square character of the outcrops introduce the principle of apparent dips. A dip direction and/or angle of a bed, lamina or other sedimentary feature as observed on a single wall will hardly ever be its real orientation. Instead, it is more likely that one observes the so-called apparent dip. Figure 3.1 illustrates this principle. By definition, the apparent dip is always smaller than or equal to the real dip.

## 3.2 Sampling

During the fieldwork, eight samples were taken in order to 1) test the rock for reservoir properties; and 2) describe the microfacies; of the Favignana calcarenite. A rock hammer and chisel were used to cut the samples out of the outcrop walls. The size of the samples was kept large - cubes of around 20 cm - to ensure that enough cores could be drilled back in the TU Delft core drilling facilities. Moreover, the size also prevents the samples from breaking during chiselling.

In the core drilling laboratory, the sides of each sample were trimmed to be able to expose a fresh rock face. Without weathering and debris that was present on the samples, the grain orientation and/or size is easier to examine. Where possible, a number of horizontal and vertical cores were drilled from the large samples. Finally, the obtained cores were cut to a length of about 3 cm, creating the plugs for



**Table 3.1** – Overview of the samples, the type and the number of plugs and thin sections obtained in the laboratory. Note: sample 7 could not be used because of poor cementation conditions.

Sample	Origin	Horizontal plugs	Vertical plugs	Thin sections
1	Parallel laminated units	8	2	1 (1.2)
2	Massive, rich in bioclasts	4	2	1 (2.1)
3	Tabular cross-stratification	5	0	1 (3.2)
4	Small scale trough cross-stratification	2	0	1 (4.1)
5	Massive bioturbated units	4	3	1 (5.1)
6	Tabular cross-stratification close to fracture	3	1	1 (6.1)
7	Through cross-stratified, rich in bioclasts	-	-	-
8	Relatively fine, rich in bioclasts	3	0	1 (8.1)
<b>Total</b>		29	8	7



(a) Core drilling process.



(b) Resulting cores.

**Figure 3.2** – The principle of drilling cores from samples, and the result when the cores were washed from drilling debris.

the porosity and permeability tests. From the trimmed parts of the cores, thin sections were made. A blue dye in the pores was used to enhance the detection of the pore space under a microscope. Table 3.1 summarises the amount of both horizontal plugs, vertical plugs and thin sections examined in this study. Figures 3.2a and 3.2b show the drilling process and the resulting cores.

The final quality of the plugs and thin sections was variable. Some (parts of) samples were not suitable for core drilling because of poor cementation between grains. In these cases, the hollow drill bit erodes too much of the surface of the plug, generating non-cylindrical plugs that are not suitable for tests on reservoir quality. Sample seven is an example where sub-sampling of plugs was not possible.

### 3.3 Reservoir properties

The link between a sedimentary facies and the behaviour as a hydrocarbon producing reservoir can be described with a number of parameters, including porosity and permeability.

*Porosity* is defined as the volume of open space (void space) as a fraction of the total volume of a piece of rock. The effective porosity is used to exclude any non-connected pores, or in other words, pores that do not contribute to the total amount of fluid that can potentially be extracted. For a porosity - permeability relation an effective porosity is preferred, as this represents the amount of pore space contributing to the flow through a porous medium (Dake, 1978). Porosity is measured as either a percentage or a fraction, and is therefore dimensionless. For calculation matters, a fraction to describe porosity is favourable, so this will be the unit used for porosity in this report.

*Permeability* is a parameter that describes the ability of a fluid to flow through a porous material. In the oil industry this refers to the flow of oil, gas or water through a reservoir rock. This parameter can then be used in for example Darcy's law to describe flow through a hydrocarbon bearing reservoir (Dake, 1978). Permeability is measured in square meters [ $\text{m}^2$ ], and is therefore a sort of representative cross-sectional area. Because permeability expressed in square meters leads to very small numbers it is more common to use darcy [D] - one darcy is  $10^{-12} \text{ m}^2$  - or in most cases even millidarcy.

#### 3.3.1 Porosity

Porosity can be estimated by using 1) an ultrapycnometer which measures the matrix volume; 2) the measurement of a saturated core submerged in water; or 3) thin section analysis. Using multiple measurement procedures has the advantage that a quality check can be done when comparing the results of different methods. For simplicity, only the results from the ultrapycnometer will be used — this gave the most accurate results — with a few quality-checks from other methods.

An ultrapycnometer uses a controlled volume of Helium gas to measure the matrix volume  $V_{ma}$  of a plug. The volume  $V$  of the sample container is reduced by the matrix volume when the core is placed inside the chamber. The volume of gas is exposed to isothermal expansion from pressure  $p_1$  to  $p_2$ , so the following equation can be applied:

$$(V - V_{ma})p_1 = (V - V_{ma} + \Delta V)p_2 \quad (3.1)$$

The chamber volume  $V$  is entered when calibrating the device. During the measurement procedure values of  $p_1$ ,  $p_2$  and  $\Delta V$  are recorded. The output consists of a series of matrix volumes and as a quality-check matrix densities (derived from the weight of the plug and  $V_{ma}$ ). Porosity can then finally be calculated

using:

$$\Phi = \frac{V_b - V_{ma}}{V_b} \quad (3.2)$$

In here, the bulk volume  $V_b = \frac{\pi}{4}D^2L_c$  is derived from the diameter and the length of the plugs, assuming a perfect cylinder. Multiple measurements of these dimensions reduced the possible errors.

### 3.3.2 Permeability

For samples with a permeability that reflect typical hydrocarbon-bearing rock — from  $\mathcal{O}$  few millidarcy up to  $\mathcal{O}$  two darcy — a Ruska gas- or liquid permeameter can be used (Wolf, 2010). Both methods measure flow rate and the pressure drop over the core. Together with the viscosity of the used fluid and the core dimensions, the permeability can be determined with Darcy’s law:

$$Q = -k \frac{\Delta p}{L_c} \frac{A_c}{\mu_w} \quad (3.3)$$

In here,  $k$  is the permeability [ $\text{m}^2$ ],  $\Delta p$  the pressure drop [Pa],  $L_c$  the length of the core [m],  $A_c$  the cross-sectional area of the core  $A_c = \frac{\pi}{4}D^2$  [ $\text{m}^2$ ] and  $\mu_w$  the viscosity of water [Pa s].

The Favignana samples, though, have a too high permeability to use this apparatus. A liquid permeameter uses a small reservoir with water, making it possible to let a fixed amount of water flow through a sample. Several canisters are available to vary the volume of the water to flow trough the samples. The largest canister available had a volume of 10 ml, and with only a very small pressure drop the time it took for this amount of water to be entirely pushed trough the sample was too short to accurately measure. First attempts to measure permeability with these permeameters resulted in values of  $\mathcal{O}$  tens of darcy. With a gas permeameter, it was not even possible to build up a high enough pressure drop over the core to obtain reliable measurements. Even with the highest possible rates, gas was flowing in such an unrestricted way that no pressure increase was observed in the upstream part of the apparatus.

In order to overcome the problems regarding the high permeability of the samples, an alternative set-up had to be created. An experimental set-up using a falling-head pressure differential was designed to eliminate the problem with the high pressure drop. The sample is fixed at the end a transparent PVC tube with a known diameter. An inner tyre of a bicycle placed around the sample restricted the flow only trough the core. The bottom end of the tube is placed in a large tank of water. Figure 3.3 gives a schematic overview of the set-up.

In order to perform the measurements, a vacuum pump is installed at the top. This serves two purposes: 1) it ensures that the core will be completely water-saturated; and 2) it will fill ensure that the tube is entirely filled with water. Appendix E.1 provides a detailed workflow with both the preparation of the

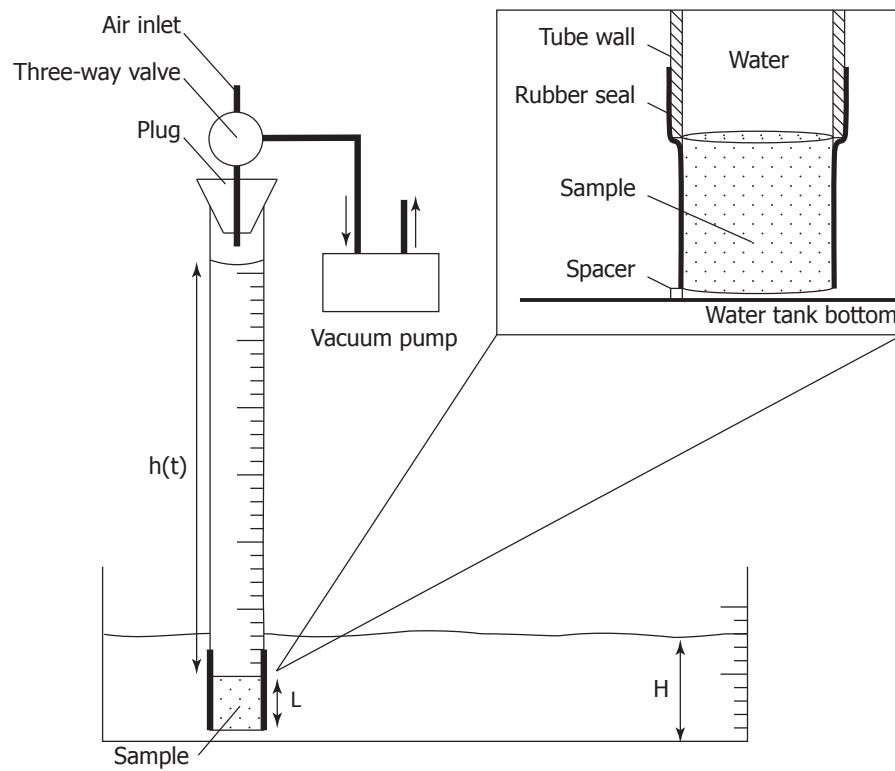
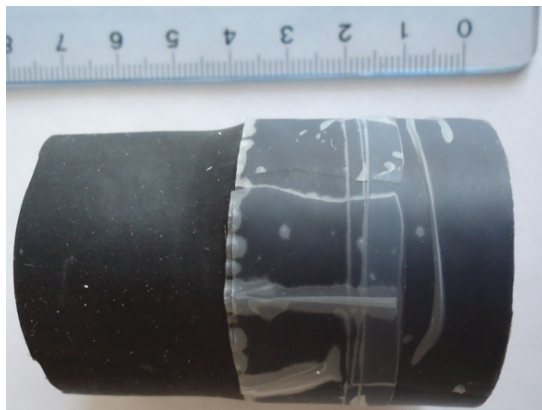


**Figure 3.3** – Schematic overview of the experimental set-up used for the permeability measurements.



(a) A prepared sample with its seal. Flow of water would in this case be from left to right.



(b) Cross-sectional view of a calcarenite sample.

**Figure 3.4** – Examples of a calcarenite plug prepared for permeability tests, including the rubber bicycle inner tyre that serves as a seal.

set-up and samples, and the actual implementation of the experiment. The basic principle is that after the tube is filled with water, a valve is opened at the top, causing the water level to drop. Time starts when the water reaches the one metre above the sample level, and at fixed intervals the intermediate times are recorded. This results in a time versus height plot for each sample.

Calculation of permeability from *time-vs.-height* plots, obtained by performing falling-head experiments requires some modification of Darcy's law. First of all, recapitulation of Darcy's law for flow through a core is

$$Q = -k \frac{\Delta p}{L_c} \frac{A_c}{\mu_w} \quad (3.4)$$

Application of the experimental set-up gives expressions for flow rate

$$Q(t) = \frac{dh A_t}{dt} \quad (3.5)$$

where  $A_t$  is the cross-sectional area of the tube [m<sup>2</sup>] and  $dh/dt$  the drop velocity of the water level in the tube, expressed in [m/s].

and pressure drop

$$\Delta p = \rho g (h(t) + L_c - H) \quad (3.6)$$

In here,  $\rho$  is the density of the water [kg/m<sup>3</sup>],  $h(t)$  the water level in the tube as function of time [m],  $L_c$  the length of the core [m] and  $H$  the water level in the large tank [m], where the size of the tank allows for the assumption of a constant water level in this tank.

Substitution of equations (3.5) and (3.6) into equation (3.4) leads to

$$\frac{dh A_t}{dt} = -k \frac{\rho g (h(t) + L_c - H)}{L_c} \frac{A_c}{\mu_w} \quad (3.7)$$

Reworking the equation makes it possible to integrate on both sides

$$\int \frac{dh}{h + L_c - H} = - \int k C dt \quad (3.8)$$

where the constant term is written as  $C = \frac{\rho g A_c}{L_c \mu A_t}$ , expressed in [1/m<sup>2</sup>s].

Now, integration with the necessary start condition for the left-hand term defined as  $t=0: h=h_0=1$  m leads to

$$\ln |h + L_c - H| - \ln |h_0 + L_c - H| = -k C t \quad (3.9)$$

By plotting the left-hand term against  $t$ , the slope of the line will be determined by the permeability  $k$  multiplied by  $C$ . Examples of some results of the falling head experiments are discussed in the results (figures 4.14a and 4.14b).

### **3.4 3D Geological modelling**

The three-dimensional geological model of eastern Favignana is made using the Petrel software package from Schlumberger. The integration from seismic evaluation to dynamic modelling makes it useful for a variety of applications, including the creation of static and dynamic models from well data. In this study the topography of Favignana is available as digital AutoCAD data, which is subsequently exported to a format suitable for Petrel (see tutorial in appendix E). The outcrop data from the fieldwork campaign is converted in pseudo-wells, which are placed at the correct location with GPS data. Finally, the facies model is generated using a multi-point statistics algorithm that uses the pseudo-well data and additional geological thoughts as input. Chapter 6 discusses the entire modelling process in more detail.

## 4 Favignana calcarenite

This chapter provides the results of the fieldwork and the subsequent data analysis and experiments. Some background on sedimentary structures and how they fit into the context of the Favignana calcarenite will be discussed first. Then the micro- and macrofacies definition and description are presented. Finally, the experimental results regarding reservoir properties complete this chapter.

### 4.1 Background

The primary sedimentary structure is a very important characteristic when trying to reconstruct the depositional environment of a sedimentary rock succession. Depending on the type of material and the energy that was present in the system, various flow regimes can develop. Figure 4.1 shows the grain size and flow velocity versus the sedimentary structures that can form when sediment is deposited due to a unidirectional flow of water under given conditions. The x-axis represents the mean grain size of the sediment that is subjected this flow, while the y-axis represents the Froude number ( $Fr$ ). This is a dimensionless number, defined as  $Fr = U/\sqrt{gd}$ , where  $U$  is the mean flow velocity [m/s],  $g$  the gravitational constant [m/s<sup>2</sup>] and  $d$  the mean flow depth [m]. This equation corresponds to the ratio of the flow velocity and the velocity of a stationary wave inside that same flow. When  $Fr < 1$ , the wave velocity is greater than the flow velocity, allowing waves to travel upstream. A Froude number of  $Fr > 1$  represents supercritical flow conditions, where the flow velocity exceeds the wave velocity (Leeder, 1999).

When velocities are too small to move sediment, there will be no layering that is caused by the transport mechanism of sediment. The absence of layering however does not imply that no sedimentation takes place. Very large sedimentation rates that need a significant amount of energy still will not develop clear lamination. In the case of Favignana it might as well be possible to have material deposited in-situ, because it concerns the remains of living material. As velocity increases sediment will be transported on the sea floor, causing a parallel lamination. No disruptions should be present, because this can cause turbulence, and therefore ripples. An even higher Froude number yields the formation of dunes; first with a linear crest, changing to an undulating crest with increasing energy. For smaller grain sizes an upper plane bed will form at high velocity conditions. The formation of this bedform is then associated with the erosion of existing structures because of its higher energy, but is not supercritical yet. Because of the

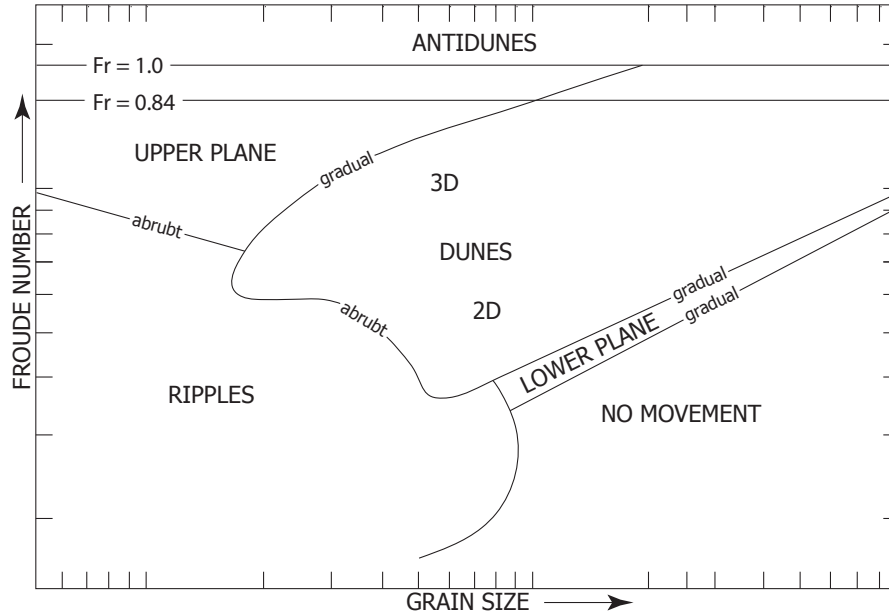


**Figure 4.1** – Bed geometries as function of the grain size on the horizontal axis, and the mean flow velocity on the vertical axis. Both axes are logarithmic, and scale of the axes has been left out to emphasise the relative position of the flow regimes without exact numbers. Plot has been modified after Southard & Boguchwal (1990).

high energy and the supercritical flow conditions undulated beds and antidunes can form. Antidunes are associated with a high degree of erosion, and are therefore generally not often well preserved. A typical phenomenon related to the formation of giant ripples and the transition to supercritical flow conditions is a scour and fill system.

## 4.2 Sedimentary microfacies

The thin sections from a selected number of samples were examined with a microscope in order to describe the microfacies of the Favignana calcarenite. Unlike the macrofacies, showing distinct differences in sedimentary structures, the microfacies focusses more on the fossil content of the samples. Therefore, this section gives an overview of the most common types of fossils found in the samples and in the field. The vast majority — around 80 % — of the calcarenite matrix is made up from three types of organisms. In order of abundance, bryozoans, red algae and foraminifera are the most common.

### 4.2.1 Foramol

In the industry and literature the bioclastic calcarenite as observed on Favignana is also known as *foramol*. One of the first descriptions of foramol is given by Lees & Buller (1972), who defined two main types of carbonates. The foramol differs from the chlorozoan with an abundance of animal matter, and except for



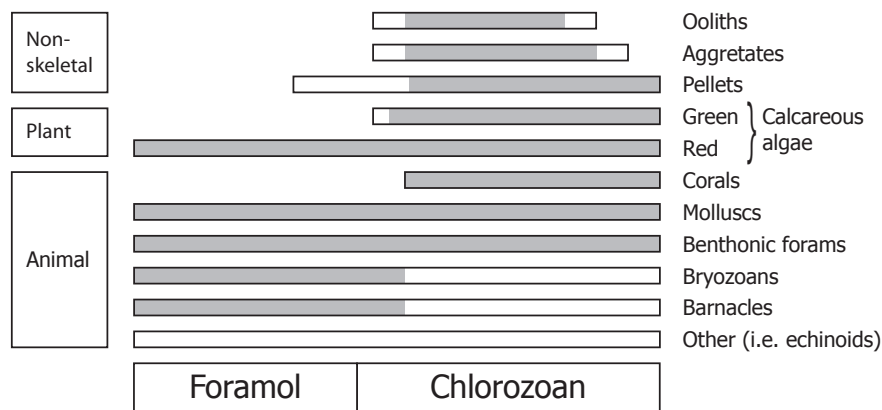


**Figure 4.2** – Classification of carbonate grain types by Lees & Buller (1972). The grey parts illustrates importance or dominance.

red algae almost no non-skeletal and vegetal particles. The classification is illustrated in figure 4.2.

Simone & Carannante (1988) describe the temperate platforms that are associated with foramol. Unlike chlorozoan carbonates foramol is believed to be deposited in temperate environments. A relation between different water depths and fossil types is given, reaching from sea meadow and molluscs at shallower depths to algae, bryozoans and forams in deeper parts. Because of the temperate nature of foramol platforms, they usually can not keep up with a sea level rise — like tropical platforms do — and will eventually drown.

Reefs in both tropical and non-tropical regions have a significant contribution from carbonate sediments (Carannante et al., 1988). Rhodalgal sediments — consisting of encrusting coralline algae and bryozoans — are mainly found on temperate shelves, however a study of several both modern and ancient foramol platforms in southeast Asia and Australia by Wilson & Vescei (2005) supports the presence of foramol platforms in tropical regions.

#### 4.2.2 Fossil content

As seen in the previous section, fossil content of a calcarenite can give indications of its origin. The results of the analysis of the thin sections in cooperation with Dr. X. Marquez are given below. Flügel (2010) is consulted for information on the type of fossils.

##### Bryozoans

Bryozoans, also known as moss animals, are a type of small invertebrate ('without a backbone') animals that feed themselves by sieving food using a network of tentacles. Almost all bryozoans form colonies. Figure 4.3a shows an example of a common types of bryozoans as seen in the thin sections.

## Red algae

This type of algae (figure 4.3b) is an important builder of carbonate reefs or platforms. Red algae appearance can be dated back to Cambrian period. In the form of Rhodoliths they can be quite abundant. This special occurrence of red algae is discussed somewhat later in this section.

## Foraminifera

Foraminifera are uni-cell organisms of generally less than one millimetre in size, which can be made of  $\text{CaCO}_3$  or agglutinated particles from the substrate. Several hundreds of thousands of species are known, and they can be split up in two main types. *Benthic* foraminifera live on the sea floor, however larger species need to be in the photic zone in order to survive. Therefore the presence of these type of foraminifera can possibly indicate a shallow sedimentary environment. *Planktonic* foraminifera are suspended in the water column during their life. They are possible indicators of more deep marine environments. The Favignana calcarenite contains approximately twice as much benthic as planktonic forams. Figures 4.3c and 4.3d show examples of both types.

## Rhodoliths

Rhodoliths are a group of coralline red algae that live in the benthic zone, drifting over the sea floor forming sphere shaped structures. Figures 4.4a and 4.4b show respectively a close up of a rhodolith encapsulating a particle and a collection of rhodoliths in calcarenite.

## Molluscs

Molluscs are invertebrate animals, in some cases showing an external skeleton. In the outcrops of Favignana they are represented in the form of bivalve shells, mostly pelecypods and scallops (figure 4.4c), and occasionally in the form of pinna (figure 4.4d) or oyster shells (figure 4.5b). Preservation is generally good, and makes it easy to find almost intact clams in outcrops. In thin sections fragments are observed, as figure 4.3e illustrates.

## Echinoids

Echinoids are sea urchins, featuring a crest of several centimetres in diameter generally covered with numerous spines. In some cases the whole skeleton is preserved — for example in figures 4.4e and 4.4f — showing the typical fivefold symmetry. On the top of the skeleton, five equal parts are radiating out to the sides. In addition, fragments of both the skeleton and the spines are observed in thin sections (figure 4.3e).

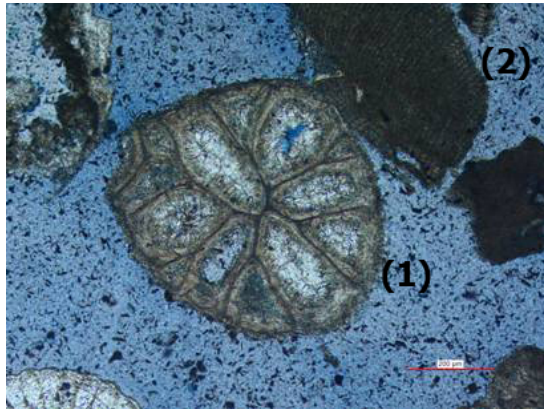
## **Shark tooth**

In one occasion, the calcarenite contained a tooth, which was later interpreted as most likely originating from a shark (figure 4.5c). Because the sedimentary facies (scour infill, see later) of the sediment containing this remain, the tooth could have been transported over significant distances.

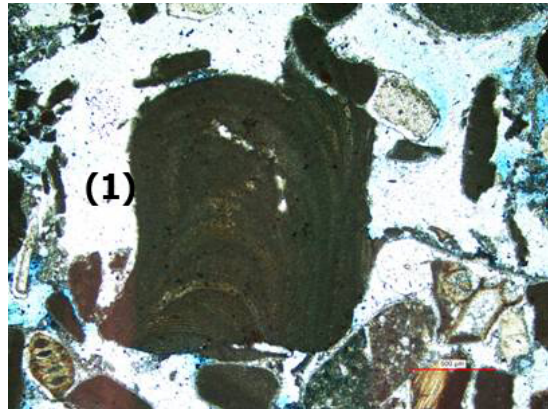
### **4.2.3 Diagenesis**

Diagenesis is defined as any chemical, physical or biological change that a sediment faces at elevated temperature and pressure after it was deposited (Tucker & Wright, 1990). In carbonates, the two most important diagenetical features are dissolution and cementation, mainly because they have huge impact on the reservoir quality of such rocks. Figures 4.3e and 4.3f show typical parts of a thin section made from the Favignana calcarenite. The cement is clearly visible, and analysis indicated that this is a syntaxial rim type of cementation (X. Marquez, personal communication). It forms a rather small layer of constant thickness around the grains. Syntaxial rim cement is typically created by marine processes, giving more indications regarding the depositional environment. Cementation is not extensive, and did not clog pores or pore throats. Because of the poor quality of the thin sections, they most likely do not represent the real distribution of grains. However, it is not likely that cementation influences pore geometry significantly, given the high porosity, grain size and small cement thickness.

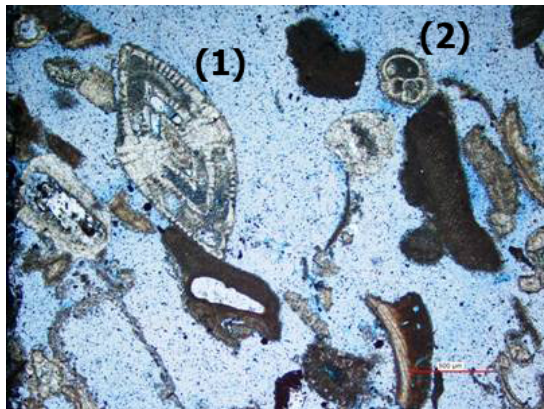
Bioturbation is technically not a form of diagenesis, however since it involves sediment reworking as well, so the phenomenon is introduced here. In figures 4.5e and 4.5f some burrows as observed in Cala Azzurra are shown. This micro- and macrofacies analysis describes the bioturbation as a macrofacies effect, therefore it will be discussed in more detail in the next section.



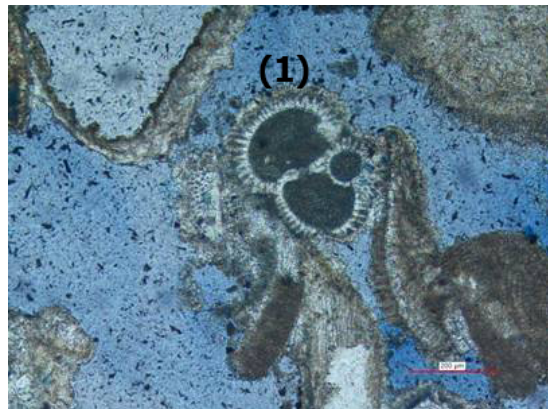
(a) Bryozoans (1) and some fragments of red algae (2). Magnification 10x.



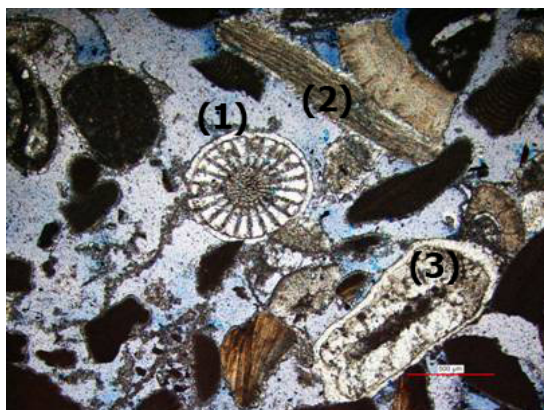
(b) Red algae (1). Magnification 4x.



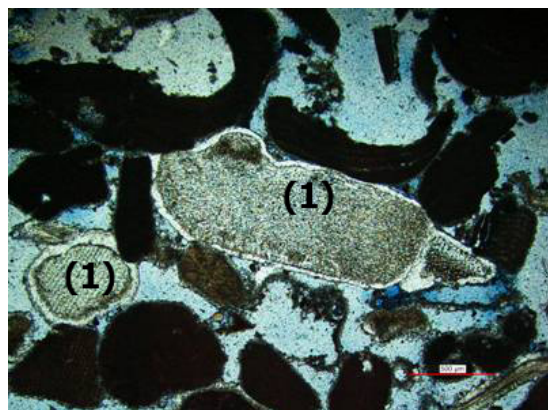
(c) Benthic (1) and planktonic (2) foraminifera. Magnification 4x.



(d) Planktonic foraminifera (1). Magnification 10x.



(e) Echinoderm spine (1), mollusk fragment (2) and syntaxial cementation (3). Magnification 4x.



(f) Syntaxial cementation developed around fragments (1). Magnification 4x.

**Figure 4.3** – Thin section examples showing fossil content and diagenetic processes. The size of the red scale bar is respectively 500  $\mu\text{m}$  and 200  $\mu\text{m}$  for the 10x and 4x magnifications. Abrasion due to the creation of thin sections may have changed the original grain orientations. Images and interpretation courtesy of Dr. X. Marquez.





(a) Rhodolith in massive calcarenite where a shell fragment is visible in the core.



(b) Several rhodoliths 'floating' in the calcarenite matrix. Lens cap for scale.



(c) Intact pecten shells with hammer tip for scale.



(d) Fragmented parts of pinna molluscs.



(e) Cross-section of an echinoid skeleton.



(f) Almost intact skeleton of an echinoid, partially squeezed due to sediment compaction.

**Figure 4.4** – Examples of fossils as observed in the field. Unless indicated otherwise, hand lenses for scale.





(a) Byozoan branch revealing internal structure. Hand lense for scale.



(b) Large oyster shell. Hand lense for scale.



(c) Shark tooth found inland of the Bue Marino area. Scale in centimetres.



(d) Bivalve shell of approximately 3 cm in size.



(e) Burrows in a bioturbated part of Cala Azzurra.



(f) Close-up of a large vertical burrow.

**Figure 4.5** – More examples of fossils as observed in the field.

## 4.3 Sedimentary macrofacies

*"A sedimentary facies is a body of rock with specified characteristics"* (Reading, 1996).

This section describes the different macrofacies as observed in the fieldwork area. The facies are distinguished by properties like lithology, sedimentary structure, and the presence of bioclastic material — either in preserved or fragmented state. The Favignana bioclastic sands show sedimentary structures of variable nature, which will be the most important characteristic in the macrofacies distinction. In general, the Upper Pliocene to Lower Pleistocene deposits found on the eastern part of Favignana consist of coarse grained fragments of bioclastic material, and internal differences are not very well pronounced on the rock face.

Each facies has been interpreted as being formed under specific sedimentary conditions, from which sediment supply and the amount of associated energy can be derived. Table C.1 in appendix C summarises the facies as recognised in the field, of which the interpretation given will be used to establish the conceptual geological model.

### 4.3.1 Massive calcarenite

#### Description

Well sorted calcarenite, generally showing a large amount of non-fragmented fossils like urchin shells, molluscs, foraminifera and bryozoa. Figures 4.7a and 4.7b show examples from the field. Grain size varies between 0.5 and 2 mm, with occasionally rhodoliths up to 4 centimetres in diameter floating in the matrix. Sedimentary structures are generally absent in these deposits, however some faint lamination can be seen. Such hardly visible lamination can be partly caused by the alignment of rhodoliths or other fossils. The most typical location where this facies is observed is the northern end of Punta San Vituzzo, where it can reach a visible thickness of over three metres.

#### Interpretation

The massive deposits must have been most likely associated with a very fast sedimentation rate. This is the only way of preventing the development of internal sedimentary structures. The occurrence of large fossils like rhodoliths floating in the matrix is also consistent with a very fast sedimentation process. A slower sedimentation would allow a better sorting. In order to achieve this amount of sedimentation, the system must have been 1) facing a very high sediment supply; and therefore also be 2) subjected to a high amount of energy to transport the particles.

There are some similarities with the scour fills that are described somewhat later in this section, because they show similar properties. The difference is the shape of the bodies. The facies in this section forms more laterally continuous bodies, while the latter is characterised by more lateral variability.

### 4.3.2 Parallel laminated units

#### Description

Straight parallel laminated beds consisting of relatively fine grained material, which is illustrated by figure C.1 in appendix C. Laminae thickness varies from a few to 15 centimetres. A relatively low amount of preserved fossil content is observed within these deposits. The southwestern part of Cala Rossa shows significant units that have parallel laminated bedding.

#### Interpretation

The parallel lamination can develop in two totally different types of energetic environments. On one side, the lower flow regime beds can form parallel lamination, with the tendency to form ripples or dunes when energy increases. On the other side, this type of lamination can be formed by a high energy upper flow regime. In this case existing dunes will be eroded, so a flat surface will remain to accommodate other sediment. An increase in energy would potentially become supercritical and will have the possibility to form antidunes or a scour system.

Outcrop data reveals that stratigraphically the parallel laminated units are in proximity to other low energetic deposits. For example, most of the outcrops near Cala Rossa show a distinct upward trend. Starting with massive homogeneous layers, the structure changes to parallel lamination. On top of that, dunes start to form. This might indicate that the parallel laminations are developed in a transition stage between no visible lamination and the formation of ripples or dunes.

### 4.3.3 Undulated lamination and scour fills

Both the *undulated lamination* and the *scour fill* facies are described in a single section, as they are in some cases strongly interrelated.

#### Description

The undulated lamination shows sinusoidal behaviour, with wavelengths of order of magnitude one to two metres. They often erode the lower structures, creating an inter-cutting system. Two different scales of scour fills are observed. The first type consists of very large — up to 20 metres thick — scour fills, mainly located in the area around Scala Cavallo and further south. The second type of fill is deposited in



the lower parts of the undulated structures. Both scour fills generally show the same sedimentological characteristics with a higher concentration of coarser grains and rhodoliths at the bottom, and a fining upward trend. Lamination is absent, making the scour fills displaying as a massive and structureless facies.

### **Interpretation**

The large scours are interpreted as eroded channels that incised the previously deposited calcarenite. After that they were filled with massive deposits. Both the undulated lamination and smaller scour fills are interpreted as *scour and fill system*. Undulated features are created in the transition between the upper flow regime parallel lamination and the antidune bedforms, i.e. in high Froude number conditions. If the energy increases even more, flow might become supercritical. The combination of bed load transport and gravity effects causes the depositional system to erode itself, creating the scours. As a consequence of the increased energy a hydraulic jump is likely formed. The eroded and transported sediments are subsequently deposited in the scour, generating the fining upward sequence observed in the outcrops.

## **4.3.4 Tabular cross-stratification**

### **Description**

These deposits consist of up to two metre thick tabular cross bedded calcarenite bodies (figures 4.8c and 4.8d). Some foresets tend to onlap on their base, while others make a sharper angle. Another important feature in some outcrops is the show cyclic behaviour regarding the deposition of laminae.

### **Interpretation**

The large scale cross laminated bodies are interpreted as sub-tidal prograding dunes of fragmented bioclastic material, with relatively low-energy conditions which would allow the preservation of a linear dune crest (figures 4.1 and 4.6a). Palaeo-transport occurred in the direction of the highest dip angle, corresponding to the foreset of a dune. The typical transport direction for these dunes as observed in the field was south-southeast (figure 4.12).

## **4.3.5 Large scale foresets**

### **Description**

This type of sedimentary structure shows up to five metres high tangential-shaped dune foresets, with a laminae thickness of on average 25 centimetres. The length of the foreset — of which probably only the

toe is visible in the outcrops — can be up to 15 metres.

### **Interpretation**

As the name of the facies suggests, these deposits are interpreted as large — most likely isolated and storm-related — prograding dunes. Outcrop data analysis shows that the crest of these dunes is parallel to the Sicilian shoreline. The fact that no separate beds are present suggests that no interruption in the amount of energy and/or sediment supply occurred — indicating a relatively steady depositional environment without much variation.

#### **4.3.6 Trough cross-stratified units**

##### **Description**

These deposits consist up to several metres thick trough cross bedded bioclastic sands, with beds of typically 10 to 40 cm thick. Locally a large amount of semi-broken bioclastic material is present, especially at the base of a bed. This facies is dominating in several areas, such as the eastern part of Cala Rossa and the outcrops of Bue Marino.

##### **Interpretation**

A higher energy supply to the system than in the case of dunes with a linear crest, implying higher Froude numbers, induce a prograding dune to form an undulated crest. Troughs are forming in the concave parts of the lee side of the dune. The undulating character causes these dunes to erode each other much faster than a linear-type of dune — thick tabular foresets will not be able to develop — resulting in bed thickness that differs significantly from the tabular dunes. A possible explanation for this observation might be found in the increase in energy and the constant undulating crest, which partly erodes an earlier deposited dune. The result is a system of intersecting troughs, showing a more chaotic architecture. Figure 4.6b illustrates the geometry of such a dune system, including the appearance of so called 'troughs' that are clearly visible on outcrop walls perpendicular to the main transport direction.

#### **4.3.7 Massive bioturbated units**

##### **Description**

The massive bioturbated units on Favignana show extensive burrowing, in some cases completely obliterating the original sedimentary structure, while in other cases some bedding might still be visible. Burrows can be both vertical and horizontal. The southern part of Favignana shows the most extensive

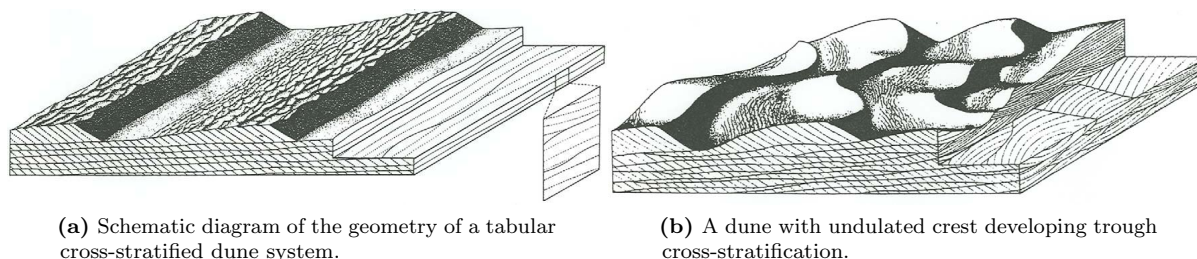


**Figure 4.6** – Two main types of cross-lamination as observed on Favignana. Note the difference in geometry visible on the cross section perpendicular to the main flow direction. See also figure 4.1 for flow regimes. Figure courtesy of Southard (1996).

burrowing, especially parts of Cala Azzurra, the south coast and Punta Lunga. The latter shows large networks of burrows up to five centimetres in diameter (figure 4.9d)

## Interpretation

Bioturbation is sediment reworking by any living organisms, either flora or fauna. They can create extensive systems of burrows. Depending on the degree of bioturbation, the primary sedimentary structures may be entirely destroyed. The effect of burrowing can on one side homogenise an initially heterogeneous unit, mixing particles of different size and composition. On the other hand, an initially homogeneous layer can be mixed up because burrowing reworks sediment and aligns them in a preferred orientation. Regarding reservoir connectivity, bioturbation can potentially interrupt continuity of shale layers, improving the overall vertical fluid communication. Bioturbation is an indicator for 1) a string decrease in sedimentation; and 2) a relatively calm palaeo-environment. A too high energy does not allow the organisms to develop a system of burrows, because the youngest layer of sediment — where most of the nutritious material is present — will be constantly reworked or buried.

### 4.3.8 Clay

#### Description

A sharp contrast in grain size is observed between the calcarenite and the stratigraphically lower clays in some outcrops (4.9e). The clay is a yellowish to grey structureless unit, of which the base is not observed in the field. The contact between the clay and the calcarenite locally shows a dark layer which is interpreted as an iron and manganese mineralisation band (visible in figure 4.9f).

## Interpretation

Abate et al. (1997); D'Angelo et al. (2005) interpreted the clay as the Trubi formation, that can be found on several locations around the Mediterranean. It is commonly found on the mainland of Sicily and is assumed to be deposited in a calm marine environment in the middle to late Pliocene — the Zanclean stage (Couvering (van) et al., 2000). Because the Trubi clay dates from the Upper Pliocene and the Favignana calcarenite from the Lower Pleistocene, the Plio- Pleistocene boundary on Favignana is defined at the contact between the clay and the calcarenite. This is observed at three main locations in the fieldwork area: 1) at the lowest part of eastern Cala Rossa, see figure 4.9e; 2) beneath the large foresets in the northern part of Cala Azzurra; and 3) below the calcarenite of the western part of Cala Azzurra, shown in figure 4.9f.



(a) Massive unit with vertical fracture. Book for scale.



(b) Punta San Vituzzo with massive calcarenite and Levanzo in the background. Note the horizontal marks made by the quarrying equipment.



(c) Parallel lamination in the southwestern part of Cala Rossa. Ruler is ca. two metres high.



(d) Parallel lamination, overlain by bioturbated calcarenite, just east of the Cala Rossa bay. Section approx. two metres thick.



(e) Undulated lamination and low angle parallel lamination. Section is ca. two metres high.



(f) Undulation in the Bue Marino area. The SE part of panel B.4, exposing a wall of ca. eight metres high.

**Figure 4.7** – Field examples of sedimentary structures outcropping in eastern Favignana. The photographs illustrate massive calcarenites and parallel- and undulated lamination.





(a) Homogeneous scour fill showing a large quantity of bioclasts at the bottom. Erosion by wind formed the protruding banks. Ruler is four metres long.



(b) Scour fill in the San Francesco quarry, in the southern part of Favignana town. The wall is two metres high.



(c) Tabular cross-stratification. Thickness of each bed is ca. one metre.



(d) Bottom part of this section in Bue Marino shows tabular cross stratification. Ruler of approx. two metres for scale.



(e) Large foresets forming a bed of approx. eight metres thick in the Scala Cavallo cliff.



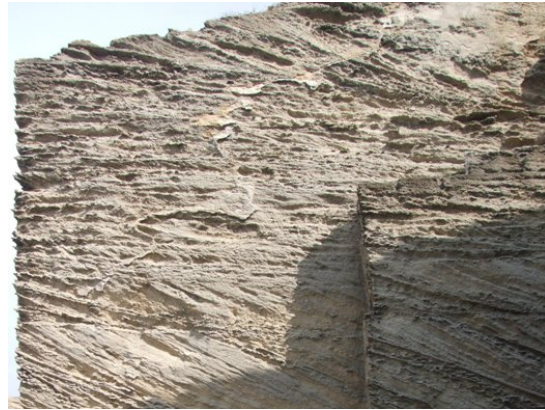
(f) Situation in the northern part of Cala Azurra, showing large foresets up to six metres high.

**Figure 4.8** – Field examples of scour fills, tabular cross-stratification and large foresets.





(a) Trough cross-stratification looking in the orientation of the transport direction. Thickness of sequence ca. two metres.



(b) Approximately three metres thick unit showing trough cross-stratification (Cala Rossa bay).



(c) Inclined beds of Cala Azzurra showing almost vertical burrows caused by bioturbation. Book for scale.



(d) Extensive bioturbated level on the Punta Lunga peninsula with locally large burrows. Book for scale.



(e) The massive grey clays — interpreted as the Trubi Formation — in Cala Rossa. The contact with the calcarenite is well visible. Book for scale.



(f) The contact between underlying clays and extensively bioturbated calcarenite at the western part of Cala Azzurra. The visible part of the clay is ca. 30 cm thick.

**Figure 4.9** – Field examples of trough cross-stratification, bioturbation and the (Trubi) clay.

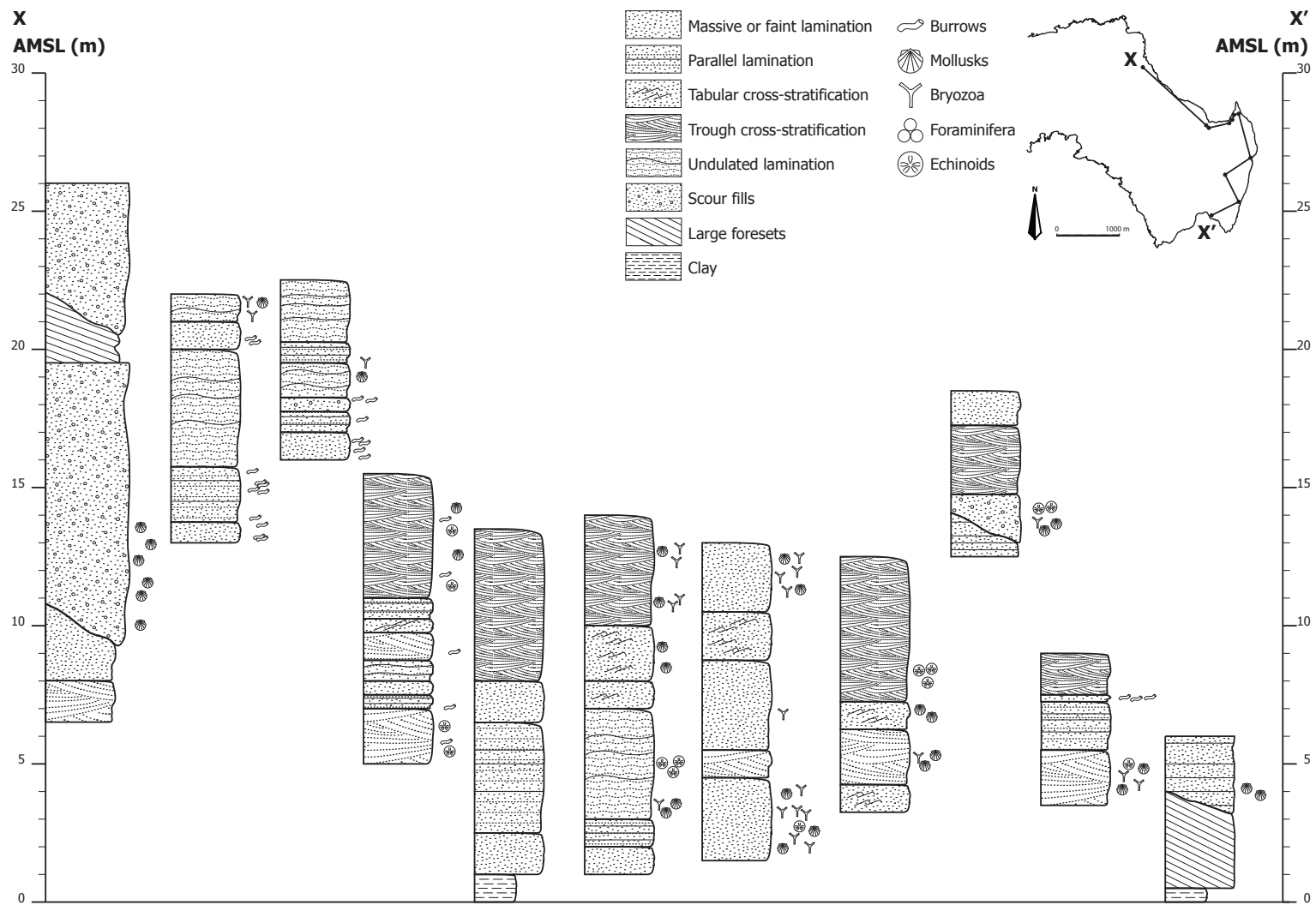


**Figure 4.10** – Sedimentary logs from fieldwork at eleven pseudo-well locations, which are illustrated in the map. Well spacing varies significantly and is therefore not to scale.



## 4.4 Stratigraphic logs and facies distribution

The micro- and macrofacies together with stratigraphic logs have been combined and the result is shown in figure 4.10, which represents a panel crossing through the eastern part of Favignana. A correction for elevation is applied, making it easier to correlate various depositional environments across the logs. The logs show primary sedimentary structures, fossil content, and an attempt to illustrate grain size variation. These data were then used to establish a conceptual geological model by correlating the logs as the basis for a 3D facies distribution.

A different way of visualising the fieldwork results is a map with pie charts (figure 4.11). Each pie chart shows the relative distribution of facies at a particular pseudo-well location. In order to distinguish larger outcrops from smaller ones, the pie charts are scaled to the thickness of the outcrop where the measurements were taken. Unlike the detailed stratigraphic logs presented earlier, all fieldwork locations are included (see figure D.1 in appendix D), so observations from a distance and photographs are presented here as well. Again, the map will be useful in a later stage when the conceptual model is created.

## 4.5 Palaeo-transport directions

Orientations of foresets, propagating dune beds, undulations and scour geometry are all indicators of the direction of the flow that deposited such structures. Other sedimentary structures, like as massive beds or parallel lamination makes extracting palaeo-directions difficult. Where possible, palaeotransport directions were obtained in the field (figure 4.12). This information can be useful when establishing a conceptual geological model of the Favignana calcarenite.

Two main transport directions can be inferred from the data. The main system seems to build out to the southeast, while there is a secondary main direction to the south-southeast. These directions are good indicators when revealing the sedimentary history of the island. Moreover, the data indicate that the eastern part of Favignana can be split up in roughly two regions with their own characteristic palaeo-transport directions. The majority of the island — from Favignana town to Cala Azzurra — shows a dominant direction to the southeast. A considerably smaller part, concentrated around Cala Rossa and Bue Marino, has recorded transport to the south.

To a minor extent other transport directions are found, especially in the eastern part of the fieldwork area. They are indicated with the smaller arrows and show transport to — on average — the north.

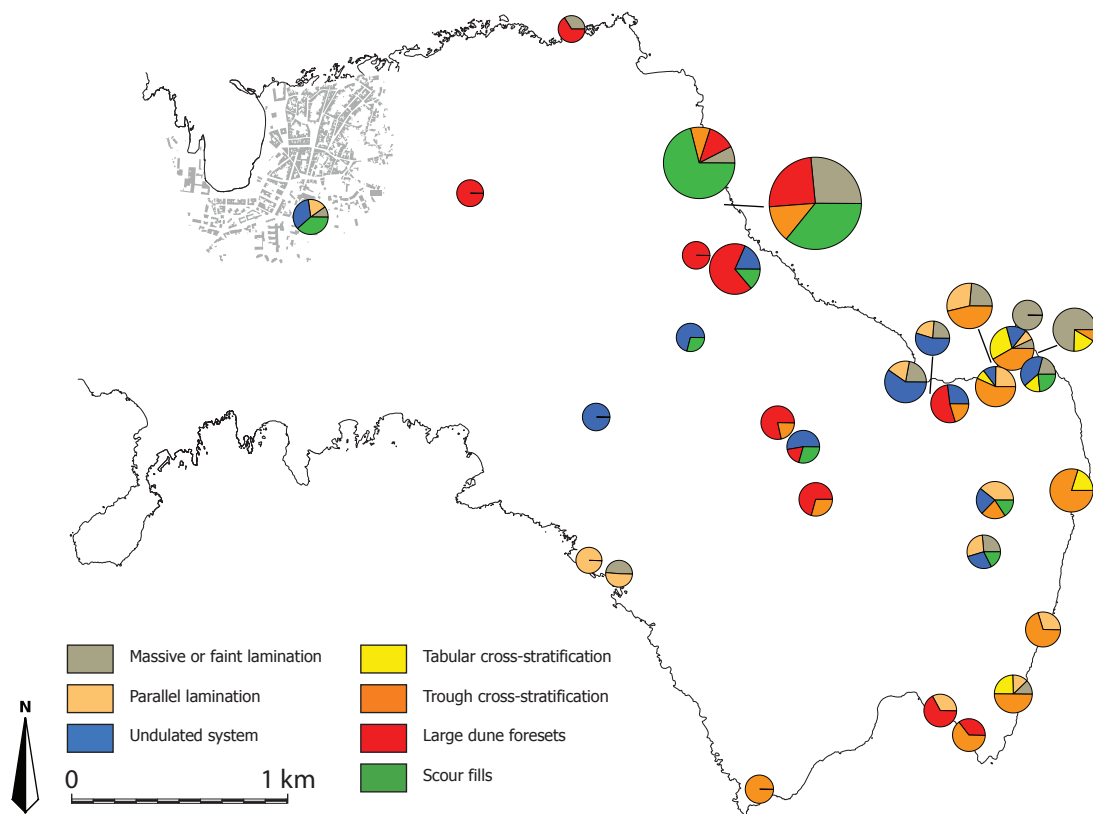


**Figure 4.11** – Pie chart data obtained from field observations and facies assemblage.

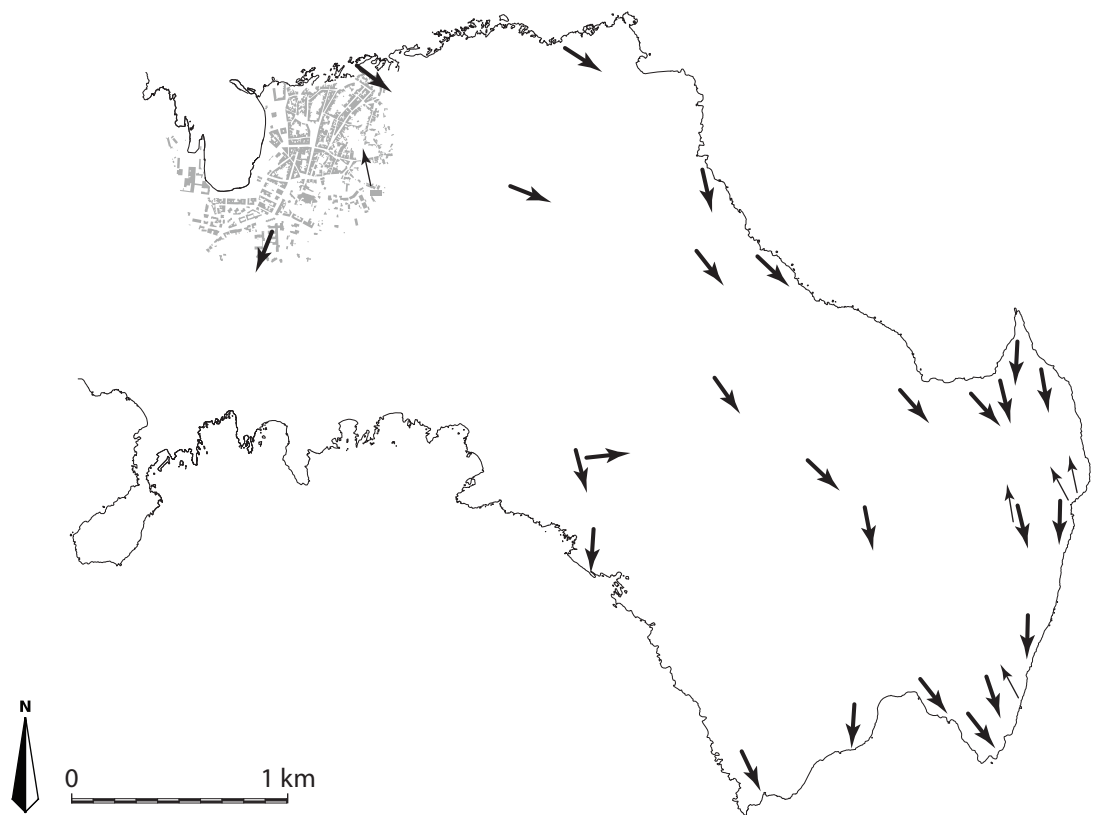


**Figure 4.12** – Overview of palaeo-transport directions as observed in the field.

## 4.6 Reservoir properties

This section presents the results of the laboratory tests described in section 3.3. Table C.2 in appendix C provides a general overview of the reservoir properties, and figure 4.13 illustrates the porosity-permeability correlation with the results from the samples.

### 4.6.1 Porosity

The porosity of the Favignana calcarenite is approximately between 0.45 and 0.65, thus showing extremely prolific values, when compared to typical hydrocarbon reservoir properties (Flügel, 2010). Lowest porosities can be found in the massive calcarenites, but even those values are rather high with a fraction of 0.45 or higher. The most porous samples originate from the parallel laminated unit (up to 0.65), which is striking because thin section analysis points out that these samples are relatively fine grained. Because almost no dissolution or extensive cementation has taken place all porosity is intergranular. Because the low degree of diagenesis, secondary types of porosity that are common in subsurface carbonate reservoirs — like vuggy or intragranular — are not observed.

### 4.6.2 Permeability

All the results of the permeability laboratory experiments described in section 3.3.2 are presented table C.2 and figure 4.13. For two samples, the resulting time versus height plots are displayed in figure 4.14a. This plot confirms the repeatability of the experiments, as the two different measurements match reasonably.

As expected from the porosity results, also the permeability values are high — between 20 and 100 darcy — compared to subsurface reservoir properties. Permeabilities of tens of darcy generally do not occur in the deep subsurface. The fact that the Favignana calcarenite has not been buried several kilometres deep can explain this highly permeable sedimentary rock.

In contradiction to the porosity results, the variation of permeability is less dependent on the origin of the samples. Values of tens of darcy occur for most of the samples, with an exception for some cross-laminated units. These tests resulted in abnormal values of up to 320 D, which might be caused by the bad sample quality. Section 7.2 discusses this problem.

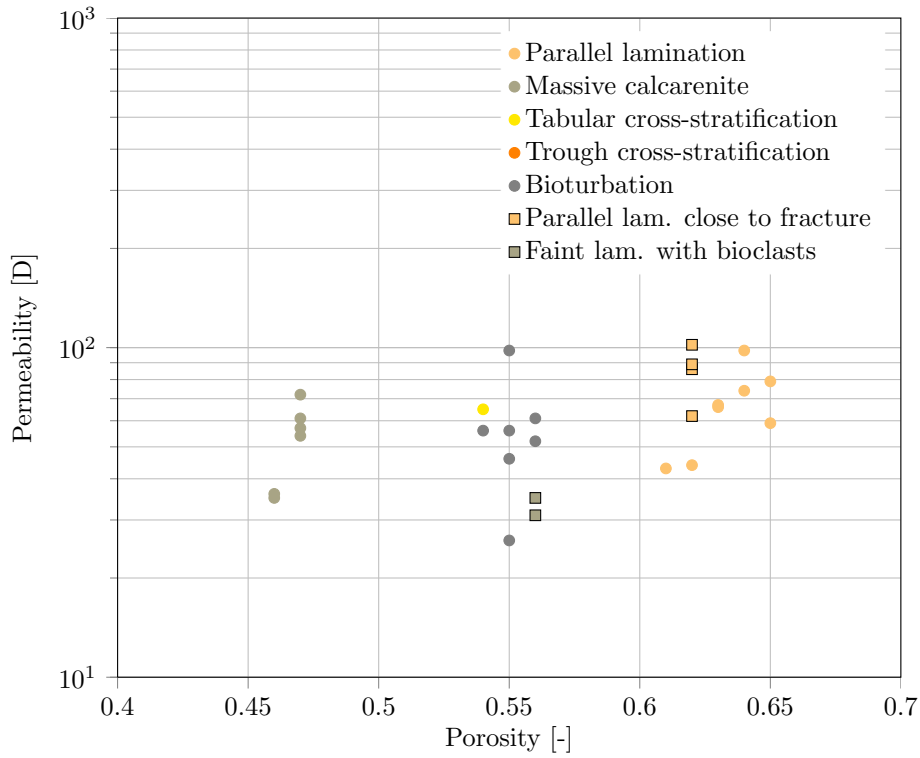


**Figure 4.13** – Cross plot showing porosity versus permeability obtained from core analysis of the samples. Sections 3.3.1 and 3.3.2 describe the laboratory experiments.

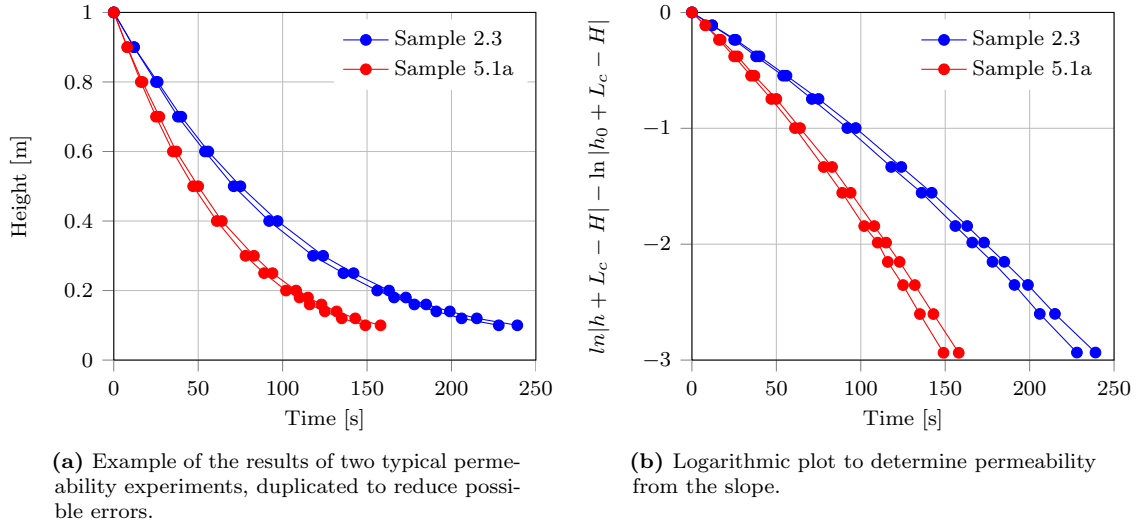


**Figure 4.14** – Experimental results of the permeability tests on samples. Figure 4.14a shows the direct results, and in figure 4.14b the results are plotted in such a way the permeability can easily be derived from the slope of the lines. Section 3.3.2 explains the principles of this method. Sample 2.3 yield with a permeability of 35 D, while sample 5.1a — showing a steeper slope — has a higher permeability of 56 D.

## 5 Conceptual geological model

The conceptual geological model of the Favignana calcarenite is an attempt to combine all interpreted sedimentary facies and their vertical and lateral distribution by placing them in a specific sedimentary environment. First, the sediment supply mechanism will be discussed, followed by the transport mechanism and finally the sedimentation processes. The aim is to present an overall schematic model of where, how and in what geometry the calcarenite is deposited. This will be used to as the basis to build a three-dimensional sedimentary model of eastern Favignana.

### 5.1 Sediment supply

The sedimentary structures show a predominant transport direction of southeast to south-southwest — corresponding to the 140 to 210 compass degrees. Structures in both directions indicate that flow was reversed from time to time. Given the amount of fragmentation of the bioclastic material, it is clear that it must be either transported from the place it was generated, or reworked extensively.

Assuming that the sediment is generated somewhere north of Favignana, a location must have been present where vast amounts of living material could develop. Other studies indicate that similar deposits are cool-water biocalcarenes (Massari & Chiocci, 2006; Hansen, 1999). The investigation of thin sections — described earlier in this report — points in the direction of cool-water carbonates as well (X. Marquez, personal communication). These carbonates were able to flourish in the relatively temperate Mediterranean of the Pleistocene, however the dependence of sunlight limits the water depth in which they can develop. Figure 5.1 shows the Aegadian archipelago and the location with respect to the Sicilian mainland. The present-day shelf edge is marked with the dashed line. According to Cohen & Gibbard (2010) the Lower Pleistocene sea level was relatively high, and started to fall without large disruptions. Therefore the location of the shelf edge is assumed to be not too far from the present day situation.

The production platforms of cool water carbonates probably have been located on the continental shelf. Figure 5.1 indicates some possible locations of the platform that provided a breeding place for living material. Geological investigation showed earlier that the limestones that form Monte Santa Caterina and the two islands of Levanzo and Marettimo have a Triassic to Miocene age, and the deformation process

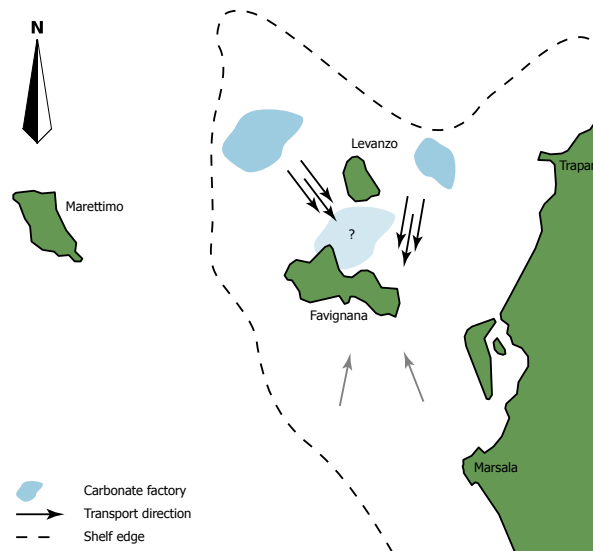


**Figure 5.1** – Schematic map of the Aegadian islands showing the major transport directions and possible locations of carbonate generation platforms.

that formed thrust structures started in the Alpine orogeny (Tavarnelli et al., 2003). During the Pliocene the start of the uplift process introduced the transition from compression to extension, so the positive Monte Santa Caterina structure was therefore already present during the sedimentation of the Favignana calcarenite, which can have important implications for the transport mechanisms.

An alternative to the assumption of a platform in the north is a single system at the same location. The studies of Massari & Chiocci (2006) and Hansen (1999) do not provide a clear explanation of sediment supply, because they assume that the calcareous material is generated on the shelf and subsequently reworked by storm events. This can be the case in Favignana as well, however the transport directions point to a system that develops towards the coast. Because water depths are limited, organisms could develop, be reworked by storm events, after which new matter was created and the cycle could repeat itself. This supports the observations of cyclic behaviour in the smaller scale foresets.

## 5.2 Transport mechanism

Dead calcareous material originating from the carbonate platform needs a mechanism in order to be transported to the location that at present time forms eastern Favignana. The Mediterranean Sea is not characterised by a strong tidal influence or predominant continuous currents. Still, the sedimentary macrofacies description showed sedimentary structures that are associated with a significant amount of energy at the time of deposition.

A possible explanation to the origin of the sediment transport might be found in the predominant wind directions in this part of the Mediterranean. The western Sicilian fetch — the length of water over which

a wind has the possibility to create waves — is the largest at a northwestern wind. More than 700 kilometres of open sea are situated between western Sicily and the Ligurian coast in the northern part of Italy. The regional name for the strong north-south wind is the Mistral (*It: Maestrale*), which can be remarkably powerful and can therefore potentially transport coarse grained sediments in case of major storm events. The impact of the Mistral winds on eastern Favignana can potentially be intensified when water pushes itself through the channel between the Levanzo and Favignana limestone platforms.

The hypothesis of storm-related events as a main driving force of sediment transport is reflected in the outcrop data. As mentioned earlier, predominant directions are observed to be around southeast to south (figure 4.12). Outcrops show very few subsequent palaeo-directions, approximately opposite to the main orientation, indicating minor storm events from the south occurred during the sedimentation of the calcarenite complex. Another explanation can be found in the fact that some of the subsequent directions are found in sequences that show upper plane flow regimes. This can lead to an interpretation where the structures are seen as backsets of antidunes. At this stage it is not certain what process caused the — apparent — reversal of the flow direction.

A summary of observed palaeo-transport directions and possible locations of cool water carbonate factories is provided in figure 5.1. An important observation in here is the orientation of the flow with respect to the other Aegadian islands and the mainland of Sicily. The southeast direction is more or less aligned with the channel between Levanzo and Monte Santa Caterina. Moreover, the other dominant southwest direction shows transport parallel to the coast. This indicates alongshore currents to have played a role in the system.

Outcrop analysis shows that also gravity processes most likely had an important role in the transport of sediment. In particular the large scour systems may have been favoured and/or generated by gravity processes. It is therefore reasonable that the start of erosion at the crest of a calcarenite wedge started a self-inducing process driven by gravity, scouring into the earlier deposited sediments.

### 5.3 Depositional environment

The character of the internal sedimentary structures and the processes that formed the Favignana calcarenite are fairly complex. The base of the Lower Pleistocene system on Favignana is the top of the Trubi clay, which can be found at several locations on the island, in particular Cala Rossa and Cala Azzurra (figures 4.9e and 4.9f). The top of the clay is both bioturbated and eroded, but bioturbation did not continue across the boundary between the clay and the bioclastic Favignana deposits. This indicates either a stop in sedimentation or an erosive event at this stage — no deposits dating from the uppermost Pliocene (Piacenzian stage) are found — which also confirms the difference in age between the Zanclean Trubi Formation and the Favignana calcarenite.

During the Lower Pleistocene, the Mediterranean area faces a relatively high sea level (Cohen & Gibbard, 2010). The chronostratigraphical correlation presented in figure A.5 (appendix A) presents the sea level curve — represented by marine isotope analysis — from the Lower Pleistocene to present. The uplift phase ongoing since the stage ended in the Plio-Pleistocene period (Tavarnelli et al., 2003) is causing the existing structures of Favignana, Levanzo and Marettimo to experience an inversion process. As a consequence of the uplift carbonate producing platforms started to become prone to erosion by storm-induced currents and wave action.

Because of the position of Monte Santa Caterina with respect to the early mountains of Marettimo and in particular Levanzo, a negative structure — such as a channel — existed. The high thickness of the Plio-Pleistocene between Favignana and Levanzo reported by Abate et al. (1997) suggests that this hypothesis is likely. Large amounts of bioclastic material were delivered to the area, and deposited on top of the Trubi clay. Similar Mediterranean calcarenites described by D'Angelo et al. (2005) and Hansen (1999) are interpreted as being deposited on the shelf, and then reworked by storms which induces the build up of bioclastic wedge that builds out towards the open sea. More discussion on similar deposits is provided later. The two main transport directions on Favignana indicate progradation towards the mainland of Sicily.

Based on the observations mentioned above, the development of the Favignana calcarenite, the resulting stratigraphy and the overall geological model can be reconstructed in the following three phases:

1. The deposits that characterise the base of the Favignana calcarenite sequence generally have a rather massive character. Vast amounts of sediments were transported and deposited at a very high rate on top of the Zanclean Trubi clay. As water depth decreases, due to 1) the accumulation of bioclastic material on the seafloor; 2) uplift of the area like observed in the Marsala calcarenite by D'Angelo et al. (2005); or 3) sea level drop that steadily occurred during the Lower Pleistocene, lamination starts to develop. The lower plane parallel laminated sands are in some cases relatively extensive. As the accommodation space starts to decrease more, small scale dunes with either undulated or straight crest start to develop. Because of the directions of the storm-driven current and wave action, propagation is mainly to the south-southeast. Minor storms from the south reversed the process from time to time. A high degree of fluctuations in depositional energy is observed in the field, which is illustrated by erosive features and the varying thickness of smaller dune foreset beds.
2. Due to the processes described in phase one, accommodation space continued to decrease, resulting in a further increase in energy under which the Favignana calcarenite is deposited. Locally 15 metre high giant dunes are observed in large parts of the fieldwork area, which can be relatively laterally continuous. More storms induced incidental supercritical flow conditions, providing energy to develop undulated bedding. During this stage, a substantial complex with submarine prograding calcarenite dunes is generated.
3. A high positive structure — like the crest of a giant bioclastic calcarenite dune — is in case of



major storms easily affected by erosional processes. Parts of a dune crest face a small degree of erosion, likely creating a preferred path where the flow could be concentrated. Gravity processes enhanced the erosive processes and created large scours of up to 10 to 20 metres deep. Because of the storm-related nature of these processes energy supply suddenly dropped which filled the deepest parts of the scours with structureless sediment, locally showing a high amount of rhodoliths and other coarse bioclastic material at the base. Figure B.3 in appendix B shows part of the Scalo Cavallo cliff with several scour-related features. The downstream part of the scours induced the possibility to develop small scale trough cross-stratification. Interpretation of the field data led to the hypothesis that the big scours created in the northwest — Scalo Cavallo and its surroundings — provided a concentrated energy fanning out to the southeast. The small scale troughs that are observed in Cala Rossa, Bue Marino and Cala Azzurra can possibly be explained with this lobe-like geometry. The transition from tabular cross-stratified dunes to troughs is very well visible in the Cala Rossa photo panel (figure B.2 in appendix B).

Some of the undulated beds are associated with upper flow regime structures related to the scouring nature of parts of the stratigraphy. In particular the inland area of Bue Marino, western Cala Rossa and the central part of the island show these structures. They are interpreted as an intermediate step when moving towards the end of a scour fan — from massive infill to undulated beds and finally to troughs. The undulations are in some cases associated with smaller scale scour and fill systems (figure B.4). Therefore the nature of these features differs from the large scours. The high energy and the gravity based flow can create a scour which has an orientation perpendicular to the flow direction. Because of the hydraulic jump that is associated with such a system, large amounts of sediment are instantly dropped into this structure, with the coarsest material at the base.

Summarized, the reconstruction of the eastern Favignana depositional framework consist of three phases. The first two phases are general for the entire area, where a system builds up with low energy deposits at the base, and large prograding dunes towards the top. Local erosive events created the deep scours and the associated lobe structure. This explains the lateral variability of some of the sedimentary structures related to this phase.

Figure 5.3 illustrates the resulting architecture based on the described stratigraphical evolution of the Favignana calcarenite. The phases described above are schematically positioned next to the Monte Santa Caterina structure. Sediment supply in this situation is from the northeast, indicated with the arrows. Only one scour and its interpreted fan geometry is drawn to emphasise the conceptual nature of this diagram. It is likely that in reality an interplay between different scours and their lobes exists. The cross section parallel to the flow direction shows how the undulated scour and fill system is positioned in the framework. The end of the fan — with its trough cross-stratification — is situated at the top left part of the frame.

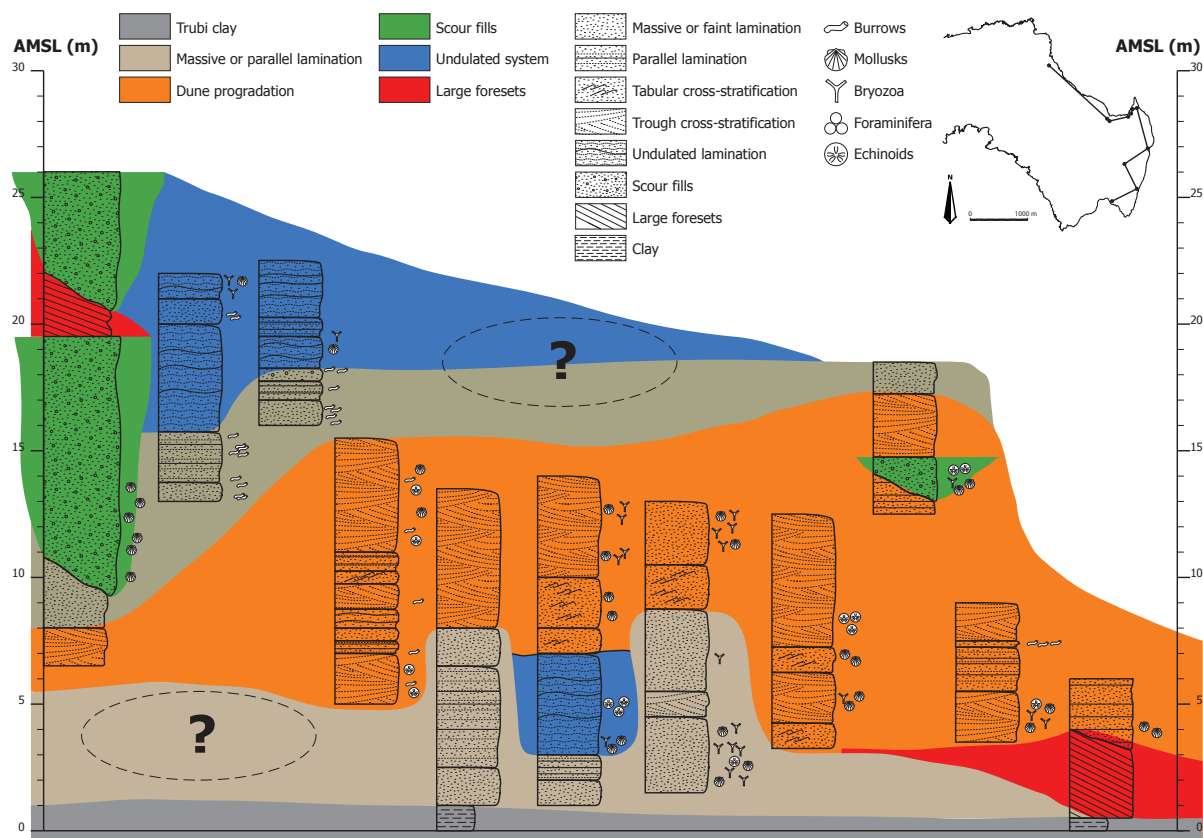


**Figure 5.2** – The well logs from the fieldwork data (figure 4.10) with an interpreted conceptual facies model.

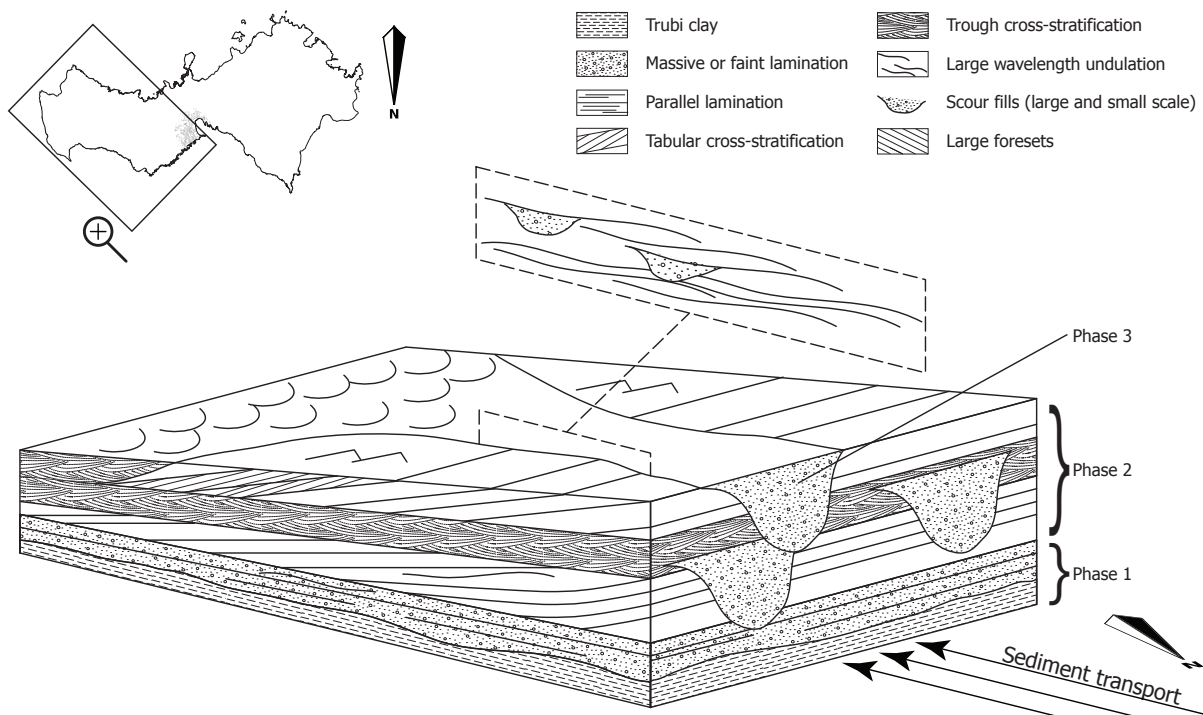


**Figure 5.3** – Conceptual model of the Favignana calcarenite with respect to the present-day situation.

## 6 Reservoir modelling

The results from the fieldwork campaign, consisting of the facies description, the inferred conceptual geological model and the reservoir properties, will be used to generate a model of the eastern part of Favignana. The geological modelling will be performed as a (potential) reservoir model, and will therefore not aim for accuracy to a metre or centimetre scale. As all upscaled geological models, it is an attempt to capture key architectural and sedimentological characteristics of these deposits. Therefore, a model will never be as accurate as the reality, but it will try to be as useful and correct as possible. To quote a well known statistician:

*'Essentially, all models are wrong, but some are useful.'* (Box & Draper, 1987)

In order to build a model, the present boundary surfaces have to be gridded. Before this step, data for those surfaces was available in a vector-like grid with high resolution. Gridding introduces the concept of averaging certain properties and geometries over a 3D volume. In order to limit the time needed for calculation to acceptable dimensions, a grid size of 25 by 25 metres was chosen. Compared to reservoir models used in dynamic simulations, this is a rather high resolution. However, compared to the amount of details observed in the field, this grid could be considered a gross oversimplification. Because this study focusses on the reservoir implications, this trade-off was made. The layers are defined between the sea level and the surface of eastern Favignana, with a varying thickness. Some lower areas like Cala Rossa and Cala Azzurra require more detail than others, so a proportional approach is chosen where the layering builds up from the bottom.

### 6.1 Facies model

The facies model is the starting point of a reservoir model. The flow behaviour of a reservoir is strongly affected by petrophysical properties of the rock it consists of. These parameters can be tested in a laboratory. However, the results of these tests only represent a very small piece of reservoir rock. The aim of a facies model from a reservoir engineering point of view is to visualise the subsurface in order to populate the reservoir model with petrophysical properties. For example, a rock sample originating from a certain facies influences parts of the reservoir that are modelled as the same facies.

### 6.1.1 Geostatistical algorithm

Various geostatistical methods are available to create a facies model, such as object modelling, kriging, and sequential indicator simulation. These are all based on two-point statistics, and because their little importance for this research they will be discussed later. A relatively recent development is multi-point facies modelling, which uses the multiple point statistics (MPS) technique (Daly & Caers, 2010; Zhang, 2008). This method was introduced in Schlumberger’s Petrel<sup>®</sup> 2009 software package, that is being used in this project.

Multi-point facies modelling uses so-called training images. The images used in this facies model are manually made, and used to instruct the software how the different facies are located in a three-dimensional image. Training images are not meant to — and therefore should not — represent a conceptual geological model or map detailed fieldwork data. The multi-point facies modelling algorithm only uses them to create a template of how facies are interrelated.

A training image should be a trade-off between repeatability and accuracy versus size. A too big image requires a lot of computer time, while a small image might not be useful. Another requirement is that the images are stationary, i.e. on average the characteristics should not vary too much. This is solved by dividing the area into regions. Between the regions, differences and trends may exist, while inside a region a unique stationary image is used. In this way, a reservoir - typically non-stationary - can be modelled by using stationary training images. The region concept also reduces the number of facies in a training image, increasing representativeness and calculation speed.

In order to make a facies model, several types of input can be given. The most important one is the training image, which is a representation of the way facies are interrelated. Besides training images, additional hard and soft data can be used. Hard data, such as channels and other outcrop observations, can be used to fix a certain facies in three dimensional space. In this way, the algorithm will model this specific facies at exactly the same place. Soft data is usually expressed as trends, such as a probability property, or azimuth maps. In addition to the concept of regions, it is a good way to introduce certain trends in the model.

### 6.1.2 Training image

The well section given in figure D.1 — appendix D — presents all fieldwork locations and their interpreted stratigraphy in terms of facies.. There is a clear trend from the more low energy features to the higher energetic environments (undulation, large foresets and scour fills) when moving stratigraphically upwards. Because training images are required to be stationary, no horizontal trends can be incorporated. Zhang (2008) describes the concept of the use of regions. In here, the prospective reservoir model is split into different regions, which are assumed to have different conceptual geological properties. Each of

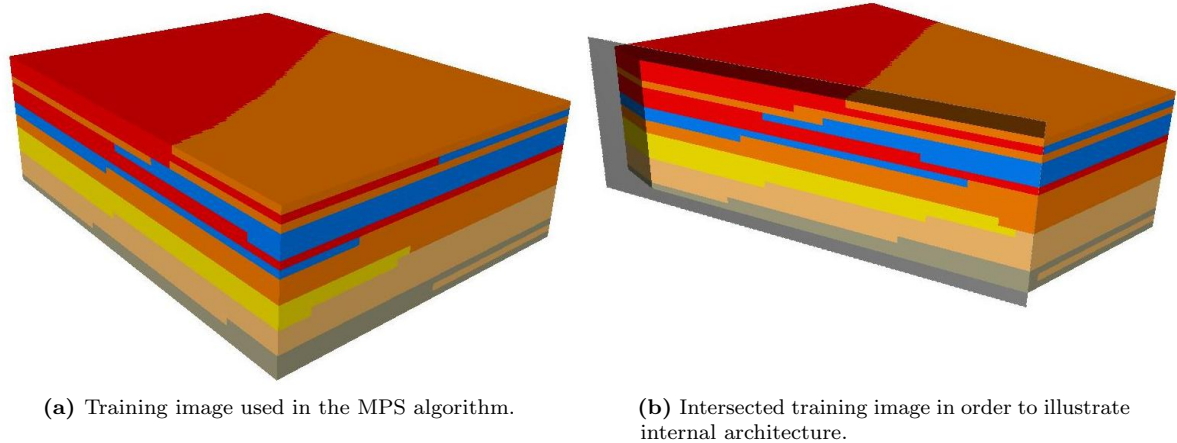


**Figure 6.1** – Training image grid for the MPS algorithm. North is upper left, facies colour according to general facies legend.

those regions is thereafter modelled with a separate — stationary — training image. Modelling eastern Favignana with the concept of regions would imply a clear boundary between the different regions that is not observed in this fieldwork campaign. Moreover, the complex internal architecture that exists throughout the island is not suitable for this type of modelling. Instead, an approach with a single training image for the entire fieldwork area is suggested. The thoughts of the conceptual geological model - described in section 5 are attempted to be included in this training image.

Training images can be given in various formats such as hand-drawn sketches, digital (areal) photographs, or basically any 3D model one can imagine (Schlumberger, 2009). The ideal training image is a rectangular 3D grid, which will be used in this modelling exercise as well. The Petrel software package offers the option to draw arbitrary facies patterns in a grid. Filters on *i*, *j* or *k* values are used to address facies only to designated grid cells. The most convenient method was to filter every *k* layer, and draw the desired facies positions for each layer separately. The training image grid can then be quality-checked with intersections in a three dimensional view.

Figure 6.1 shows the final training image used to model the Favignana calcarenite. The entire block — consisting of 100 by 125 by 20 grid cells with a size of one metre in all directions — as well as an intersected grid is shown. It is attempted to include the interpreted depositional environment as described in the conceptual geological model. Because the training image cannot include too much variation, one of the conditions was that only two facies can be next to each other in a single *k* layer. Some examples of intermediate *k* layers are given in figure D.2 in appendix D. The images show an attempt to include the propagating nature of the calcarenite complex, with preferred orientation to the southeast.

### 6.1.3 Additional data

Despite the non-regional approach of the model building process (see the previous section), trends of facies distribution in outcrops can be recognised in different areas of the island. These data are therefore converted into probability maps that can be used as additional input for the model. The tutorial in appendix E provides further details on the process of making such probability maps in the Petrel software package.

Facies occurrence and their relative proportions are linked to the outcrop thickness and represented as pie charts (figure 4.11). The same outcrop thickness is also used to generate probability maps. A convergent interpolation method converted data points at the pseudo-well locations to probability maps of a certain facies. The downside of this approach is that no conceptual thinking can be included in the maps. Therefore the probability maps generated directly from outcrop data are only used as a starting point. The interpolation method assumes that when no data are present, a certain facies is not present at that location, resulting in some unusual patterns.

A solution is found by manually creating the probability maps using both the conceptual thinking as well as the maps generated from outcrop data. This method implies the manual generation of polygons representing lines of equal probability. In this way, areas without data or parts of the island that are not quarried to a deep level can be filled in using geological knowledge. The contour lines are subsequently converted to surfaces and in turn to properties of the static model grid.

Finally, the property volumes presented in figures D.3 and D.4 are included in the MPS facies modelling algorithm. Probabilities are normalised by Petrel and used as a medium-influence soft data input, which is the degree of influence recommended by the software. Once the facies model with all the non-scouring features is created, the scours have to be modelled. This is done with an object modelling based algorithm. The locations of scours are determined by 1) the well logs; and 2) the probability volumes. In particular no information is present about the length of the scours. The few examples observed in the field only showed a cross-section rather than the full length of the scour. Thickness — or depth of the original scour — can be up to 20 metres, with a width that more or less equalises this depth. Scour-fill facies only replace the large foresets and undulated beds, because those facies occur in the top layers where the scours are believed to be occurring.

### 6.1.4 Facies modelling results

The modelling process of outcrop areas require some trial and error. The algorithm will always honour the pseudo-well logs with the facies information, but in the inter-well area often more information is known by the geologist, especially in this case study where parts of the island with high outcrop density — like Cala Rossa, Bue Marino and Cala Azzurra — show a lot of available information. A quality check

between reality and model is therefore essential, because it is a unique opportunity to improve the model. Especially scaling issues between the training image and the model grid are sensitive for features like noise or continuous layers. Two relatively closely spaced wells can give problems as well when for instance their stratigraphy differs significantly.

The final result that is believed to represent the Favignana calcarenite on a hydrocarbon reservoir scale is thus obtained (figure 6.2). Two cross-sections are created;  $XX'$  is approximately parallel to the transport direction, while  $YY'$  is orientated perpendicular to the main flow direction. In order to compare the resulting model with the field data — the stratigraphic logs at pseudo well locations — a well fence is shown in the  $ZZ'$  window. The trajectory from Scalo Cavallo via Cala Rossa, Punta San Vituzzo and Bue Marino to Cala Azzurra covers all the pseudo well locations. A series of close-ups of respectively Scalo Cavallo with Cala Rossa, Bue Marino, and Cala Azzurra is provided in figure D.5 in appendix D.

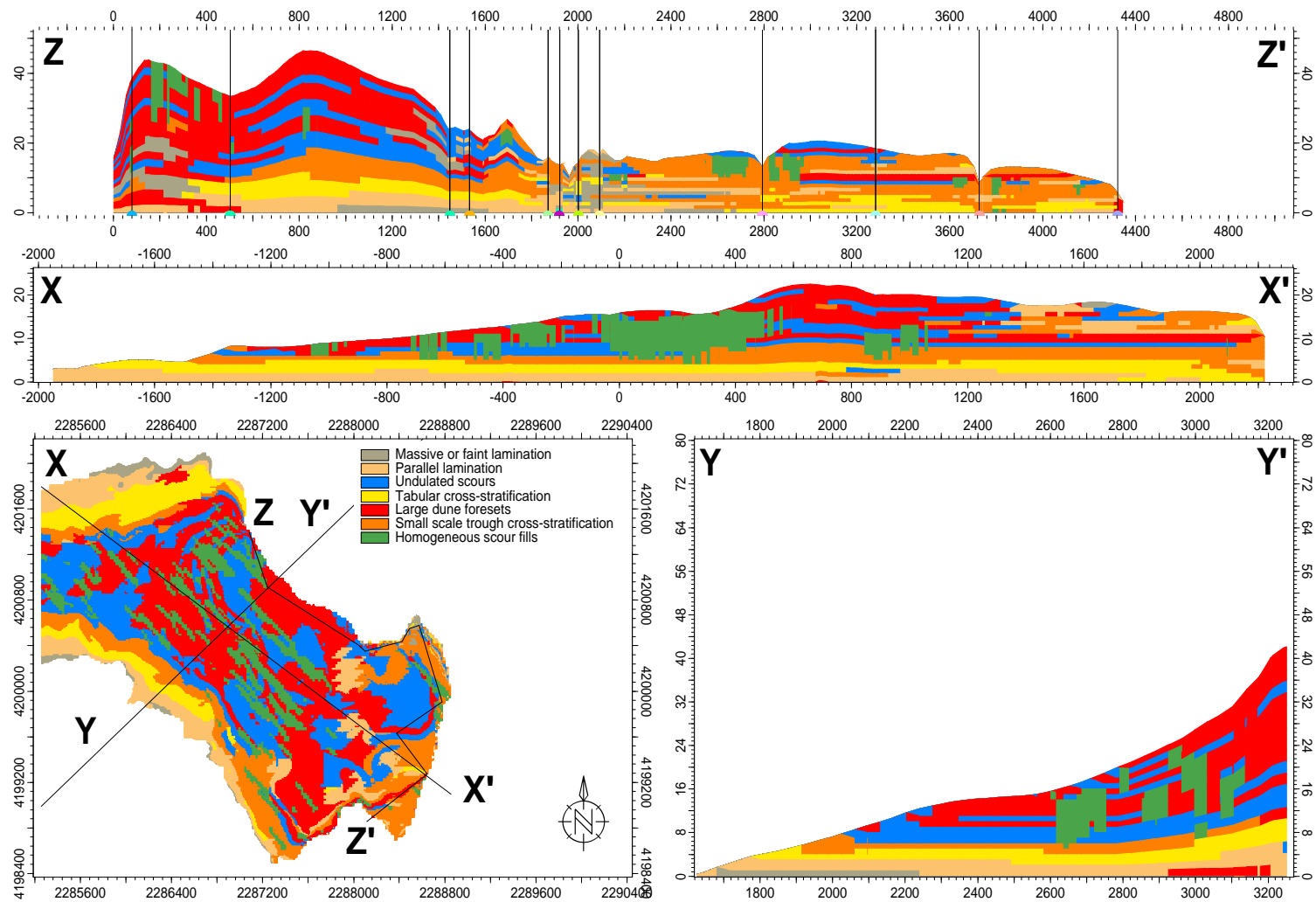


**Figure 6.2** – Facies model resulting from the MPS method showing a plan view, two cross sections and a fence with stratigraphic log locations. The values of Y-axes in cross-sections are in metres above mean sea level.



**Table 6.1** – Average petrophysical properties of the facies in the model, including the sample sources. Numbers according to table 3.1.

<b>Facies</b>	$\phi_{\text{avg.}}$ [-]	$k_{\text{avg.}}$ [D]	<b>Source</b>
Massive calcarenite	0.46	52	2
Parallel laminated units	0.63	66	1
Undulated lamination	0.63	66	1
Tabular cross-stratification	0.57	65	3
Large dune foresets	0.57	65	3
Small scale trough cross-stratification	0.58	65	3,4
Homogeneous scour fills	0.46	52	2

## 6.2 Property modelling

Results from the laboratory tests on the samples, are modelled into the reservoir model grid. Each grid cell has at this stage only an assigned facies code. In addition two additional properties can be given to all the cells: porosity and permeability. The most convenient approach is to establish a specific property distribution for each facies. In practice results from wireline logging result in for example a porosity log with values every couple of centimetres. The data from the field has a much lower resolution. Moreover, not every facies as they appear in current subdivision is sampled. Therefore some assumptions have to be made. In table 6.1 an overview of these assumptions and the reservoir properties used in the modelling process is given. Because of the lack of samples, the large dune foresets properties are assumed to be equal those of the tabular cross-stratified beds. Erroneous results from permeability tests on trough cross-stratified samples resulted in the same permeability for all cross-stratified units. Both the homogeneous deposits on the bottom of the sequence and the scour fills share the same average properties. The last assumption is the fact that the undulated lamination is equal in porosity and permeability to the parallel laminated units, as they are both relatively fine grained. The final porosity model of eastern Favignana is presented in figure D.6 in appendix D. A permeability model was not created because no dynamic simulations are part of this study.

## 6.3 Reservoir implications

As indicated earlier, the Favignana calcarenite has a very prolific reservoir quality. This is caused by several reasons: 1) a high porosity; 2) high permeability; 3) very few faults and fractures; and 4) a low degree of diagenesis. The main explanation of these excellent reservoir properties is that on eastern Favignana almost no compaction has taken place. If these deposits were buried, all these parameters would have changed significantly. The compaction causes a reduction in porosity and therefore permeability, fractures can develop due to differential load, and more cementation can form over time. However, the

calcarenite is still potentially an excellent hydrocarbon producing reservoir.

A wedge provides good structural perspective for hydrocarbons to be trapped. Although not an entire wedge is observed in the field, it might have been deposited and eroded. Other studies — which will be discussed in the next chapter — produce wedge shaped conceptual models as well. Figure 6.3 is a schematic cross section of how such a trap works. Of course it is assumed that a seal — like an impermeable clay or salt layer — is present to prevent the hydrocarbons from escaping the reservoir rock. An illustrative oil water contact (OWC) and gas oil contact (GOC) is shown as well.

The volume of oil in place is an important factor that influences the development of a field. A rather elementary expression to calculate the STOIP (Stock Tank Oil Initially In Place) from average properties is:

$$STOIP = \frac{V_b \phi (1 - S_w)}{B_o} \quad (6.1)$$

In some cases the expression is subsequently multiplied with N/G, which represents the *net-to-gross* ratio. This is used to separate the net producing reservoir units from the non-producing parts. Other variables include (Schlumberger, 2010):

- $V_b$ , which is the bulk volume of the reservoir [ $m^3$ ]. Usually this volume is bounded by the reservoir seal, faults, stratigraphic traps, and the oil water contact (OWC)
- $\phi$  is the porosity [-], which is obtained from the volume property described in the property modelling section
- $S_w$ , which is the water saturation [-] of each grid cell. For simplicity an initial water saturation of 0.2 is assumed, which is not unusual for such high quality reservoir rock.
- $B_o$  is the oil formation volume factor, expressed in reservoir barrels per standard barrel [rb/st]. It is used to compensate for oil shrinkage due to gas that comes out of solution because of the pressure drop during production, so it is in the majority of the cases larger than one.

The Petrel software calculates all these variables for each grid cell that will be part of the bulk volume, and then sums everything to obtain the STOIP [ $m^3$ ]. For simplicity it is assumed that only oil — gas will be ignored — is present, with a water saturation given before. Table 6.2 presents the results of the calculations. Apart from values for the entire pseudo-reservoir, the contributions of each separate facies are given as well. The total potential volume of oil in place is approximately 35 million cubic metres, which corresponds to 220 million barrels. These volumes, however, need some careful consideration before they can be adopted:

1. As seen before, a calcarenite wedge system can potentially be much larger than the outcrops observed on Favignana, increasing the oil in place and associated reserves.
2. The fact that the Favignana calcarenite has never been buried significantly affects the reservoir

properties. A hydrocarbon producing reservoir — typically over two kilometres deep — will theoretically never show porosities of  $\mathcal{O}$  0.4 to 0.6 bulk rock fraction. Potentially this can be simulated in laboratory experiments. In here, cores are subjected to confined pressure comparable to the pressure regime in a typical hydrocarbon producing reservoir. The compaction that will occur as a result of the pressure increase can be an indication for the degree of porosity decrease in the burial process.

3. Hardly any indication of diagenesis can be observed in the thin sections. Only a very small amount of rim cement is present, which does not have a big influence on the pore network and hence the potential hydrocarbons in place. A deeper burial and therefore higher pressure and temperature will increase the speed at which cement forms. Potentially this can significantly reduce porosities, especially in carbonates, because these sediments are associated with precipitation of dissolved calcareous material. This effect is harder to reproduce in a laboratory, because a geological time scale is impossible to simulate.

The permeability is the second parameter which is important for in particular the production behaviour of a hydrocarbon producing reservoir. Because dynamic simulations are not considered in this project, permeability has not been modelled across the reservoir grid. Table 6.1 gives — apart from the porosity — values for the average permeability of the facies. These values are obtained with a falling head experiment described before and with a limited number of samples.

Implications for the productive behaviour are often found in high differences in permeability. A relatively small unit with a very high or very low permeability can influence the production significantly. Although the differences in permeability measurements are not large, it does not exclude the possibility of the presence of low permeability zones. For example, the cementation near fractures is significant (see figure 4.7a) which will form an obstacle for flow of reservoir fluids, even in horizontal direction.

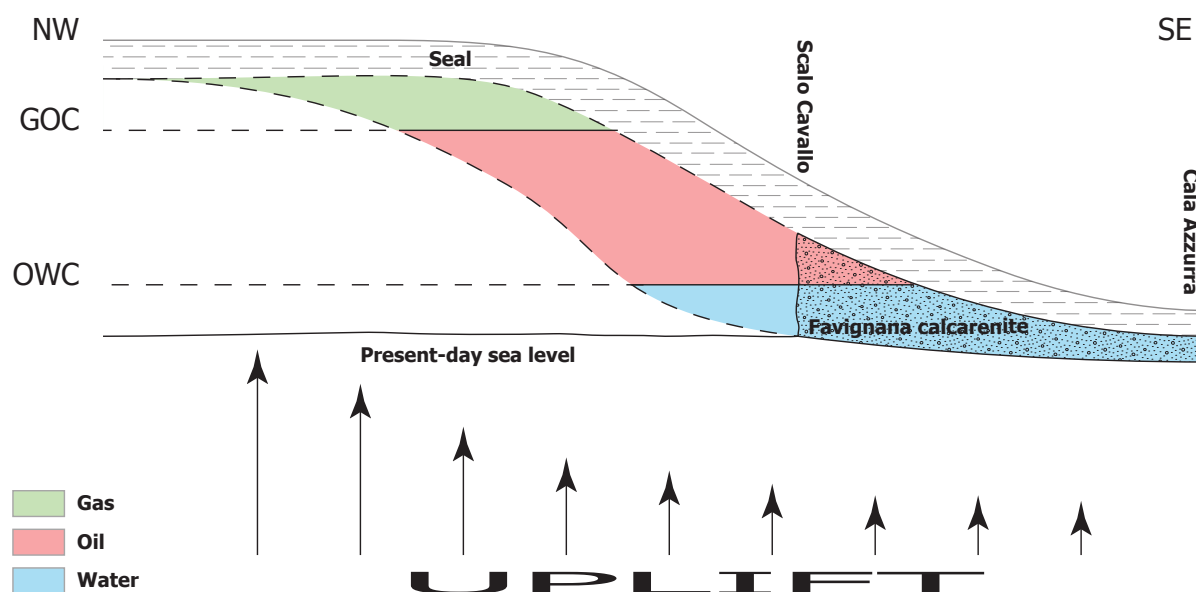


**Figure 6.3** – Conceptual structural reservoir prospective of the Favignana calcarenite. A cross section from northwest to southeast is given, with Favignana on the right. Vertical scale is exaggerated.

**Table 6.2** – Results of the volume calculation of the potential Favignana oil reservoir. BV is the bulk volume, PV the pore volume and HCPV is hydrocarbon pore volume — or the pore volume occupied by hydrocarbons. All volumes are in  $[10^6 \text{ m}^3]$ .

	BV	PV	HCPV	STOIIP
Total reservoir	97	56	45	35
Massive calcarenite	3	1	1	1
Parallel laminated units	16	9	8	6
Undulated lamination	15	9	7	6
Tabular cross-stratification	14	8	6	5
Large dune foresets	19	11	9	7
Small scale trough cross-stratification	21	13	10	8
Homogeneous scour fills	10	4	3	3

## 7 Discussion

### 7.1 Sedimentation deformation structures

The assumed high sedimentation rate associated with the extensive massive deposits and the large foresets may be supported by several features observed in the field, that are not yet discussed. Some locations show sedimentary structures formed after deposition (figure 7.1). They are interpreted as post-sedimentary structures and perturbations which could be caused by several mechanisms. Water escape structures, formed when water between the grains of the sediment suddenly escapes due to the increased load and pressure are associated with a high sedimentation rate, which does not allow the water to gradually escape. Similarly this can be generated by sediment shaking — due to earthquakes, which are still common in the area — or by fast movement of pore water induced by gravity processes.

### 7.2 Reservoir properties

The porosity and permeability measurements obtained using the test described in respectively section 3.3.1 and 3.3.2 are considered to be reliable. Measurement did not differ much between different runs, and samples with the same origin appeared to have more or less the same properties (see section 4.6). A high variability of results from the different samples derived from the same type of sediment facies would either suggest that the measurement method is not reliable, or that the heterogeneity of the deposits is very high. The small diameter plugs could not be tested with the picnometer. No reliable result could be obtained because the gas chamber that houses the sample was too large compared to the dimensions of those plugs. The same holds for the permeability tests, where no small enough seal was available.

Porosity determination from thin sections was not possible because the blue dye did not penetrate the samples perfectly, making it impossible for an image detection program to separate pores from grains. Secondly, some mechanically induced disturbance of rock fabric appears to have taken place during the thin section preparation procedure. Grains must have undergone a change in position or orientation which did not allow any reliable porosity measurement.



(a) Bed deformation structure in Lungo Mare at the north coast of Favignana, most likely as a result of water escape or instability during deposition. Ruler of one metre for scale.



(b) Smaller scale dish-and-pillar deformation structures in Cala Azzurra, observed in the yellowish deposits visible on the panel in figure B.5, appendix B. Chart for scale, which is 10 centimetres wide.

**Figure 7.1** – Water escape structures at two different scales.

The very high permeability of the Favignana calcarenite (30 to 100 D, with some outliers to little above 300 D) have to be interpreted carefully, because they might be caused by side effects of the test method, and not by the matrix permeability itself. All samples show approximately the same variance in permeability values (see porosity-permeability plot in figure 4.13). This implies that in the stratigraphical units where the sampling was done no major flow barriers have been observed and/or sampled. The number of samples, however, is too small to extrapolate this statement to the entire calcarenite complex. Very small features like recrystallised fractures can have major implications on reservoir flow (see for example figure 4.7a). A set of plugs with a size as used in these experiments can never be representative of a such large scale accumulation.

### 7.3 Location on shelf

Many examples of calcarenite complexes described in the Mediterranean area suggest that large foresets as seen on Favignana usually indicate that the sedimentary system is prograding on a shelf edge, towards the open sea. Multiple examples can be found in the literature. Below some of these examples will be discussed:

1. Massari & Chiocci (2006) describe a cool-water carbonate body with large foresets in the central part of Sicily. Pleistocene deposits can be found several hundreds of metres above present day sea level, indicating that a substantial amount of uplift has occurred since deposition. Their conceptual depositional model proposes a situation where bioclastic sediment is deposited on the shelf, partly at depths lower than the storm-wave base. Storms and wave interaction reworks the sediment and creates a wedge-type system that builds out towards the open sea.

2. Martín et al. (2004) investigated temperate carbonate sedimentation in an embayment in Spain. Storm-related winds provided sediments transported by longshore currents. The steep slope of the basin, together with the rising sea level of the Lower Pliocene resulted in large longitudinal foresets. In this case however the system builds out towards the centre of the embayment, and not towards the open sea.
3. Hansen (1999) describes comparable bioclastic sequences in the Lower Pleistocene of Rhodes, Greece. This research interpreted the units as being deposited during a relative sea level fall. Again, roughly the same depositional system as suggested by Massari & Chiocci (2006) is given.
4. In the strait of Messina (northeastern Sicily), a mixture of siliciclastic and bioclastic sediments is deposited on the shelf (Di Stefano & Longhitano, 2009). Like on Favignana, Lower and Middle Pleistocene sediments are deposited on top of the Trubi Formation. They provide two depositional models, both showing a system that builds out towards the sea. Similarities to Favignana that are not addressed by the other research projects are the erosive channels that are observed here. They are interpreted as being caused by downwelling storm-driven currents.
5. Pedley & Grasso (2002) describe the interaction between sea level and cool-water carbonate sediments. There are similarities between this research and an investigation by D'Angelo & Vernuccio (1996), which will be used later to elaborate on the influence of eustatic and tectonic processes on the area of Favignana and western Sicily. These sediments are also uplifted considerably since their deposition.
6. Pomar & Tropeano (2001) investigated the *calcarenite di Gravina* in the Basilicata region, southern Italy. Again, storm-driven currents are interpreted as the cause for sediment avalanches to occur on the depositional slope. Different terraces are deposited on top of each other as a result of sea level fluctuations.

Almost all the bioclastic systems of the Plio- and Pleistocene as described above build out towards the open sea, with the exception of the system investigated by Martín et al. (2004). The Favignana calcarenite prograded to the south-southeast, which is more or less towards the mainland of Sicily. In the Mediterranean this has not yet been reported, making eastern Favignana unique for this area. The reason for this different behaviour of the calcarenite deposition compared to the rest of the Mediterranean is unknown. A possible explanation is the existence of a topographic low — like a channel — in which a system can prograde.

The thickness of the Lower Pleistocene between the islands of Favignana and Levanzo — locally 600 milliseconds in a seismic survey (D'Angelo et al., 2005) — suggests the presence of a channel or depression in which a wedge can build out. Figure 7.2 shows an isopach map of the part of the archipelago just west of the fieldwork area. The channel mentioned before is clearly visible on the map, with an orientation of the longest axis that corresponds more or less to the main transport direction to the south-southeast. At

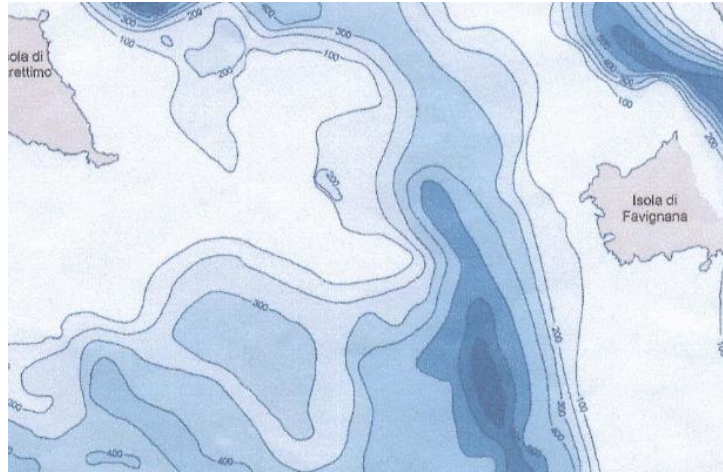


**Figure 7.2** – Isopach map of the area west of Favignana, showing the thickness of the Plio-Pleistocene. Favignana is located on the right. Unfortunately no data from the eastern part of Favignana exists up to date. Note the high thickness north of the island, between Favignana and Levanzo. The isopach values are in milliseconds, image after D’Angelo et al. (2005).

the edge on the right side of the image is the isopach line of 200 milliseconds just visible, suggesting that this is the minimum thickness of the Plio-Pleistocene on eastern Favignana.

## 7.4 Tectonic and eustatic processes

Marine deposits are always subject to changes in sea level, and the active tectonism of Sicily will have consequences for the uplift in the area. During the fieldwork no investigations of sea level fluctuations recorded by the Favignana calcarenite was carried out. Similar — somewhat younger — deposits are however chronostratigraphically evaluated. D’Angelo & Vernuccio (1996) investigated the Middle to Upper Pleistocene calcarenites on the Sicilian mainland, situated between Trapani and Mazara del Vallo (see figure A.1 as a reference for the geographical location). These deposits are locally known as *Calcareniti di Marsala* — or Marsala calcarenite — which are used as a building material just like the *tufo* from Favignana. A number of terraces are distinguished, spanning in elevation from over 100 m AMSL inland to sea level at the shore. The authors suggest a correlation between the terrace formation and the Pleistocene sea level chronostratigraphy. The marine isotope correlation chart in figure A.1 shows this attempt. Terrace age corresponds approximately to periods of high sea level. However, because the present day sea level is relatively high, a terrace that is currently 100 m AMSL would have been deposited at a very different elevation. This large difference indicates that tectonic influence must have played an important role in the region. Similarly, the highest point of the eastern part of the island rises more than 50 m above the present day sea level, indicating that uplift must have been influencing the morphology of Favignana as well. It is therefore likely that the present Monte Santa Caterina structures resulted from an uplift phase which is ongoing since at least Pliocene until today as is indicated by frequent earthquakes of medium magnitude (2.5–3.5 on the Richter scale) that occurred in the area over the last two years.



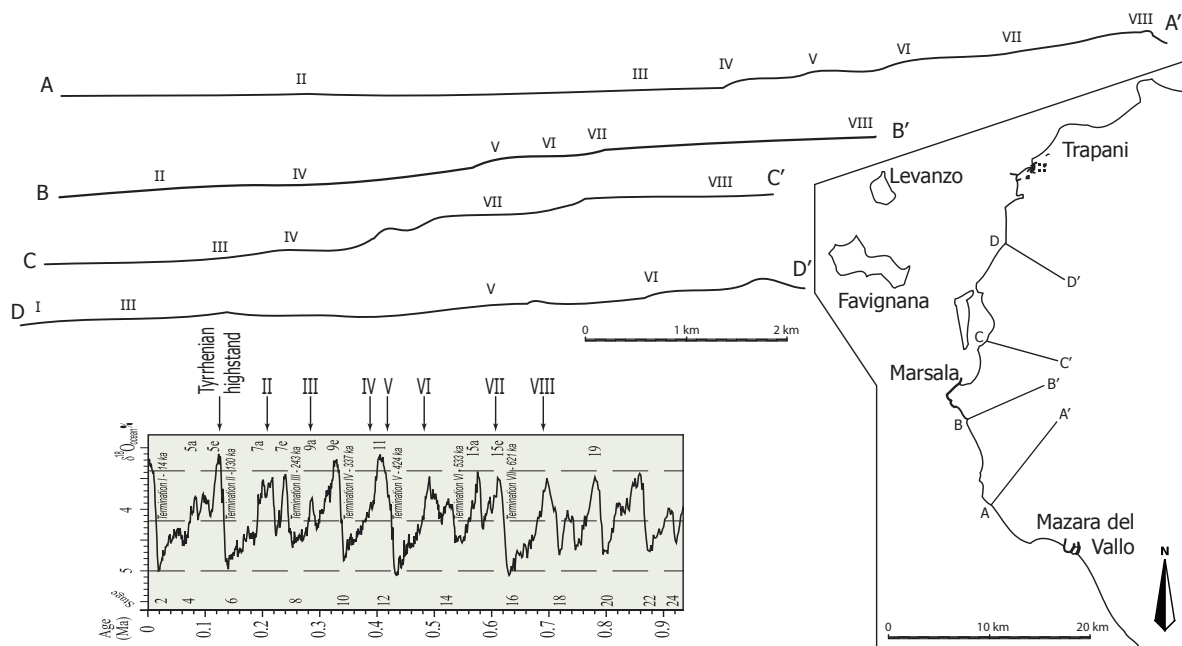


**Figure 7.3** – Terraces in the Marsala calcarenite deposits between Trapani and Marsala del Vallo on the mainland of Sicily as described by D’Angelo & Vernuccio (1996). Vertical scale is five times exaggerated. Image modified from D’Angelo & Vernuccio (1996), chronostratigraphic chart from Cohen & Gibbard (2010).

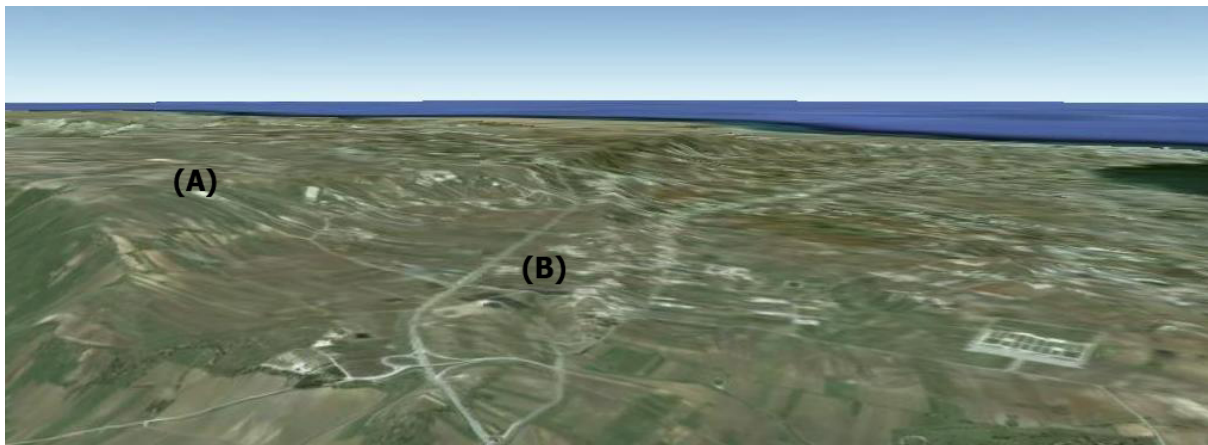


**Figure 7.4** – Example of some calcarenite terraces near the city of Marsala, looking south. Two terraces can be distinguished in this view, marked with (A) and (B) respectively. Location corresponds approximately to the BB’ line in figure 7.3. Source: Google Earth.

## 7.5 Reservoir analogues

Outcrop models can be used as an analogue for a hydrocarbon producing reservoir. Several hydrocarbon fields with similar geometry and/or lithology to the Favignana calcarenite complex can be found in the literature. It is however difficult to make a thorough comparison with the field data from Favignana based on publicly available literature, as a detailed description of the geology is often not provided. Usually publications only give a general description of the reservoir rock, but this section is an attempt to present potential reservoir analogues. Because the Middle East is the world's most prolific carbonate reservoir region, most of the reservoirs considered here will be in that area.

1. A very well known hydrocarbon producing unit in the Middle East is the Asmari limestone (Alsharhan & Nairn, 1997), with fields like Ahwaz and Bibi Hakimeh in the Iranian Zagros foreland basin. The foraminiferal wackestones and packstones from the Early Miocene are interpreted to be deposited on a marine platform to -slope. The best producing intervals in an Asmari field are however not the limestones, but interbedded sandstone units.
2. The Shaybah field in the Rub al Khali desert in Saudi Arabia consists of two units, of which the upper part is interpreted as bioclastic calcarenites with rudists (Brown & Hussein, 1977). With an average porosity of 0.23 — but a mean permeability of only 15 mD — the reservoir shows characteristics of a carbonate reservoir. In many cases a high amount of pore space is present, however connectivity is limited.
3. Qassim et al. (2003) discuss the Kharaib reservoir in Bahrain, consisting of three units that are in some cases heterogeneous and therefore challenging to model. Like many fields in the Middle East, the Kharaib is a carbonate reservoir, and is subdivided into three units. Core analysis showed clean bioclastic packstone at the top of the Upper Kharaib member, which is interpreted as being deposited on a high-energy ramp environment. Because deposition occurred above the storm wave base, according to the authors some material has been transported by storm-related events.
4. Rao & Talukdar (1980) describe the petroleum geology of the Bombay high field, which is by far the biggest oil field in India. The productive zones are interpreted as high amplitude, high velocity and continuous facies with several transgressive and regressive periods. Some intervals contain high amounts of benthonic foraminifera which are used in order to make biostratigraphical correlation. No information on primary sedimentary structures is found.
5. The Raudhatain field in northern Kuwait consists of heterogeneous Mauddud carbonates (Azim et al., 2003). These carbonates are interpreted as being deposited on a low angle ramp setting, where the best reservoir quality can be found in the high-energy upper ramp grainstones. Deposition of cross-bedded carbonates occurred in tidally influenced channels. Lower on the shelf, a transition to wackestones — supported by a fine grained matrix — is observed.

6. First investigations of the recently discovered giant Perla field, which is the largest gas discovery in Venezuela to date, associates the lithology of the reservoir with foramol (ENI and Repsol, personal communication). This study might be very useful in the understanding of the reservoir architecture.

This identification of potential analogues to Favignana is an example of the possible applications of this type of studies. It is by no means meant to be comprehensive. Further research might introduce more potential reservoirs with similar depositional background, and therefore use the Favignana dataset to improve the understanding of the reservoir facies internal architecture and the optimisation of the development of a field. For example, during the burial process some facies behave differently compared to others. This differential diagenesis and compaction might compartmentalise the complex to a larger extent than is observed in field outcrops.

## 7.6 Modelling algorithms

The multi-point statistics modelling method used in the facies model and described in section 6.1 is not the only available algorithm to model a property in a grid. The Petrel software package offers a wide range of methods, providing different results (Schlumberger, 2009). This section briefly discusses the most used algorithms and their influence — either in positive or negative sense — on the final model.

### 7.6.1 Object modelling

When the shape of the facies bodies that have to be modelled is very well known, such as channels, splays, bars or scours, object modelling is the best algorithm to use. Often this method is used in combination with other types of modelling. As described in section 6.1 this approach also has been used for the facies model of the Favignana calcarenite. After the 'background' is made, object modelling replaces parts of the that model, imitating an erosion process.

### 7.6.2 Sequential indicator simulation

In case very little is known about the shapes of sedimentary bodies, sequential indicator simulation (SIS) provides input possibilities for other data trends. Input can be upscaled well log data, variograms, trends and a random seed number. The downside of the algorithm is that if the nugget-style variograms do not match the spatial well data, very noisy results will be produced. Petrel uses the algorithm provided by the Geostatistical Software LIBrary (GSLIB).

The resulting facies model can be found in appendix D, figure D.7. It is clearly visible that such a model is not geologically meaningful. Conceptual geological thoughts can not be incorporated in the model, and although the probability maps can be used, a scattered and unrealistic distribution of reservoir

bodies is the result. Very small isolated patches are not representative for the depositional environment, with exception of few scour fills. Furthermore, the variograms were not reliable enough to use the SIS algorithm with a high degree of confidence. To conclude, the SIS method has not been used to model the Favignana calcarenite.

### **7.6.3 Truncated Gaussian simulation**

Like the SIS method, the truncated Gaussian simulation (TGS) uses an algorithm provided by the GSLIB. The same input parameters can be given. The difference between the two methods is the handling of a transition between facies. TGS handles this in a more natural way, making it suitable for e.g. carbonate depositional systems and shallow marine environments. The algorithm itself is based on a normal distribution of the facies data.

The TGS model (figure D.8) shows little improvement when compared to the SIS model discussed before. The amount of isolated patches is reduced due to the introductions of more natural transition between facies, but there is still no option to include information that is geologically meaningful. Despite the transition algorithm, especially at the boundary of two main facies regions still noisy grid cells with mainly tabular and through cross-lamination exist. Again, TGS appears not to be a suitable algorithm for a model of a fieldwork area.

### **7.6.4 Indicator kriging**

Indicator kriging is the only deterministic facies modelling algorithm in Petrel<sup>®</sup>. The algorithm discussed previously are all based on stochastic methods, which use a random seed for interpolation. Indicator kriging is a way to use a kriging method on discrete properties like facies. Main input for this algorithm is the variogram, introducing weaknesses like sensitivity to dominant facies, few data points, or bad variogram quality.

## 8 Conclusions

1. The island of Favignana, located a few kilometres off the coast of western Sicily (Italy), is the island of the Aegadian archipelago that shows the largest development of Lower Pleistocene sediments. The mountainous structures of all three islands are the result of the Alpine orogeny and subsequent uplift due to strike-slip movement, and consist mainly of limestone. Favignana is unique because of its relatively low-relief eastern part, where quarrying of the calcarenite rock has been going on for centuries.
2. The detailed sedimentological descriptions in the field and microfacies analysis of the eastern Favignana calcarenite indicates a typical foramol grain association. These bioclastic carbonate-rich sediments have been interpreted as generated in a high-energy dominated, open shelf, cool-water/temperate environment.
3. Storm-related events caused the bioclastic sediment to be either 1) transported from a productive platform; or 2) reworked and deposited at the same location. The dominance of northwestern to northern winds in this part of the Mediterranean introduced a predominant south to southeast transport direction in the sedimentary structures. The northeastern part of Favignana is influenced by storms from the north, and therefore shows a system that builds out to the south, while the rest of the complex predominantly progrades to the southeast.
4. Eastern Favignana is unique because of the progradation towards the mainland of Sicily. Comparable deposits in the Mediterranean show calcarenites deposited on the shelf of a large landmass. The habitat of the organisms was at the same location, and storm events caused the skeletal material to be reworked and deposited. The eastern Favignana calcarenite is interpreted as being deposited in a submarine environment, possibly on the shelf of an already existing channel-like depression between the older mountainous structures of Favignana and Levanzo.
5. A wide range of sedimentary structures are observed in the field, indicating a varying supply of both sediment and energy. Apart from the main progradation towards the southeast, a system that scours into the earlier deposited sediments is recognised. Scours of up to 20 metres provided a highway for sediment to be transported to the lobes of the system. Scour fills show thick homogeneous units. Locally the amount of energy was high enough to develop critical flow conditions. As a result,

undulations in the lamination and the related smaller scale scour-and-fill systems are abundant in some regions.

6. The conceptual geological model provided the possibility to create a training image for a multi-point statistics facies modelling algorithm. Compared to other conventional methods, this relatively new technique resulted in a geologically more realistic facies model which can be validated by comparison with outcrop data. This model can be used to distribute reservoir properties for volume calculation and dynamic simulations.
7. Effective porosities ranging from 0.45 to 0.65 (fraction of bulk volume) and permeability values of tens of darcy are promising regarding the hydrocarbon reservoir potential. The presence of cement around fractures and the fact that hardly any compaction has taken place however, requires a more comprehensive analysis of diagenetic processes when comparing the Favignana calcarenite to an analogue reservoir in the subsurface.
8. The Asmari limestone reservoirs in the Middle East show similar depositional environments. This study might provide new insight in the architecture of these reservoirs, and can therefore help the accurate static and dynamic modelling of these reservoirs. A new foramol-associated giant gas field in Venezuela might also be a very useful application for the result of this study.

## 9 Recommendations

This project represents an unprecedented attempt to analyse eastern Favignana’s depositional history and internal architecture from a hydrocarbon reservoir point of view. The large extension of the outcrops — together with the relatively limited time span — resulted in a very broad investigation. At the moment of writing, a similar study carried out at the University of Utrecht is focussing on the detailed sedimentological description of the calcarenite complex. An additional comprehensive microscopical description, based on a large number of samples sampling and a detailed sedimentological approach rather than a petroleum engineering perspective will hopefully increase the insight into the Favignana calcarenite.

In addition to the ongoing research, few recommendations are presented below in order to improve the scientific knowledge of the area.

1. Constraints in budget and transportation limited the number of samples large enough to produce plugs for tests on reservoir properties. In addition the samples were taken in the first fieldwork campaign, when a final facies subdivision was not yet defined. The result was a lack of samples representative of certain facies. A more extensive and comprehensive sampling campaign would therefore greatly improve the quality of the porosity and permeability dataset.
2. The creation of thin sections from calcarenite with low cementation poses some technical difficulties. Abrasion during the cutting and polishing can change the original orientation and situation of the grain particles. It is very likely that the thin sections presented in this thesis have been subjected to this kind of mechanical deformation. Other techniques in order to make thin sections were not available at the TU Delft, however more professional laboratories might be able to produce higher quality thin sections. In this way it would be possible to obtain porosity measurements from microscopical image analysis.
3. The MPS facies modelling algorithm is very sensitive to the training image input. A more experienced approach to make this image would possibly improve the quality of the facies model. Another improvement can be achieved with a higher pseudo-well density resulting from more fieldwork in the area.
4. Additional investigation of the calcarenites deposited on the mainland of Sicily, between Trapani

and Marsala can enhance the knowledge of the regional geological setting. Previously a research project by D'Angelo & Vernuccio (1996) focussed on chronostratigraphy of the depositional terraces in the so-called *calcarenite di Marsala*. A detailed stratigraphical approach is recommended for an additional fieldwork campaign in the area.

5. At the moment of writing a project by the APAT — the Agenzia per la protezione dell'ambiente e per servizi tecnici — is ongoing in order to establish a high quality geological map of the Aegadian islands. The map of Marettimo and western Favignana is already available (D'Angelo et al., 2005), however the part with eastern Favignana is still in progress. The maps include several useful features, such as bathymetry maps and isopach maps of the Plio-Pleistocene. Publication of the remaining parts can be useful to reconstruct the geological evolution Favignana calcarenite and to validate the conceptual geological model proposed in this thesis.
6. An improvement regarding the permeability tests can be made by using a portable probe permeameter. This apparatus allows permeability measurements to be taken directly on the outcrops. In this way the number and the resolution of the results can be increased.
7. A cooperation with the E&P industry improves the usefulness of Favignana as a reservoir analogue. Information about hydrocarbon producing reservoirs is often confidential, so research in that area is challenging. It is worth considering a joint project in case of a possible extension of this thesis.
8. Further research — i.e. core drilling or seismic evaluation — might improve the knowledge or confirm the hypothesis of the location and extensiveness of carbonate generating platforms contributing to the sediment supply.



# References

- Abate, B., Incandela, A., & Renda, P. (1997). Carta geologica delle Isole di Favignana e Levanzo. Dipartimento di geologia e geodesia dell'universita' di Palermo.
- Alsharhan, A., & Nairn, A. (1997). *Sedimentary basins and petroleum geology of the Middle East*. Elsevier.
- Azim, S., Al-Ajmi, H., Rice, C., Bond, D., Abdullah, S., & Laughlin, B. (2003). Reservoir description and static model build in heterogeneous Maaddud carbonated: Raudhatain field, north Kuwait (SPE 81524). In *SPE 13<sup>th</sup> Middle East oil show & conference, Bahrain*.
- Bhushan, V., & Hopkinson, S. (2002). A novel approach to identify reservoir analogues. In *European Petroleum Conference, 29-31 October 2002, Aberdeen, United Kingdom*. Society of Petroleum Engineers Inc.
- Box, G., & Draper, N. (1987). *Empirical model-building and response surfaces*. John Wiley & Sons, Inc.
- Brown, A., & Hussein, S. (1977). Permeability from well logs: Shaybah field, Saudi Arabia. In *SPWLA eighteenth annual loggin symposium*.
- Carannante, G., Esteban, M., Milliman, J., & Simone, L. (1988). Carbonate lithofacies as paleolatitude indicators: problems and limitations. *Sedimentary Geology*, 60, 333–346.
- Catalano, R., Merlini, S., & Sulli, A. (2002). The structure of western Sicily, central Mediterranean. *Petroleum Geoscience*, 8(1), 7–18.
- Cohen, K., & Gibbard, P. (2010). Global chronostratigraphical correlation table for the last 2.7 million years. *Subcommission on Quaternary Stratigraphy*.
- Couvering (van), J., Castradori, D., Cita, M., Hilgen, F., & Rio, D. (2000). The base of the Zanclean stage and of the Pliocene series. *Episodes*, 23(3), 179–187.
- Dake, L. (1978). *Fundamentals of reservoir engineering*. Elsevier science.
- Daly, C., & Caers, J. (2010). Multi-point geostatistics - an introductory overview. *First Break*, 28, 39–47.
- D'Angelo, S., Catalano, R., Mancuso, M., Agate, M., & Lo Cicero, G. (2005). Carta geologia d'Italia, foglio 604, Isole Egadi. APAT - Agenzia per la protezione dell'ambiente e per servizi tecnici.
- D'Angelo, U., & Vernuccio, S. (1996). I terrazzi marini quaternari della estremità occidentale. *Mem. Soc. Geol. It.*, 51, 585–594.
- Di Stefano, A., & Longhitano, S. (2009). Pleistocene mixed siliciclastic/bioclastic sedimentary successions of the Ionian Peloritani mountains (NE Sicily, Southern Italy): the onset of opening of the Messina Strait. *Central European journal of geosciences*, 1(1), 33–62.
- Flügel, E. (2010). *Microfacies of carbonate Rocks*. Springer Verlag, 2<sup>nd</sup> ed.
- Hansen, K. (1999). Development of a prograding carbonate wedge during sea level fall: lower Pleistocene of Rhodes, Greece. *Sedimentology*, 46, 559–576.
- Incandela, A. (1996). Deformazioni Neogeniche nelle Isole di Favignana e Levanzo. *Mem. Soc. Geol. It.*, 51, 129–135.

- Leeder, M. (1999). *Sedimentology and sedimentary basins: from turbulence to tectonics*. Blackwell Science Ltd.
- Lees, A., & Buller, A. (1972). Modern temperate-water and warm-water shelf carbonate sediments contrasted. *Marine Geology*, 13, 67–73.
- Martín, J., Braga, J., Aguirre, J., & Betzler, C. (2004). Contrasting models of temperate carbonate sedimentation in a small Mediterranean embayment: the Pliocene Carboneras basin, SE Spain. *Journal of the Geological Society, London*.
- Massari, F., & Chiocci, F. (2006). Biocalcarene and mixed cool-water prograding bodies of the Mediterranean Pliocene and Pleistocene: architecture, depositional setting and forcing factors. *Geological Society, London, Special Publications*, 255(1), 95–120.
- Pedley, M., & Grasso, M. (2002). Lithofacies modelling and sequence stratigraphy in microtidal cool-water carbonates: a case study from the Pleistocene of Sicily Italy. *Sedimentology*, 49, 533–553.
- Pomar, L., & Tropeano, M. (2001). The Calcarene di Gravina Formation in Matera (Southern Italy): New insights for coarse-grained, large-scale, cross bedded bodies encased in offshore deposits. *AAPG Bulletin*.
- Qassim, N., Jawad, W., & Abdulwahab, A. (2003). Creative modeling of a heterogeneous carbonate reservoir on Bahrain field (Karaib reservoir) (SPE 81531). In *SPE 13<sup>th</sup> Middle East oil show & conference, Bahrain*.
- Rao, R., & Talukdar, S. (1980). Petroleum geology of Bombay high field, India. In *M 30: Giant Oil and Gas Fields of the Decade 1968–1978*, (pp. 487–506). AAPG.
- Reading, H. (1996). *Sedimentary Environments: Processes, Facies and Stratigraphy*. Blackwell Science Ltd.
- Schlumberger (2009). Petrel online manual. Version 2009.1.
- Schlumberger (2010). Schlumberger Oilfield Glossary ([www.glossary.oilfield.slb.com](http://www.glossary.oilfield.slb.com)).
- Simone, L., & Carannante, G. (1988). The fate of foramol ("temperate-type") carbonate platforms. *Sedimentary Geology*, 60, 347–354.
- Southard, J. (1996). *Special topics: An introduction to fluid motions, sediment transport, and current-generated sedimentary structures*, chap. 16. MIT OpenCourseWare.
- Southard, J., & Boguchwal, L. (1990). Bed configurations in steady unidirectional water flows. part 2. synthesis of flume data. *Journal of Sedimentary Petrology*, 60(5), 658–679.
- Tavernelli, E., Renda, P., Pasqui, V., & Tramutoli, M. (2003). Composite structures resulting from negative inversion: and example from the Isle of Favignana (Egadi Islands). *Boll. Soc. Geol. It.*.
- Tucker, M., & Wright, V. (1990). *Carbonate sedimentology*. Blackwell science.
- Wilson, M., & Vescei, A. (2005). The apparent paradox of abundant foramol facies in low latitudes: their environmental significance and effect on platform development. *Earth-Science Reviews*, 69, 133–168.
- Wolf, K. (2010). Practical on Petrophysics (TA3500). *Delft University of Technology*.
- Zhang, T. (2008). Incorporating geological conceptual models and interpretations into reservoir modeling using multiple-point geostatistics. *Earth Science Frontiers*, 15(1), 26–35.

# A Maps and charts

This appendix includes a variety of maps and charts to illustrate some important aspects of the island of Favignana. An overview of the maps is given below.

**Table A.1** – List of maps of Favignana used in this study.

Map	Description
A.1	Geological map of onshore western Sicily
A.2	Nautical map of the Aegadian archipelago
A.3	Detailed map of Favignana with geographical locations
A.4	Favignana fieldwork area indicating quarried parts
A.5	Chronostratigraphical correlation

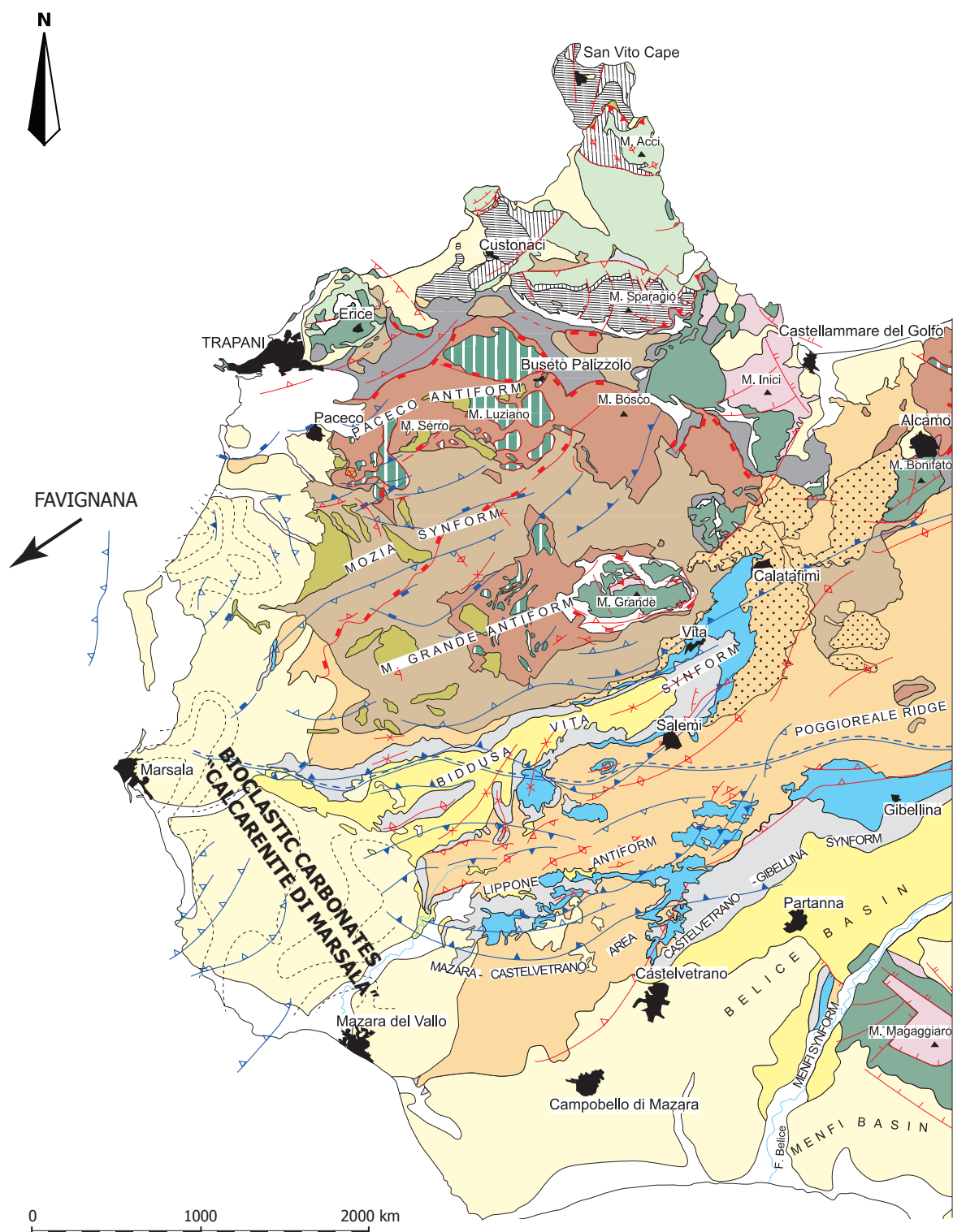


**Figure A.1** – Geological map of the onshore area of western Sicily. The complexity of the geological structures in Sicily contrasts considerably with the relatively undeformed Pleistocene clastic carbonates (marked on the map). Map modified after Catalano et al. (2002).

**Figure A.2** – Nautical map of the Aegadian archipelago showing the islands of Favignana, Levanzo and Marettimo. Image courtesy of the *Area Marina Protetta delle Isole Egadi*.

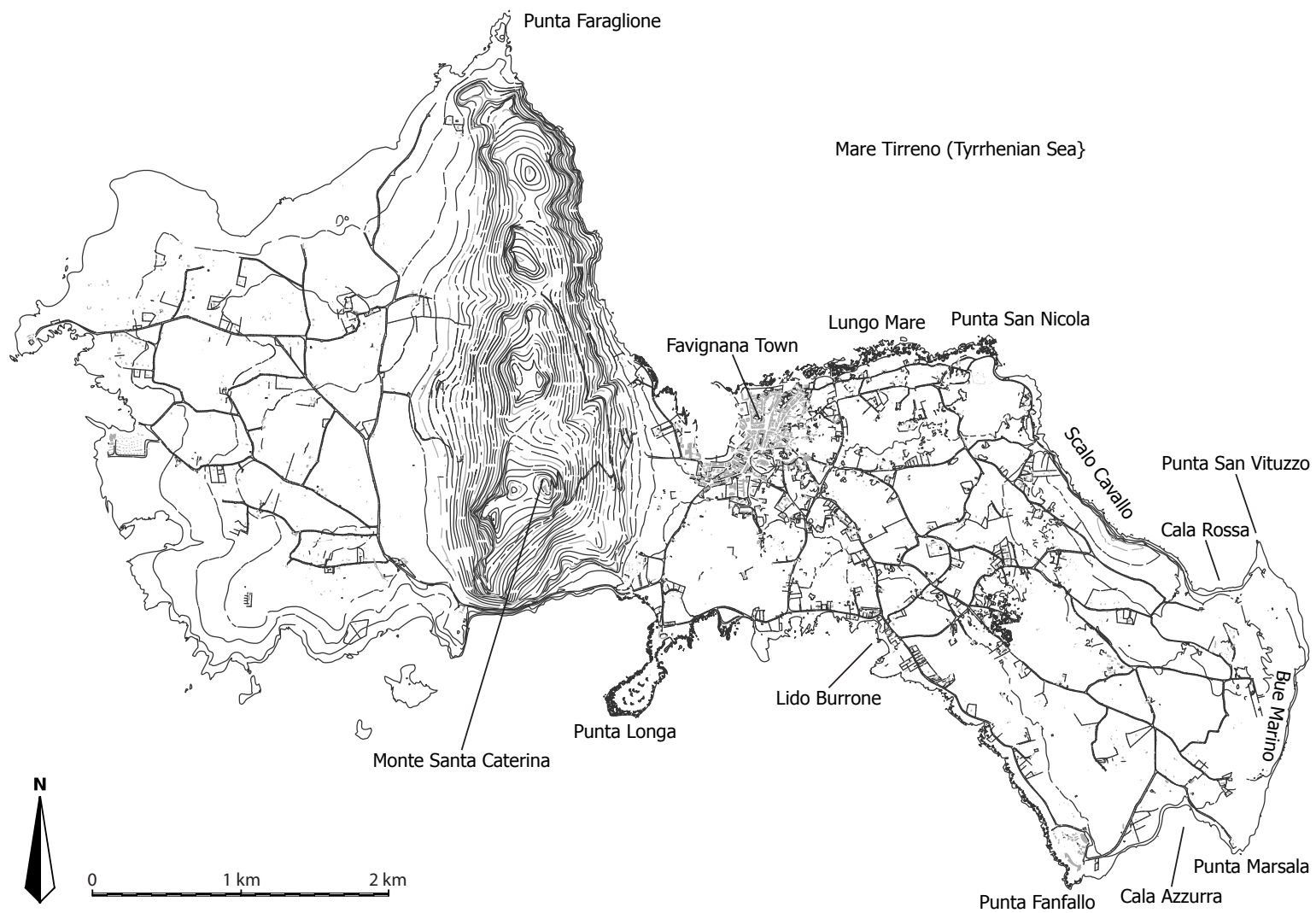


**Figure A.3** – Map of Favignana showing the locations as they are used in this report.

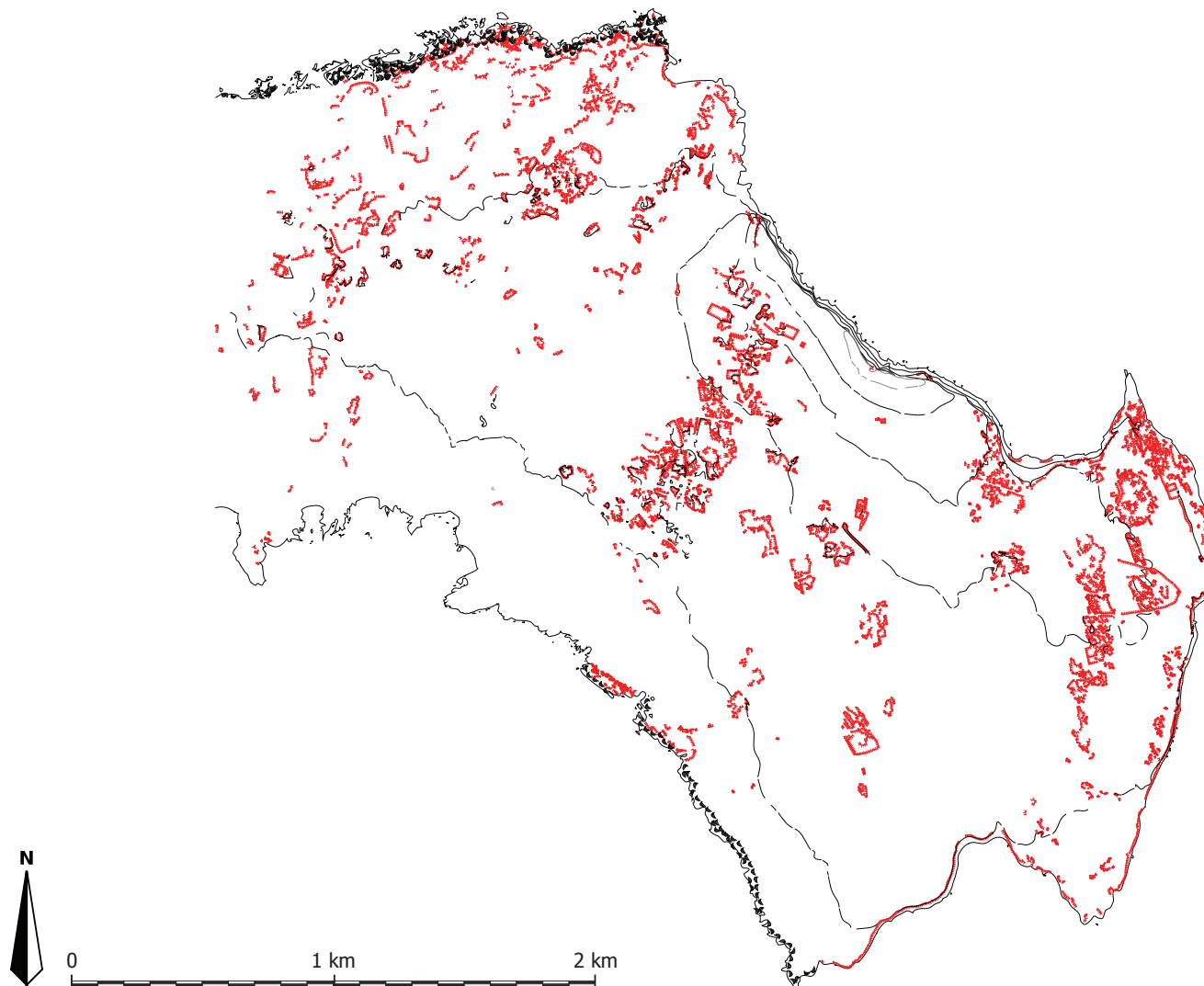


**Figure A.4** – The fieldwork area on the eastern part of Favignana. The quarries are indicated in red.



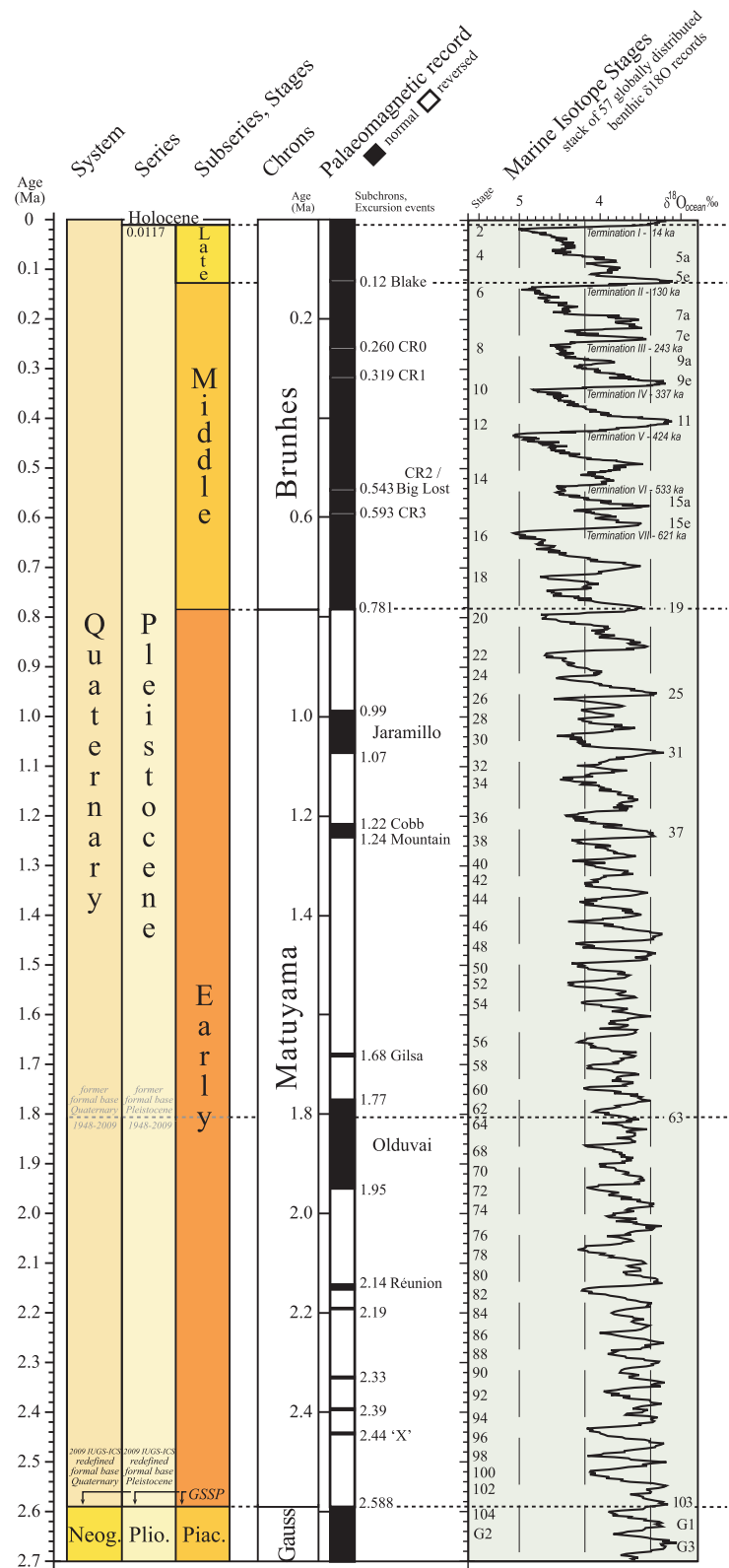


**Figure A.5** – Chronostratigraphical correlation of the Lower Pleistocene to present day situation. The sea level curve is reflected by marine isotope analysis. Chart modified from Cohen & Gibbard (2010).



## B Geological photo panels

To illustrate some interesting sedimentary structures, several photo sequences have been acquired in the field and photo panels are made. They consist of on average four to five photos stitched together to form a wide screen panorama. The interpreted structures are displayed below the panels. Below is an overview of the different interpreted locations and related panels in this report.

**Table B.1** – Overview of the geological photo panels.

Panel	Location	Feature(s)
B.2	Cala Rossa	Dune progradation
B.3	Scalo Cavallo	Big scour fills
B.4	Bue Marino	Scour and fill sequence
B.5	Cala Azzurra	Large scale foresets
B.6	South of Scalo Cavallo	Thickness and quarrying

The map below shows the location of the photo panels. The index refers to the figure number of the corresponding panel.

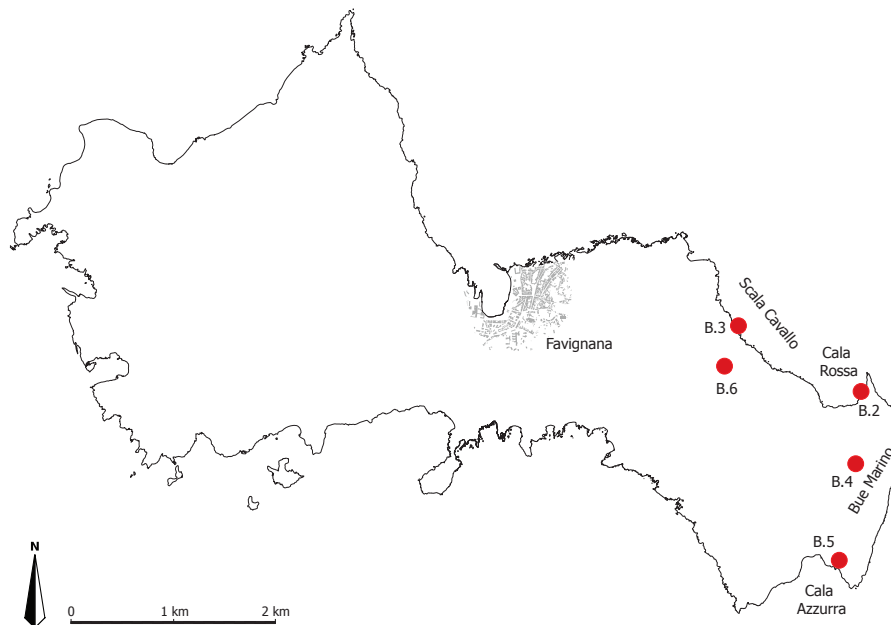


**Figure B.1** – Locations of the photo panels shown in this appendix.

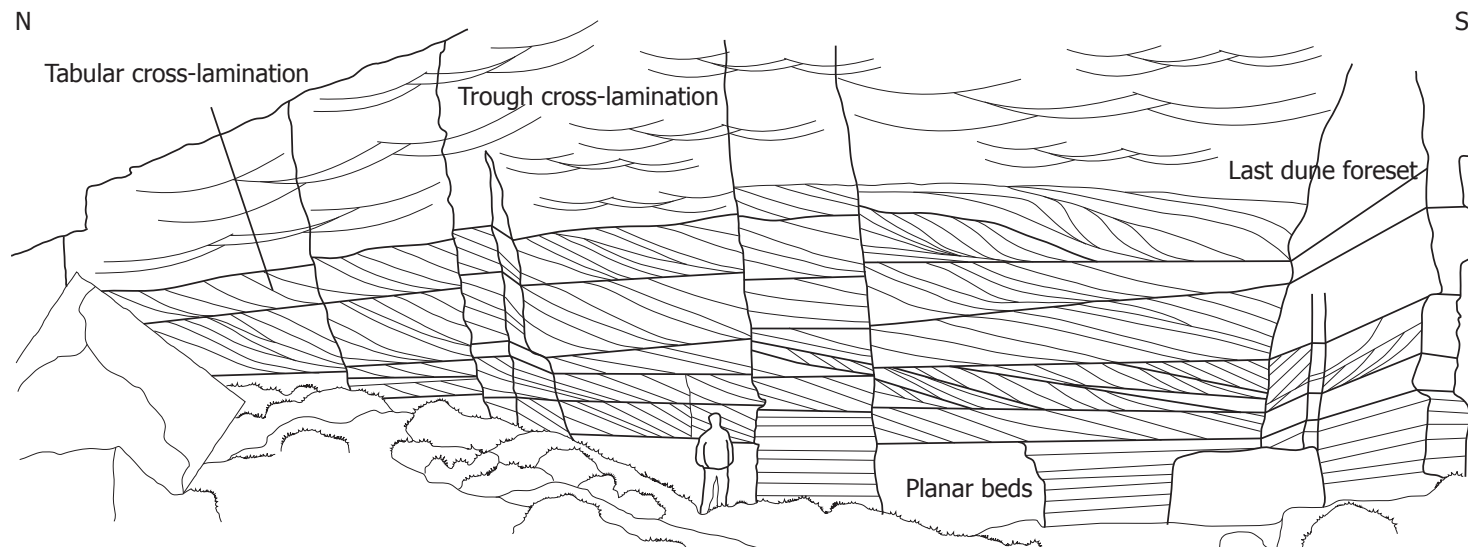


**Figure B.2** – Outcrop of the eastern part of Cala Rossa. The change from a more planar bedding to dunes with linear crest and finally undulated crest is clearly visible. Also notice the end of a set of dunes with tabular cross-lamination, overlain by trough cross-laminated units. Person for scale.

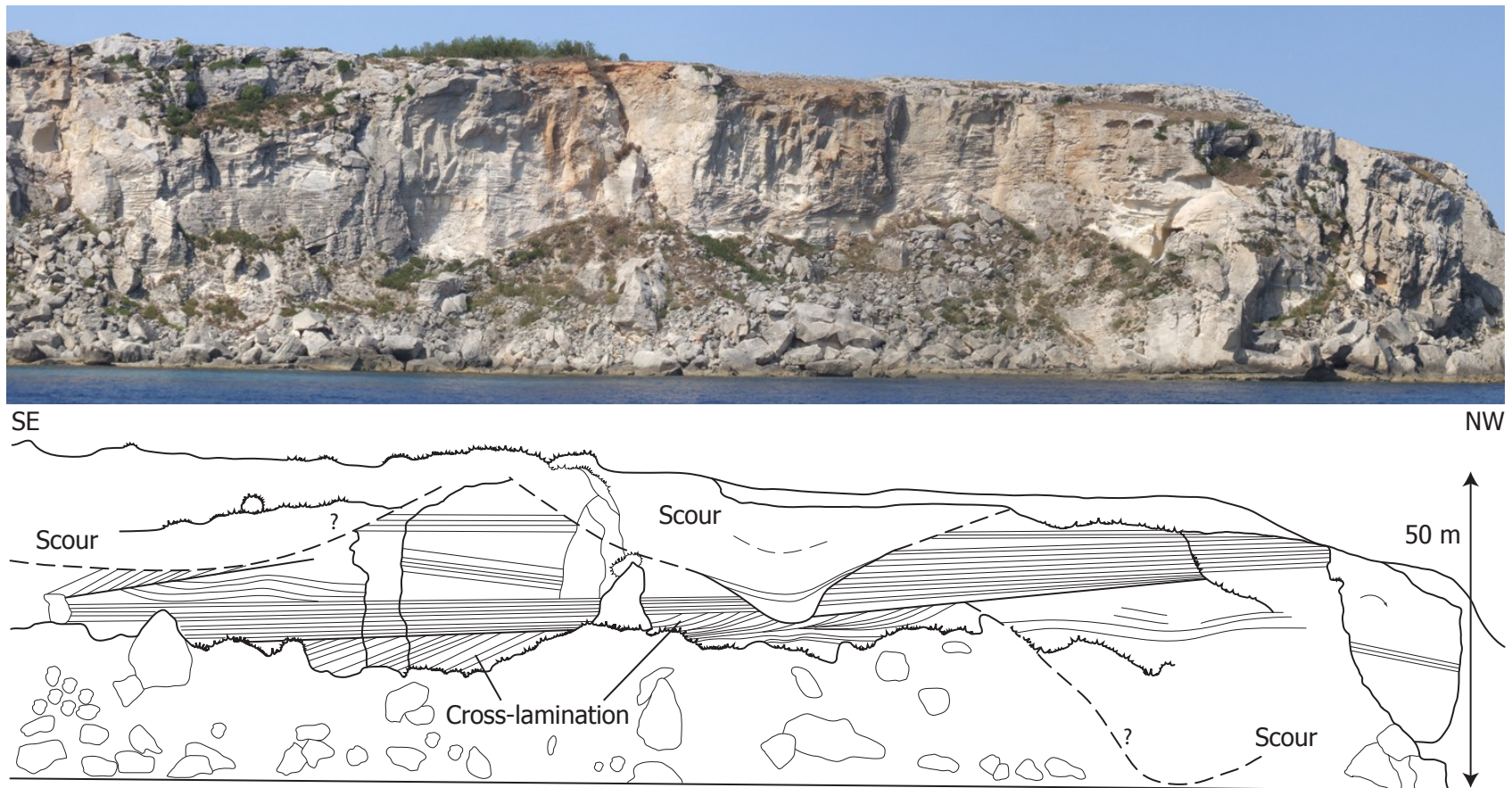


**Figure B.3** – Photo panel of the Scala Cavallo cliff face. Note the large scours incising the older sedimentary rock.



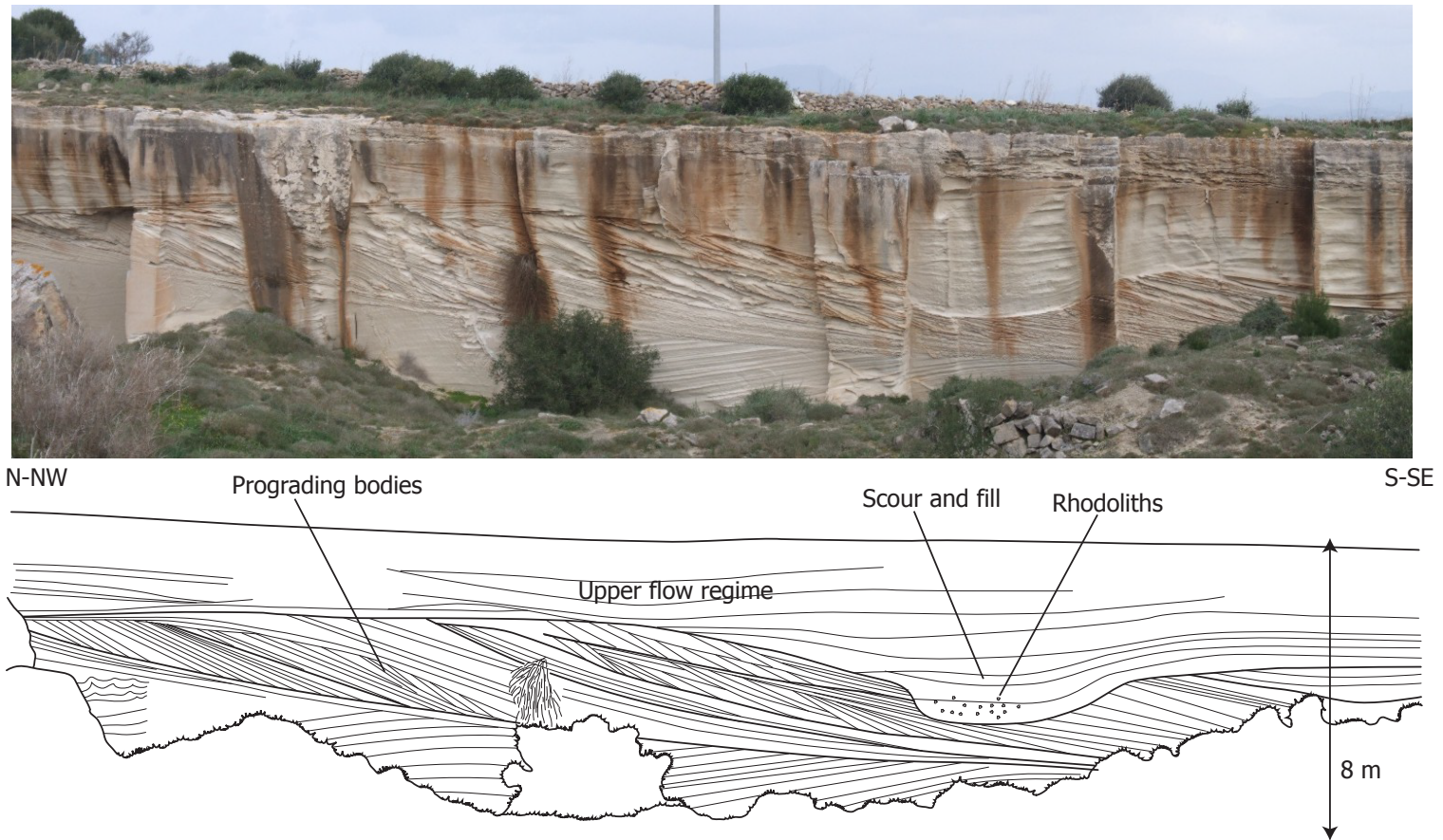


**Figure B.4** – High energy development of a scour and fill system. Similar geometries are observed elsewhere, however of smaller scale.

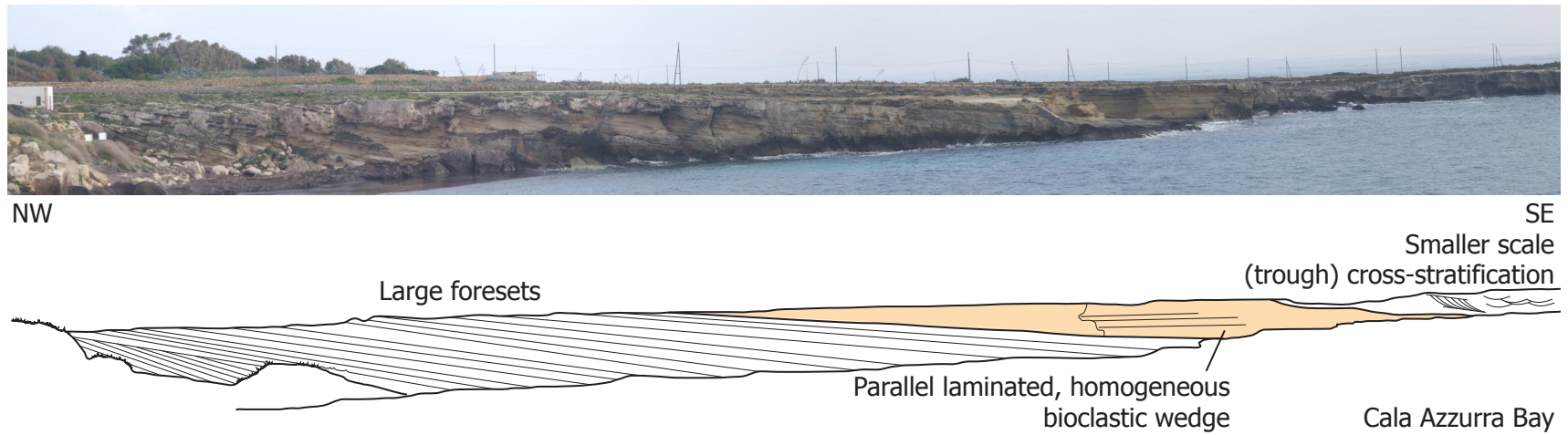


**Figure B.5** – Large foresets in the Cala Azurra bay, prograding to the southeast.



**Figure B.6** – Abandoned quarry south of the Scalo Cavallo cliff to illustrate the general thickness of the calcarenite. Note the 'skyscraper' left behind in the centre of the quarry, which is about 20m high.

## C Facies description and properties

**Table C.1** – Facies overview

Facies	Lithology	Sedimentary structure	T [m]	D <sub>gr</sub> [ $\mu$ m]	Description & Interpretation
Massive calcarenite	Calcarenite	Massive or faint lamination	up to 3	500–2000	Thick units deposited by very high sedimentation rates. Non fragmented bioclasts are abundant.
Parallel laminated units	Calcarenite	Planar beds with parallel lamination	1–3	$\pm$ 300	Relatively fine lamination parallel to bedding, most likely caused by a lower plane flow regime.
Undulated scour and fill system	Calcarenite	Undulated lamination and massive fills	2–15	—	Upper flow regime beds developing undulated lamination, in some cases small antidunes are preserved. Locally the amount of energy causes scours to form, immediately filled with homogeneous material due to the hydraulic jump. Big scours due to erosion are infilled by structureless deposits.
Tabular cross-layering	Calcarenite	Tabular cross-layering	up to 2	500–2000	Locally very large foresets, interpreted as prograding dunes with palaeo-transport direction indicated by highest dip angle. Some units on-lap on their base, and occasionally periodic cyclicity in the thickness of lamina is observed.
Trough cross bedded units	Calcarenite	Trough cross-bedding	up to 2	500–2000	The trough cross bedded calcarenites are generated by dunes with curved crests.
Large scale propagating dunes	Calcarenite	Planar foresets	up to 5	—	Very large scale foresets, up to 15 m in height. Indicates giant dunes prograding in the main transport direction. Concentrated in specific parts of the island.
Bioturbated units	Calcarenite	Massive or faint lamination	up to 1	—	Thick units with no recognizable structure, indicating long periods without energy and sediment supply. The beds are usually without any depositional dip.
Clay	Clay	Massive or faint lamination	$\geq$ 2	—	Found at the lower boundary of the East-Favignana sequence. Possibly known as the Trubi Formation across other parts of the Mediterranean.

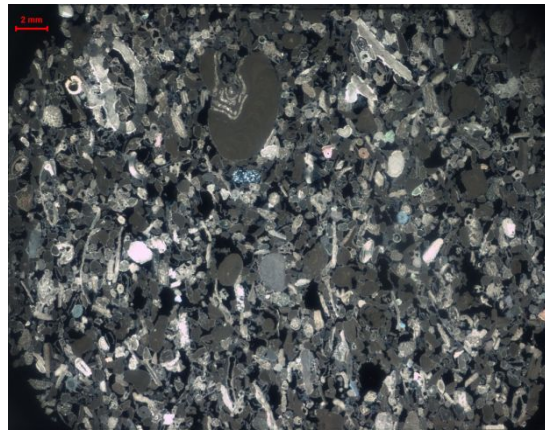
**Table C.2** – Results of laboratory experiments on plugs from the Favignana calcarenite. Porosity and permeability are listed in the rightmost columns. Plugs with indicated with H are taken horizontally, V indicates vertical plugs.

	Plug		L [mm]	D [mm]	M <sub>dry</sub> [g]	V <sub>b</sub> [cm <sup>3</sup> ]	V <sub>ma</sub> [cm <sup>3</sup> ]	$\rho_{ma}$ [g <sup>3</sup> ]	$\phi$ [-]	k [D]
1	1.1.a	H	30.4	19.6	14.8	9.2	5.4	2.75	0.41	
	1.1.b	H	30.3	19.6	14.3	9.1	5.2	2.74	0.43	
	1.2.a	H	30.4	36.4	31.5	31.6	11.6	2.71	0.63	67
	1.2.b	H	30.4	36.5	31.9	31.8	11.8	2.71	0.63	66
	1.3.a	H	30.2	36.4	33.0	31.4	12.1	2.71	0.61	43
	1.3.b	H	30.3	36.4	32.8	31.5	12.1	2.71	0.62	44
	1.4.a	V	30.2	36.3	29.5	31.3	10.9	2.71	0.65	79
	1.4.b	V	30.4	36.4	30.1	31.6	11.1	2.71	0.65	59
	1.5.a	H	30.2	35.9	29.7	30.6	11.0	2.71	0.64	98
2	1.5.b	H	30.4	36.5	31.4	31.8	11.6	2.71	0.64	74
	2.1.a	H	30.0	37.3	46.9	32.8	17.3	2.71	0.47	72
	2.1.b	H	30.4	37.3	48.0	33.2	17.7	2.71	0.47	54
	2.2.a	H	30.5	37.2	47.7	33.1	17.6	2.71	0.47	57
	2.2.b	H	30.1	36.9	46.7	32.2	17.2	2.71	0.47	61
	2.3	V	30.5	37.6	49.8	33.9	18.4	2.71	0.46	35
3	2.4	V	30.5	37.3	48.9	33.3	18.0	2.71	0.46	36
	3.1.a	H	29.7	19.9	17.0	9.2	6.2	2.75	0.33	
	3.1.b	H	30.7	19.8	16.2	9.5	5.9	2.75	0.38	
	3.2.a	H	30.1	36.6	36.4	31.7	13.4	2.72	0.58	341
	3.2.b	H	29.9	36.9	36.3	32.0	13.3	2.72	0.58	312
	3.3	H	30.5	36.6	40.2	32.1	14.8	2.72	0.54	65
4	4.1	H	30.3	36.5	35.2	31.7	12.9	2.72	0.59	324
	4.2	H	30.5	36.4	36.9	31.7	13.6	2.71	0.57	217
5	5.1.a	H	30.4	36.5	39.3	31.8	14.5	2.71	0.54	56
	5.1.b	H	30.2	36.6	38.9	31.8	14.4	2.70	0.55	98
	5.2.a	V	30.3	36.5	39.1	31.7	14.4	2.72	0.55	26
	5.2.b	V	30.1	36.2	36.7	31.0	13.5	2.71	0.56	61
	5.2.c	V	30.3	36.3	38.2	31.4	14.1	2.72	0.55	46
	5.3.a	H	30.4	36.5	38.7	31.8	14.3	2.71	0.55	56
	5.3.b	H	30.5	36.5	38.2	31.9	14.1	2.72	0.56	52
6	6.1	H	30.1	36.1	37.9	30.8	11.7	2.74	0.62	102
	6.2	V	30.2	36.5	32.8	31.6	12.1	2.18	0.62	62
	6.3.a	H	30.0	36.4	32.4	31.2	11.8	2.74	0.62	86
	6.3.b	H	30.0	36.2	31.7	30.9	11.6	2.74	0.62	89
8	8.1.a	H	30.2	35.7	36.1	30.2	13.4	2.70	0.56	31
	8.1.b	H	30.6	35.2	35.3	29.8	13.1	2.70	0.56	
	8.2	H	30.4	36.7	38.1	32.2	14.0	2.72	0.56	35

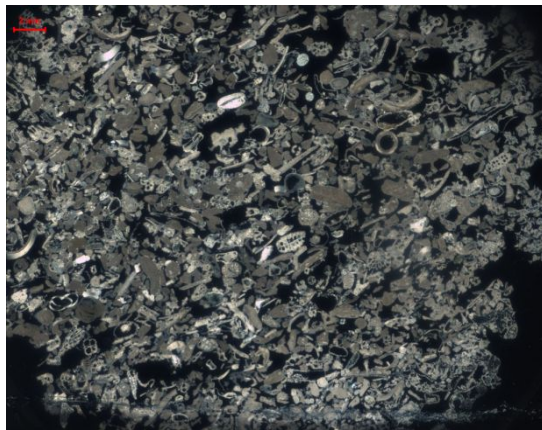




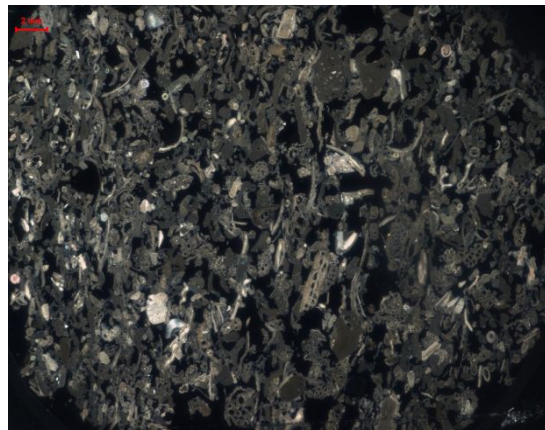
(a) 1.2



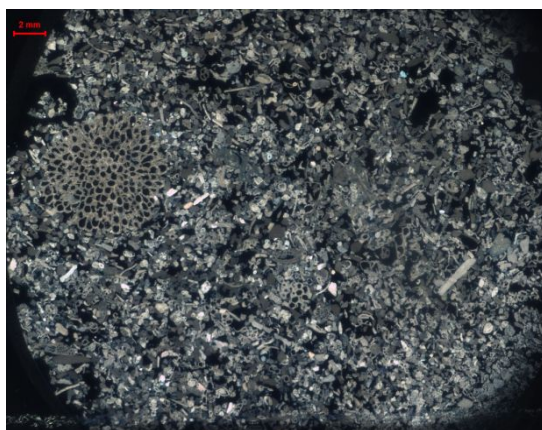
(b) 2.1



(c) 3.2



(d) 4.1



(e) 5.1



(f) 6.1

**Figure C.1** – Overview of the thin sections with polarisation filter activated. For grain-size analysis it may be useful to examine the thin sections with a small magnification. The red line in the top left corner of these images is two millimetres — or  $2000\ \mu\text{m}$  — wide. Table 3.1 can be consulted for the sample numbering.

## D Modelling results

This appendix provides an overview of the results of the facies modelling. Chapter 6 can be consulted as a guidance for the MPS modelling. After this model some the alternative algorithms —discussed in section 7.6 — are shown. The table below gives an overview of the material reported in this appendix.

**Table D.1** – List of figures used to illustrate different aspects of the Favignana facies model.

Model	Description
D.1	The facies logs from fieldwork data used as input
D.2	Examples of $\mathbf{k}$ layers of the training image grid
D.3	Probability maps
D.4	Probability maps (continued)
D.5	Close-ups of the final Multi-point statistics model
D.6	Porosity model
D.7	Sequential indicator simulation model
D.8	Truncated Gaussian simulation model

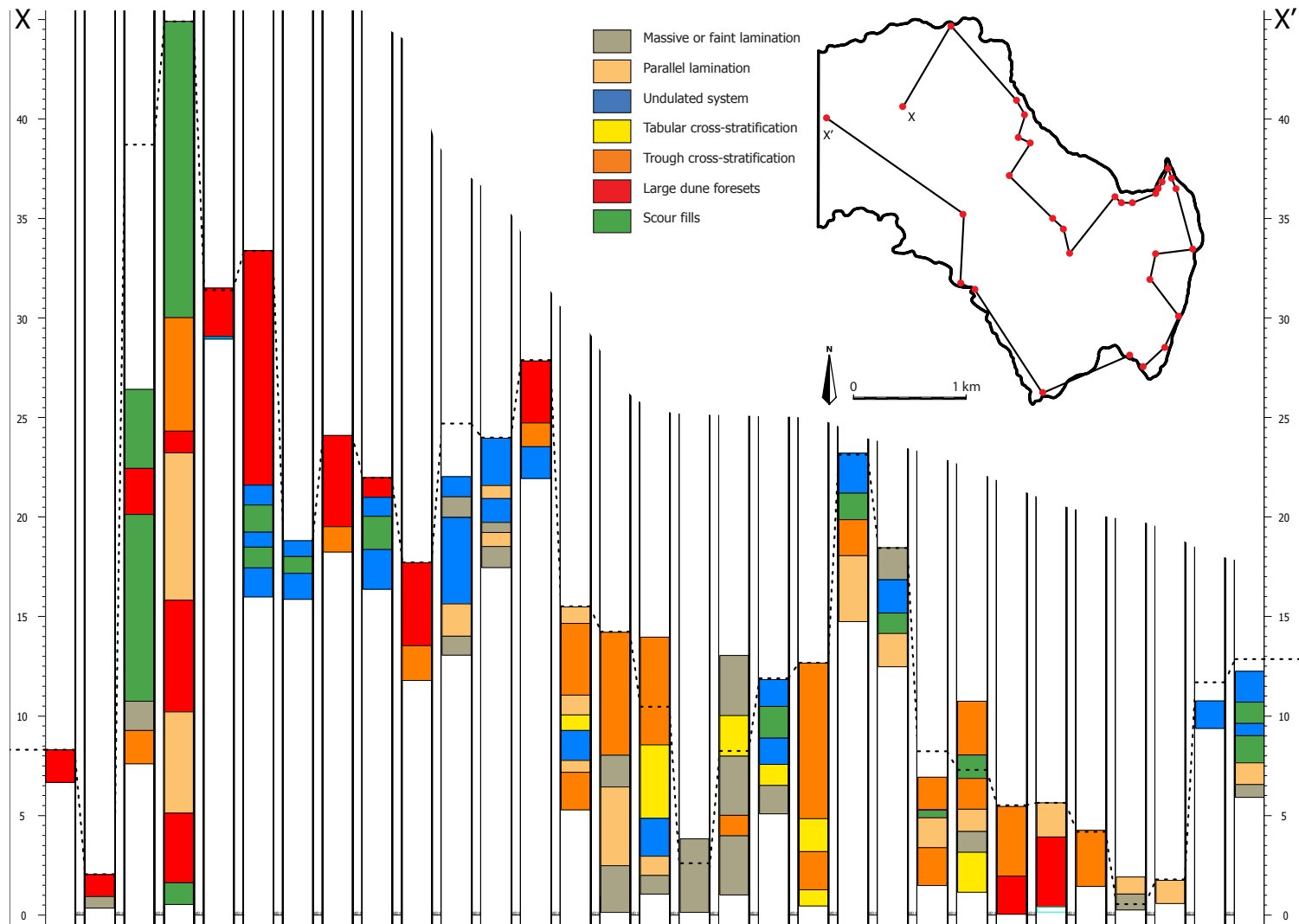


**Figure D.1** – Facies logs in all fieldwork locations, which are used as input in the facies model. The trajectory is shown in the top left, and the dotted line represents the surface of the island. Elevation in metres above mean sea level.

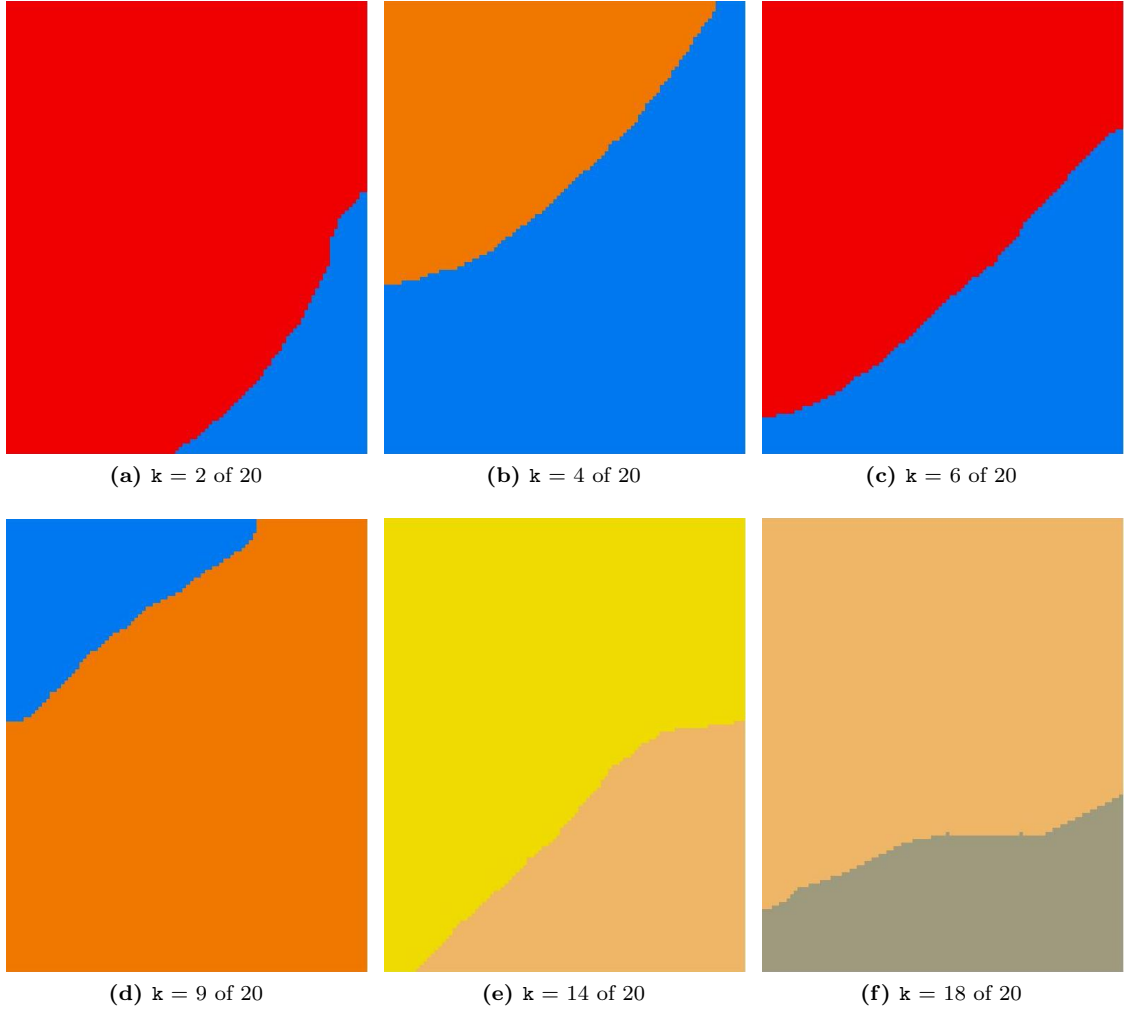


**Figure D.2** – Intermediate slices of the training image used in the MPS modelling algorithm. The north is pointing upwards, scale not relevant.

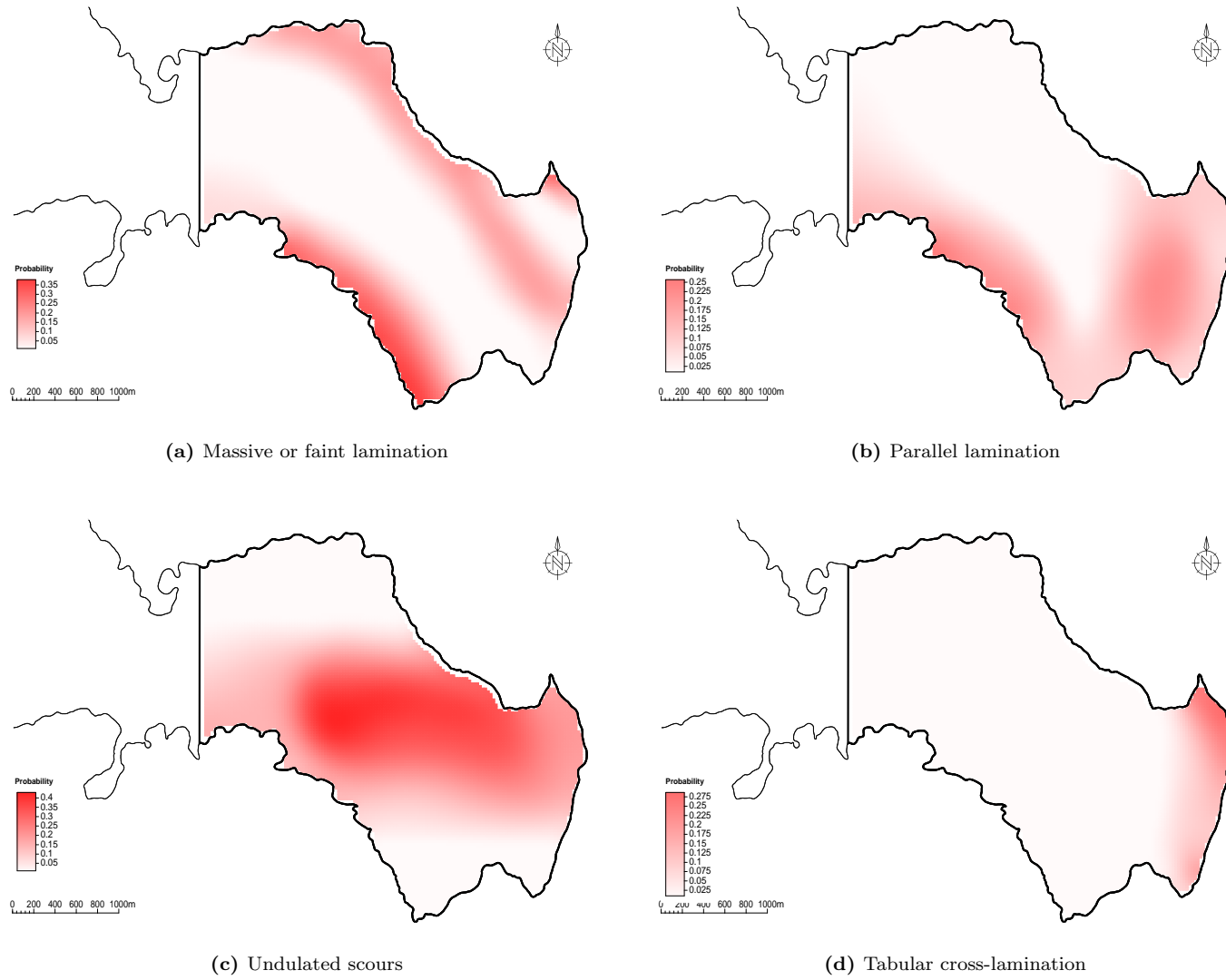


**Figure D.3** – Probability maps of the facies functioning as additional input data in the modelling process.

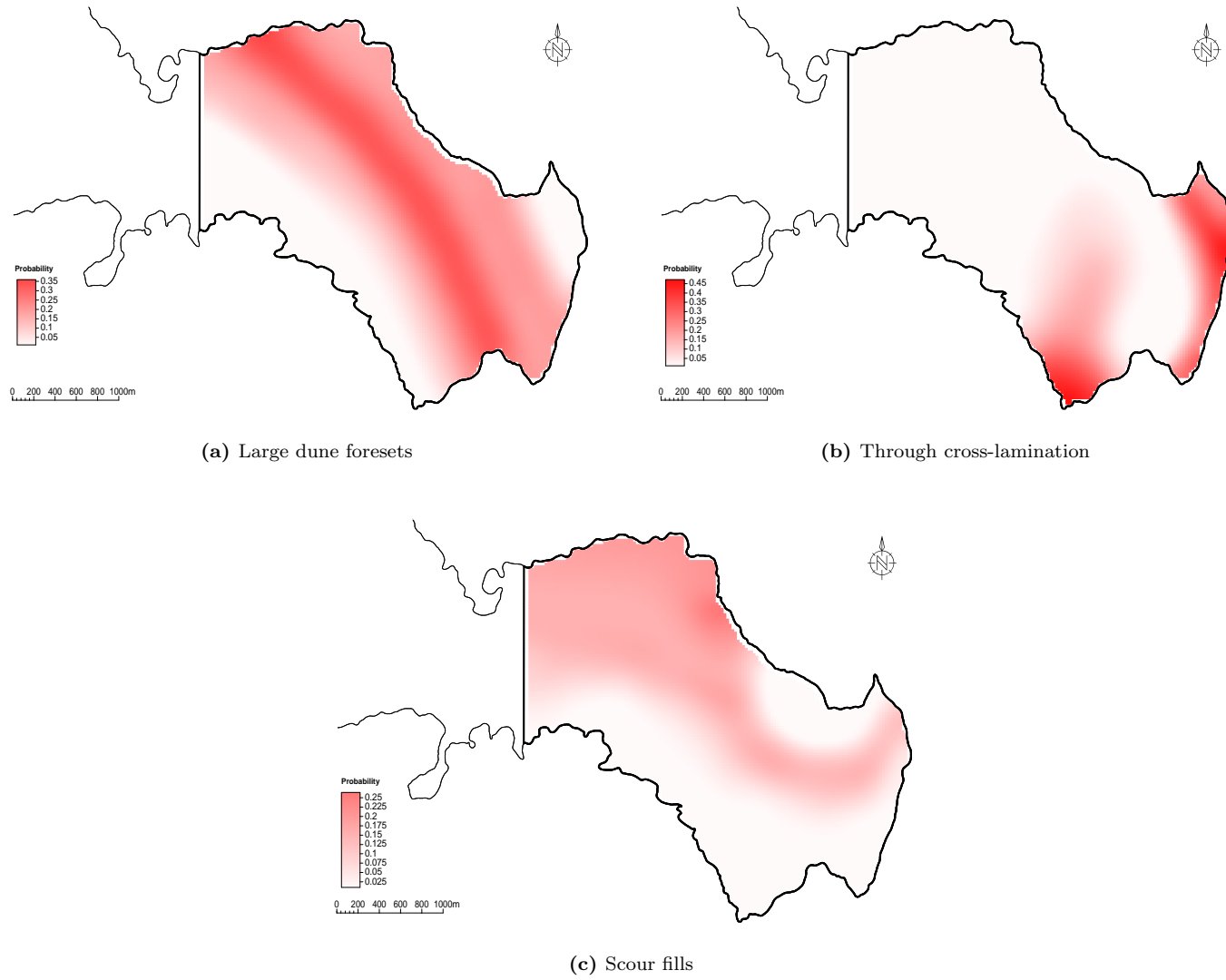
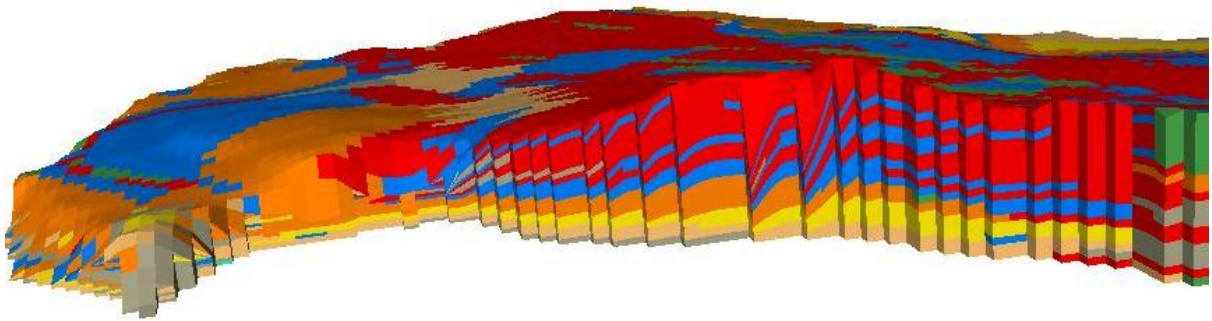
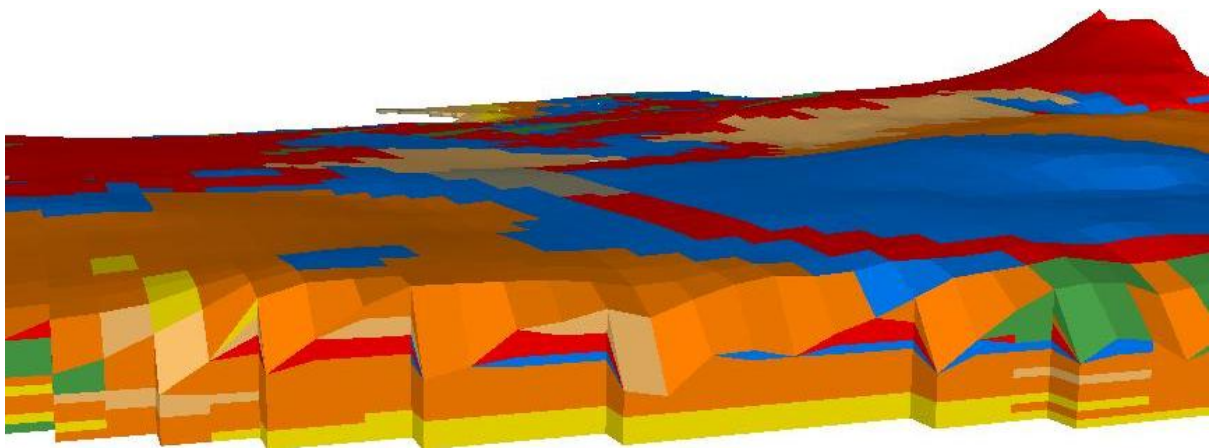


**Figure D.4** – Probability maps of the facies functioning as additional input data in the modelling process (continued).

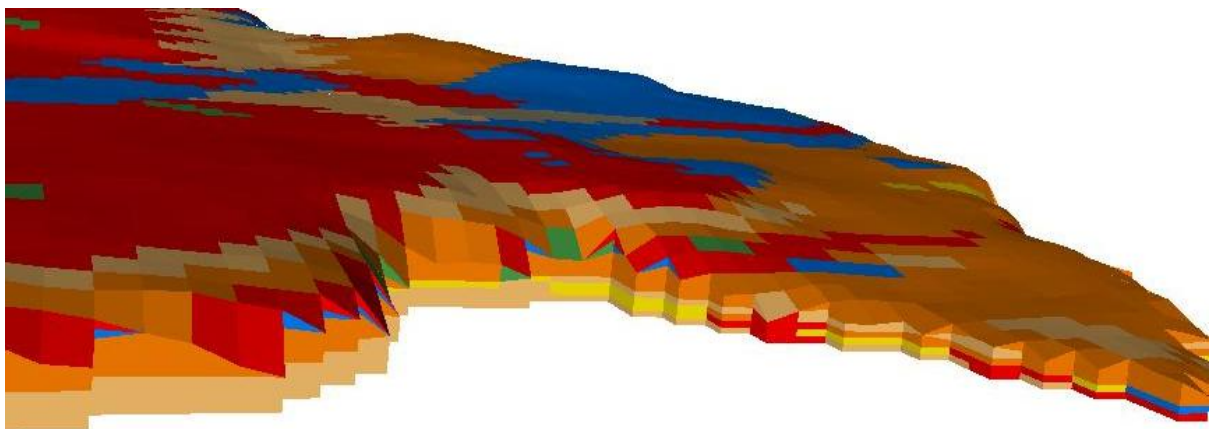




(a) Scalo Cavallo as seen from the north. Cala Rossa is on the left.



(b) Bue Marino looking inland from the east.



(c) Scala Azzurra as observed from the south, looking to the north.

**Figure D.5** – Close-ups of the final Multi-point statistics model of eastern Favignana.

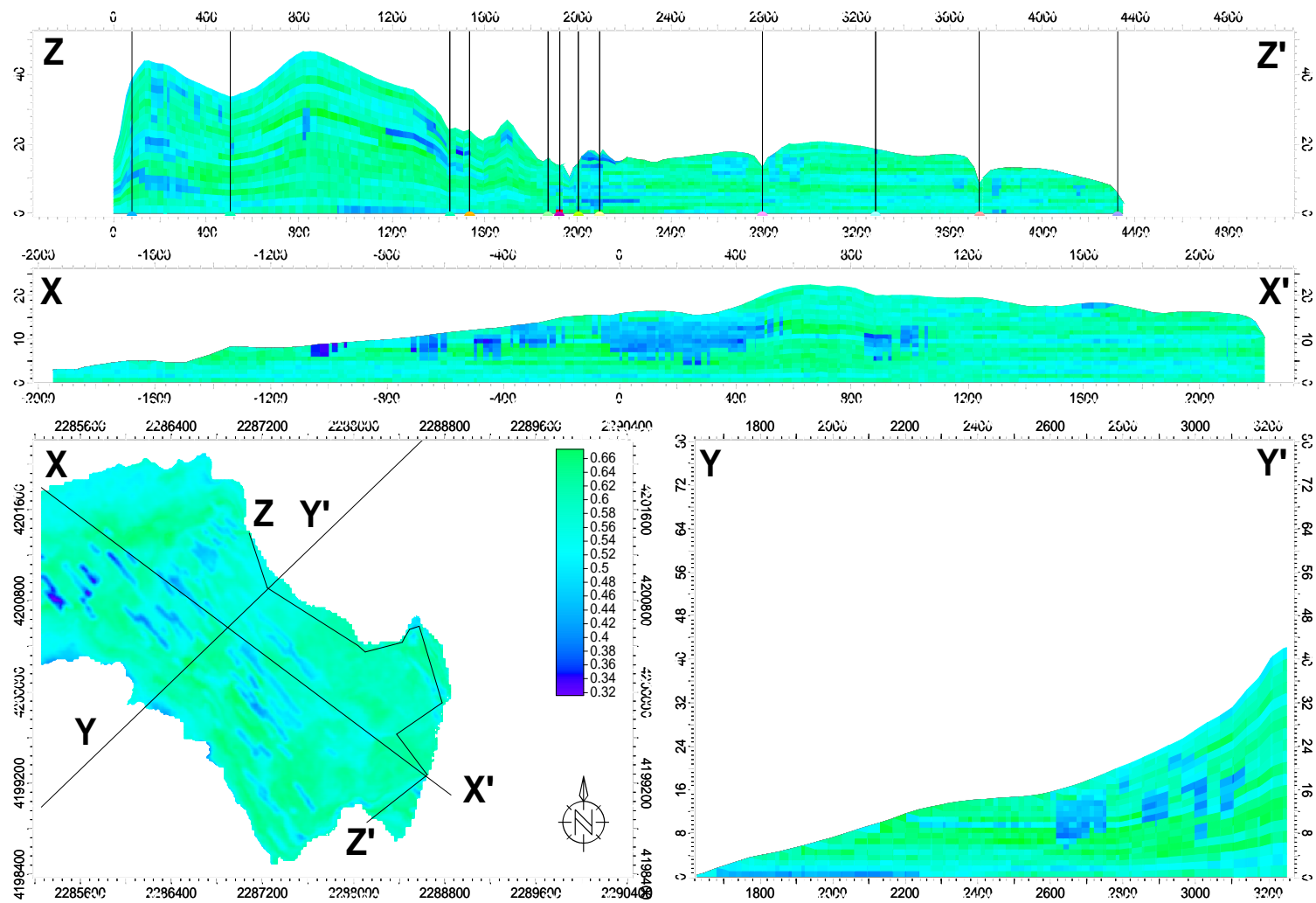
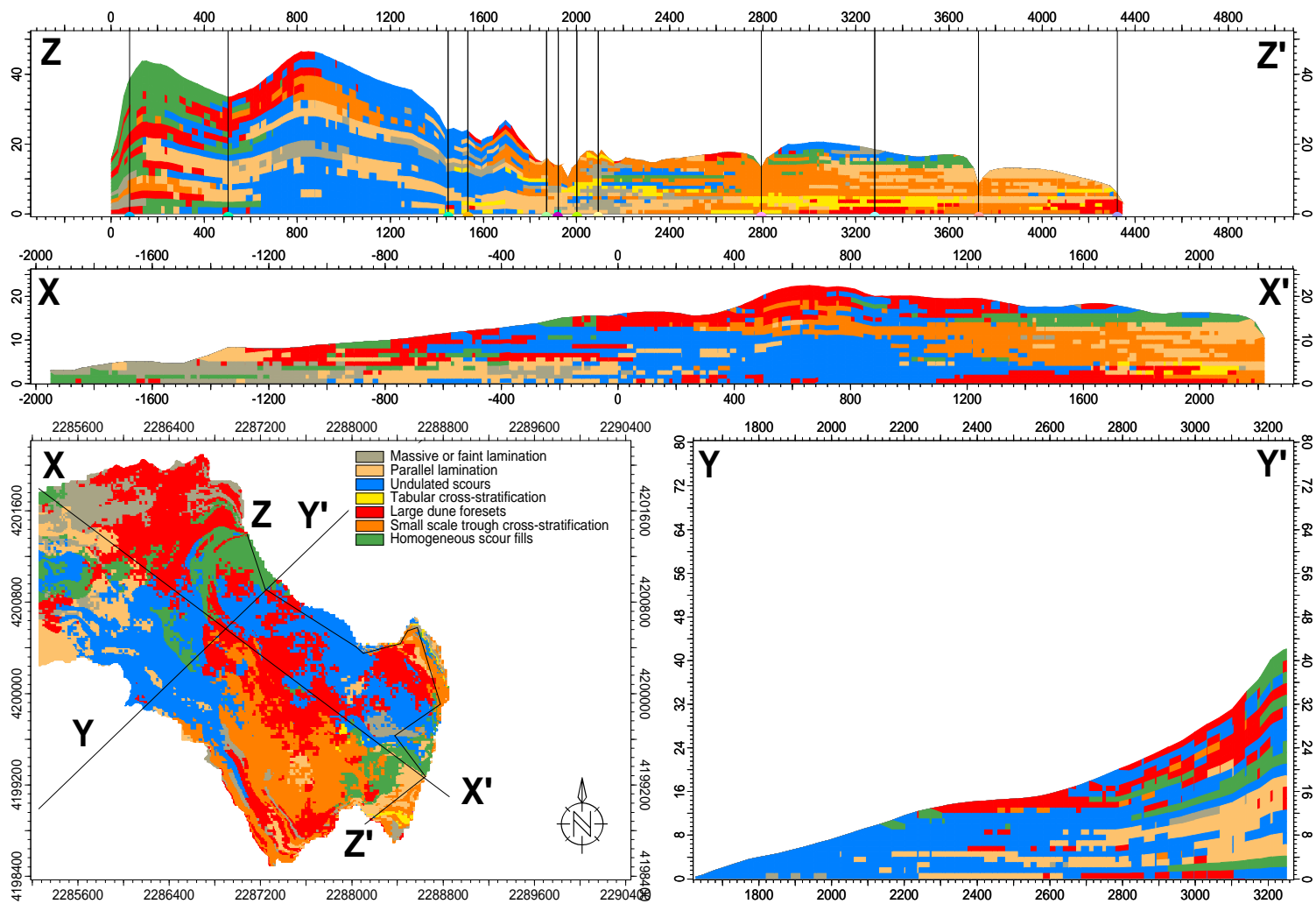
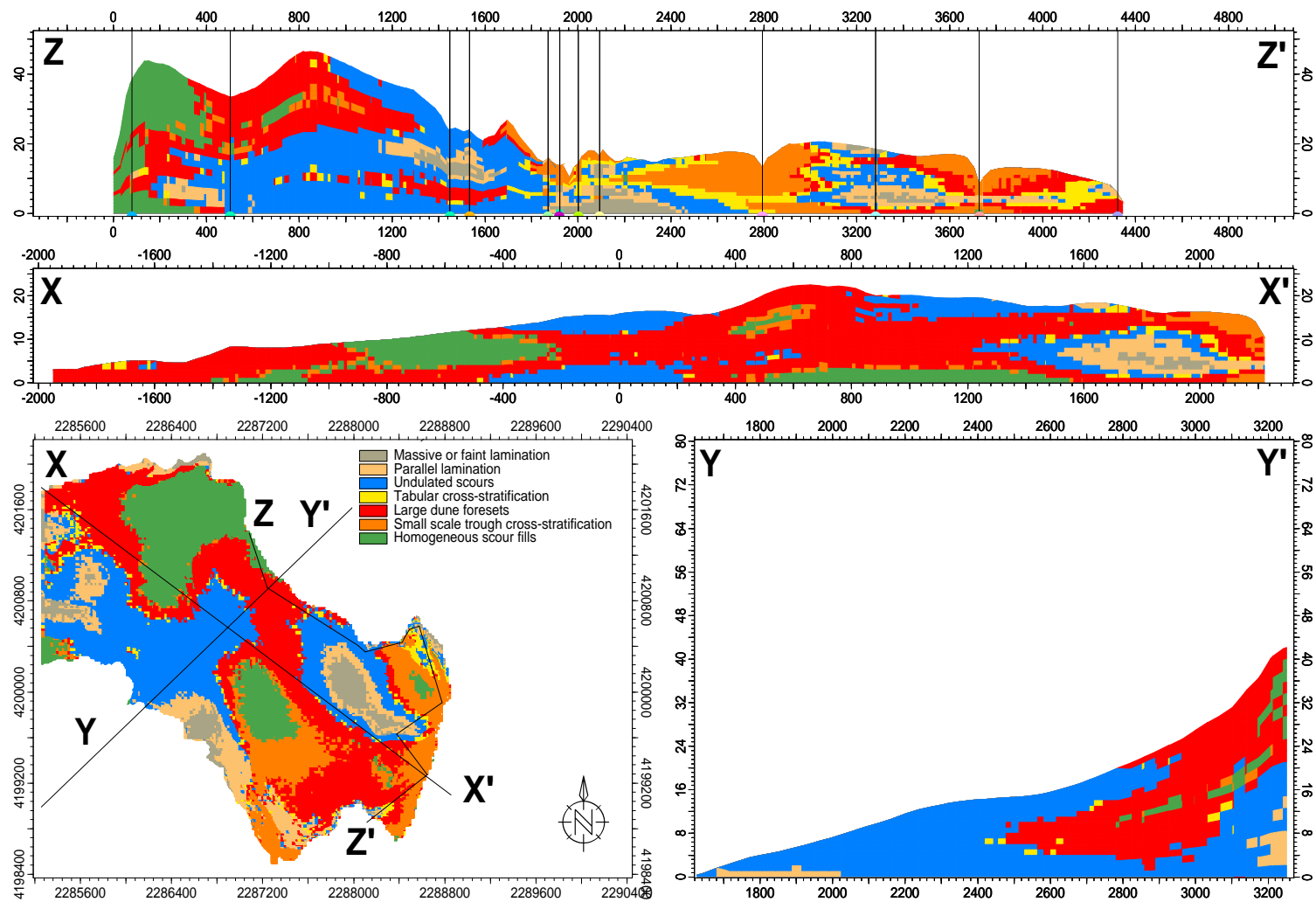


Figure D.6 – The eastern Favignana porosity model.





**Figure D.7** – Facies model of eastern Favignana resulting from a SIS algorithm.



**Figure D.8** – Facies model of eastern Favignana resulting from a TGS algorithm.

## E Tutorials

Some of the important workflows used in this research project are presented in this appendix, hopefully saving some time and preventing '*reinventing the wheel*' in ongoing future research projects. This is not meant as a comprehensive manual, but it illustrates the process used in the Favignana calcarenite research project.

### E.1 Falling head experiment

The falling head experiment was designed to overcome problems with high permeability samples. As this method does not use standard equipment, the workflow to design and execute the experiments is given here. The required equipment includes:

- PVC tube just over a metre long, and with inner diameter approx. equal to the plug diameter.
- Depending on the amount of plugs, one or more inner bicycle tyres (approx. 10 cm per plug).
- Piece of PVC tube — little longer than the plugs — with a flow valve (see figure E.1).
- Water tank, big enough to prevent water to rise significantly during the tests.
- Laboratory stand to hold the tube.
- Paper ruler.
- Vacuum pump with a three way valve and a 'cork' that fits in the tube.

#### Preparing the samples and set-up

1. The set-up of the experiment is shown in figure 3.3 (section 3.3.2).
2. Fix the paper ruler to the outside of the PVC tube with tape. The bottom of the ruler (the zero line) should align with the bottom of the tube.
3. Attach the cork, the flow valve and the vacuum pump as shown in the schematic experiment set-up.
4. Place the tube with ruler in the stand, above a tank filled with 'enough' distilled water, and connect the cork on top.
5. In order to prepare the seal around samples, use the small piece of tube with the valve. The principle is given in figure E.1, together with usage instructions.

6. Once the sample has a rubber seal, cut off one edge of the tyre. Make sure the seal aligns perfectly with the edge of the sample. The other end of the rubber sleeve is left intact.
7. In order to improve the sealing capacity, wrap tape around the seal where the sample is placed (figure 3.4. Make sure to apply enough force to create a tight seal. Especially the tape around the open end of the sample needs extra care.
8. Pull the loose end of the tyre with the sample around the long PVC tube. The sample should touch the tube, so no space may be left in between. Again, wrap tape around the rubber to improve the seal with the tube.

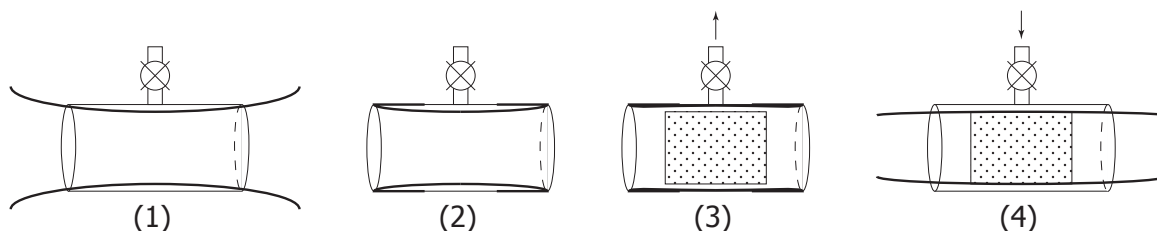


**Figure E.1** – Procedure to create a seal around the samples. **(1)** Take the small piece of tube with the valve and cut a long enough piece of inner tyre. Place it in the tube. **(2)** Wrap the excess edges of the rubber around the tube, closing off the annulus between rubber and PVC. **(3)** Open the valve and pump the air out of the annulus, so the rubber is pressed against the tube. Close the valve and place the sample in the apparatus. **(4)** Open the valve again to let air flow into the annulus squeezing the rubber tyre around the sample. Unwrap the edges.

## Performing the experiments

1. Once everything is prepared, connected and sealed properly, place the bottom end of the tube (attached to the sample) in the tank of water. Use a coin to ensure a constant space between the bottom of the sample and the bottom of the tank.
2. Start the vacuum pump leaving the three way valve closed in the direction of the sample. Turn the valve a little to create under-pressure in the tube. This will cause the water to rise.
3. The speed of the rising water can be controlled with the valve. Do not let the water rise too fast, because such a large under-pressure possibly creates air bubbles in the sample. This reduces the reliability of the outcome.
4. When the water has risen to more than a metre, stop the pump and immediately close the valve in all directions to prevent the water to flow back into the tank.
5. Prepare for time measurement, and open the valve to full extent in order to let air flow freely into the tube.
6. The water level starts to drop, with a flow velocity depending on the permeability of the sample. Start time measurement as soon as the water reaches the one metre level, and record the time at regular intervals.
7. When the water level in the tube is equal to the water level in the tank, flow will become very

slow. Stop measurement at some point little above this level, and repeat the experiment for more reliability.

## E.2 Import maps from CAD files

When fieldwork data is analysed with Petrel, often a map of the area is useful for the orientation of the user. In some cases a map is only available in hard copy. The only way of implementing these maps in a Petrel model is scanning and importing the digital picture of the map into the input folder. Tracing the contour lines with polygons having assigned the corresponding elevation leads to a digital elevation model of the area. A digital version of the map, in the case of Favignana in CAD format, is a very useful piece of information. Below is described how to exchange the data from AutoCAD to Petrel.

1. Load the digital map, and switch off all unnecessary layers. For an island it may be wise to export the data into three groups: coastline, other contour lines and single point data.
2. There is no built in function in AutoCAD to export data to text based files, but it is possible to run customised scripts created by users. A quick search on internet results in scripts with names like `ptexp.lst` or `ptexport.lst`, where `lst` is the file extension readable by AutoCAD.
3. When running one of these scripts, the AutoCAD software asks the user to select the data to convert. Select one of the data groups, and provide the name for the output file.
4. The output files are text based and contain `x`, `y` and `z` values for each point. Depending on the script, they may be comma or space delimited.
5. Petrel requires the data to be space delimited. Text editors with column edit mode can change a comma to a space easily. Another option is find and replace all the commas in the file.
6. Import the files into Petrel, selecting the appropriate options in the dialog box. The point data can then be used to make a surface, or in case of the coastline a polygon.

## E.3 Field data in pie charts

A useful way of displaying data is a pie chart map. This provides an easy to read overview of a lot of data points. Petrel supports the creation of such maps, and this workflow illustrates a way to create them.

1. Make facies logs from the fieldwork data. This includes the subdivision in facies, the creation of a facies template with suitable colours, etc.
2. When facies logs are done, make well tops for top outcrop and bottom outcrop. If the surface of the fieldwork area coincides, that well top will approximately be at the same level as the top outcrop marker.
3. These well tops make it possible to create a zone log for all the wells. Give the zones appropriate names, in particular the zone that includes the facies will be important.

4. Insert a new well top attribute. The folder with well top attributes can be found in the well tops folder. Such an attribute operates - or calculates - various properties of a well log. In this case a thickness template is attached to the outcrop part - top outcrop and bottom outcrop - creating an attribute for the outcrop thickness. This can be used for scaling later on.
5. For each facies, make a separate well top attribute. Select to operate to zones at level 1, ignoring any sub-zones. Select the facies log to be used, and the averaging method fraction (or percentage if preferred).
6. Make a map window with an overview of the field area, lay-out is up to the user. In the settings menu of the well tops folder, the style tab determines what is displayed.
7. Select the pie chart option and choose the earlier created outcrop thickness attribute as the relative size of the pie charts. After this, tick the boxes of the desired facies fraction attributes, and they will be displayed as pie charts.

## E.4 Probability maps

1. To start, first make the fraction attributes also used in order to create the pie charts.
2. Convert the attributes to points by right-clicking. This creates a point with the fraction of the specific facies for each well location. Do this for each facies. The point data appears in the input plane.
3. Point data can then be used to make a surface, displaying the fractions (or probabilities) in a surface-like manner. In order to do so, go to the make surface dialogue and select the point data from a certain facies. Other input options such as boundary and interpolation algorithms are project-specific.
4. When displaying the surfaces created from the well top attributes, some disadvantages become clear. At locations without no well data, the algorithm assumes that a facies is simply not present there. A combination of field data and the conceptual knowledge of the user is needed to make more reliable maps.
5. In addition, the creation of polygons on top of the earlier created maps provide full freedom in incorporating the geological knowledge. Draw the polygons, and with the z-value selector the desired fractions or probabilities can be assigned.
6. Create a second surface, but now from the polygons. The surfaces from well top attributes are only used as guidance when creating polygons.
7. Finally, convert the surfaces to a property in the active simulation grid. The easiest way is to make a workflow, so all facies probability properties can be created in once. Using the calculator, make an empty probability property for each facies (choose the probability template) in the simulation grid. Insert as many `Property = Surface(x,y)` functions as needed. The properties that have to be inserted are the empty properties, the surfaces on the right are the surfaces from the polygons.

8. The workflow only has to be made once. In case of an intermediate update, running such a workflow again refreshes and updates all items in the process. Note that this method does not include vertical variability. Every  $k$  layer in an  $i, j$  column of grid cells will be assigned to the same probability.





